Pesticide Residues in Frozen Beef and Fresh Tilapia "Oreochromis niloticus" Displayed in Qena Governorate Markets"

Jehan, R. Daoud, ∗Hanaa, M. R. Hegazy and ∗∗A. M. Ahmed
Food Hygiene &Control Dept., Faculty of Vet. Med., South Valley University, Qena
∗Forensic Med.&Toxicology Dept.,Faculty of Vet.Med., Kafr El-Shekh University
∗∗Food Hygiene Dept., Faculty of Vet. Med., Suez Canal University

Summary

The organochlorine pesticide "DDT, Aldrin, Dieldrin and lindane "residues in frozen beef samples and fresh tilapia" Oreochromis niloticus" (30 samples each) which collected from Qena governorate markets were evaluated using High Performance Liquid Chromatography. The recorded positive beef samples for DDT, Aldrin, Dieldrin, and Lindane were 14 (53.4%), 16 (46.7%), 20 (33.4%) and 15 (50%) respectively, meanwhile the recorded positive tilapia samples for the previous residues were 22 (73.4%), 20 (33.4%), 24 (80%) and 21 (70%) respectively. The mean concentrations of DDT, aldrin, dieldrin and lindane residues in beef were 2.0± 0.145, 0.48 ± 0.065, 0.52 ± 0.032 and 1.47 ± 0.064 ug/kg, respectively while the mean concentrations of the previous residues in tilapia were 2.56 ± 0.029, 0.26 ± 0.009, 0.16 ± 0.006 and 0.0020 ± 0.00008 ug/kg, respectively. The concentrations of pesticide residues in all positive samples (beef and fish) were below the permissible limits which set by WHO(1989)and FAO/WHO(1987). The public health significance and the toxicity of recorded pesticide on human health as well as the preventive measures for decreasing these residues in meat and fish were discussed.

introduction

Environmental pollution and food contamination are considered as the most serious problems challenging investigators allover the world. The hazards of pesticide residues in food have been addressed at international level through several Committees sponsored by some United Nations Organizations (FAO/WHO, 1986 and Hashim & Salem, 2006).The deleterious effect of the environmental pollution by pesticides has been considered as one of the principal research activities (David et al. 2008).

The wide spread usage of pesticides in Egypt led to many problems and constituted hazard in food animals. Pesticides residues in food arise as an important problem of serious public health hazards which may lead to acute or chronic hepatic toxicity for human being (Hassouba et al, 2007).

Organochlorine pesticides (OCPs) are a class of non polar toxic chemical compounds classified as dichlorodiphenylethane cyclodienes and chlorinated benzenes (Ademoroti, 1996). OCPs are ubiquitous environmental contaminant which have spread globally and have been detected in food stuffs, meat, drinking water and sediments as well as wide range of biota including fish (Ize-Iyamu et al., 2007). Numerous studies on both human and laboratory animals provide strong evidence of the toxic potential of the exposure to OCPs. The health effects associated with OCPs include reproductive failures, birth defect, endocrine disruption immune system dysfunction and cancer (Bouman et al., 1990; winter, 1992 and Olea et al., 1998). Other investigations confirmed that OCPs have strong potential to cross placental barriers even in minute concentration and cause serious neonatal damage (Saxena et al., 1981 and Jurewicz & Hanke, 2008).

Pesticides have been used in the public health sector and agriculture for controlling disease vector and eradicate crop pests. OCPs are widely used by farmers because of their effectiveness and their broad-spectrum activity (Ntow et al, 2006; Darko & Acquaah, 2007 and Ashujohri et al., 2008). Moreover, OCPS showed very resistant to microbial degradation and employed to control ecto-parasites of farm animals and pets.

They may concentrate in the adipose tissues and in the blood serum of animals leading to environmental persistence, bioconcentration and biomagnification through the food chain (Ntow et al., 2001). Acute hepatic and renal toxicity as well as the long term effect of organochlorine and organophosphorous pesticides are responsible for non specific symptoms like dizziness, headache, nausea, weakness, disturbance of vision, nervous symptoms, rashes, alternation of genes, disturbances of fertility and promotion or induction of cancer (Clark & Clark, 1978; Gergis, 1983; Beise, 1992 and Hashim, 2002 and Pathuk et al., 2009).

Beef may contain considerable levels of pesticide residues as a result of dipping of cattle or contamination of feedstuffs with these chemicals, increasing in these pesticide residues over their permissible limits in the food chain may pose serious health hazards to the general populace (Jeyashree and Vasudevan, 2007). Therefore this study was conducted to determine the concentrations of dichlorodiphenyltrichloroethane (DDT), Aldrin, Dieldrin and Lindane in frozen beef and fresh Tilapia" Oreochromis niloticus" samples that collected from Qena governorate by using High Performance Liquid Chromatography (HPLC).

Materials and Methods

Samples collection:

A total of sixty samples, 30 frozen beef (900g each) and 30 Tilapia "Oreochromis niloticus" (150g each) samples were collected from markets located in Qena, Egypt. The collected samples were separately packed in polyethylene bags in ice box and immediately transferred to laboratory to be cut into small pieces, thoroughly mixed and kept in aluminum foil, labelled and frozen at –20°C until evaluated. The collected samples were examined for determination the concentrations of DDT, Aldrin, Dieldrin and Lindan residues (ug/kg) by using HPLC.

Determination of organochlorine pesticide residues:

Frozen beef and fish samples were extracted according to AOAC (1980) and Pesticide Analytical Manual (1978). Fifty grams of each sample were ground with 100g of anhydrous sodium sulphate in presence of 150 mL of petroleum ether for two minutes, the extract was decanted through 500 ml Buchnur funnel containing two Whattman filter papers. The extract was poured through 40×25 mm column of anhydrous sodium sulphate then diluents were collected in 500 ml flask and placed in rotary evaporator to concentrate the extract. The pesticide residues were extracted from fat by using acetonitrile saturated with petroleum ether and clean up on florisil adsorbent. Extraction with 6% diethylether in petroleum ether. The dilute was concentrated in rotary evaporator, after which it was dried in a test tube at 50°C. The dried extract was dissolved in 0.5 mL n-hexane before injection in HPLC apparatus (ISCO model 2350) HPLC and 205 UV / vis detectors with hyper sil HPLC column 250×4.6 mm B DS. 180 SM.

Results and Discussion

The existence of the organochlorine pesticides with varying concentrations in examined food samples reflect the accumulation of pesticides in the tissue of the cattle and fish that may be attributed to way of nutrition (graze in different pastures) and continuously exposure to the spraying with insecticides to control external parasites. The persistence of DDT in the environment means that much of the material used for control of insect borne diseases and elimination of agricultural pests still contaminates soil, water and air (Ralls & cortes, 1972; Darko & Acquaah, 2007 and Hassouba et al., 2007).

Chemical Residues in Beef

The results in (figure 1) revealed that the recorded negative beef samples for DDT, Aldrin, Dieldrin, and Lindane were 16 (46.6%), 14 (53.3%), 10 (66.6%) and 15 (50%) respectively. Meanwhile the recorded positive beef samples for DDT, Aldrin, Dieldrin, and Lindane were 14 (53.4%), 16 (46.7%), 20 (33.4%) and 15 (50%) respectively. The mean concentrations of organochlorine Pesticide residues (ug/kg) in Beef samples showed in table (1). The mean

concentrations of DDT, Aldrin, Dieldrin, and Lindane in beef samples were 2 ± 0.145, 0.48 ± 0.065, 0.52 ± 0.032 and 1.47 ± 0.064 ug/kg, respectively. The recorded data were lower than the permissible limits established by WHO (1989) which was 5 ppm in meat for DDT, 1.01 ppm for Aldrin, Dieldrin and 1.1 ppm for Lindane.

Figure (1)

Frequency Distribution of Organochlorine Pesticide Residues in Frozen Beef

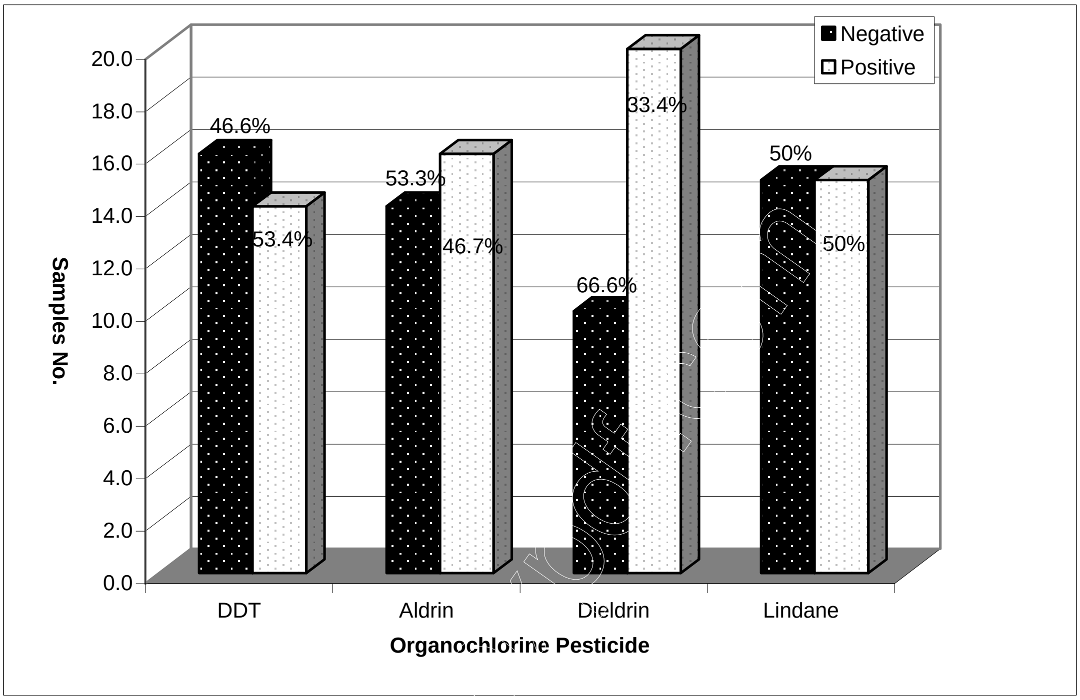

Table (1)

Concentrations of Organochlorine Pesticide Residues (ug/kg)in Frozen Beef (N=30)

OCPS	Samples No.< LOD	Min.	Max.	Mean ± S.E.
DDT	16	0.90	4.20	2.00 ± 0.145
Aldrin	14	0.04	1.10	0.48± 0.065
Dieldrin	10	0.10	0.80	0.52 ± 0.032
Lindane	15	0.70	1.80	1.47± 0.064

± S.E: Standard Error.

The concentrations of DDT in frozen beef were lower than those detected by Gadalla (1999) and Darko and Acquaah (2007), and Hassouba et al. (2007) in beef and Shrestha et al. (2009) in buffalo meat. DDT is still ubiquitous in the environment due to its past wide use and its chemical and physical characteristics. DDT persists for more than 10 years in the soil and accumulates in the organisms through the food chain. After absorption, a part of the DDT is metabolized, the products in mammals being DDE, DDA and DDT (Batrik and Piskac, 1980).

The obtained data of Aldrin and Dieldrin in frozen beef in table (1) were higher than those recorded by El-Shafi (1988) and Falandyeze and Kannan (1992) in frozen beef and lower than those detected by Darko and Acquaah (2007) in beef meat, Hassouba et al. (2007) in frozen beef.

The levels of Lindane in frozen beef in table (1) were nearly similar with those reported by Zasadowski et al. (1991) in cattle's meat, Darko and Acquaah (2007) in beef meat and lower than those recorded by Hassouba et al. (2007) in frozen beef.

Chemical Residues in Tilapia

The results in figure(2) revealed that the recorded negative tilapia "Oreochromis niloticus" samples for DDT, Aldrin, Dieldrin, and Lindane were 8 (26.6%), 10 (66.6%), 6 (20%) and 9 (30%) respectively. Meanwhile the recorded positive tilapia samples for DDT, Aldrin, Dieldrin, and Lindane were 22 (73.4%), 20 (33.4%), 24 (80%) and 21 (70%) respectively. The mean concentrations of organochlorine Pesticide residues (ug/kg) in tilapia, Oreochromis niloticus, samples showed in table (2). The mean concentrations of DDT, Aldrine, Dieldrin and Lindane in tilapia were 2.56 ± 0.029, 0.26 ± 0.009, 0.16 ± 0.006 and 0.0020 ± 0.0008 ug/kg, respectively. The obtained data were within the permissible limits of FAO/WHO (1987) and were nearly in accordance with those reported by Hashem and Salem (2006) in cultured and wild fish, Tilapia species.

Figure (2)

Frequency Distribution of Organochlorine Pesticide Residues in Tilapia “Oreochromis niloticus”

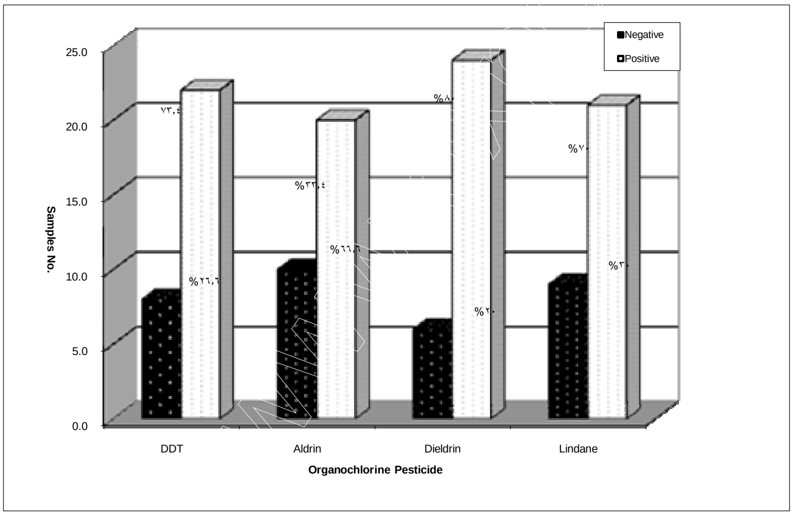

Table (2)

Concentrations of Organochlorine Pesticide Residues (ug/kg) in Tilapia "Oreochromis niloticus" (N=30)

OCPS	Samples No.< LOD	Min.	Max.	Mean ± S.E.
DDT	22	2.30	2.85	2.56 ± 0.029
Aldrin	20	0.19	0.38	0.26 ± 0.009
Dieldrin	24	0.11	0.23	0.16 ± 0.006
Lindane	21	0.0011	0.0032	0.0020 ± 0.00008

± S.E: Standard Error.

The recorded results of DDT in fresh fish were lower than those reported by Hashem (2002) in fish products, kipcic et al, (2002) in domestic fish, Marsalek et al. (2004) in domestic fish, Ejobi et al. (2007) in Nile perch "Lates nilotica" and David et al (2008), and higher than those detected by Ownby et al. (2004) in fish fillets.

The concentrations of Aldrin in fresh fish were lower than those recoded by Hashem (2002) fish products. Also the Lindane concentrations in fresh fish were lower than those detected by Kipcic et al. (2002) in domestic fish. Meanwhile the levels of Dieldrin in fresh fish in table (2) were lower than those reported by Ejobi et al. (2007) in Lates nilotica and david et al. (2008) in Tilapia zille (red belly Tilapia) and higher than those recorded by Therdteppitak and Yammeng (2003) in Nile Tilapia "Oreochromis niloticus".

The detectable level of such residues were varied in quantities dependent on the way of nutrition and the fat content of particular species of fish, type of tissue examined and exposure of examined fish to different pesticides before caughting and processed as well as the degree of accumulation of these compounds in examined samples.

References

Ademoroti, C. M. A. (1996): Environment Chemistry and Toxicology. Foludex Press Ltd. Ibadan, pp: 79 – 208.

AOAC "Association Official Analytical Chemists" (1980) "Official methods of the Association Official Analytical Chemists" Washington D.C. Chapter 29 (Pesticides) Bed.

Ashujohri, A.; Dhawan, A.; Singh, R.L.; Parma, D. (2008): Persistence in Alterations in the Ontogeny of Cerebral and Hepatic Cytochrome P. 450, Following Prental Exposure to low doses of Lindane. Toxicological Sciences 101 (2): 331 – 340.

Bartik, M. and Piskac, A. (1980): Veterinary Toxicology, 137. Elseveier Scientific Publishing Company Amsterdam – Oxford – New York.

Beise, S. (1992): Pesticide residues in food as a potential health hazard in 3rd world congress, food born infections and intoyications volume 11, Berlin 706.

Bouman, H.; Coetzee, A. and Schutte, C. H. (1990): Environment and health implication of DDT contaminated fish from the Pongolo flood plain. J. Afr., 104 : 275 – 286.

Clark,G. C. and Clark, M. L. (1978): “Veterinary Toxicology” Bailliore and Tindal England 196.

Darko, G. and Acquaah, S. (2007): levels of organochlorine pesticides residues in meat. Int J. Environ. Sci. Tech. 4 (4): 521 – 524.

David, A. Grace, U. Chimezie, A. and Johnpaul,U. (2008): Organochlorine pesticide residues in fish samples from lagos lagoon, Nigeria. Am. J. Environ. Sci., 4(6): 649 – 653.

Ejobi F.; Muller, P.; Opuda – Asibo, J. and Kruger J. (2007): Polychlorinated Biphenyls and organochlorine pesticides residues in Nile Perch (Lates nilotica) from lake Victria, Uganda J. of Fisheries International, 2 (2): 158 – 161.

El-Shafi, M. E. (1988): Monitoring for Pesticide residues in Egyptian livestock in middle Egypt. Ph.D. Thesis Meat Hygiene, Fac. Vet. Med. Cairo University.

Falandyez, J. and kannan, K. (1992): Organochlorine pesticide and polychlorinated biphenul residues in slaughtered and game animal fats from the northern part of Poland. Zeitschrift Fuerleben smitleunter suchnug and Forschung. 195 (1): 17 – 21.

FAO/ WHO (1987): Food Standard Programme. Codex Alimentairius Commission Rome.

Food Agricultural Organization / World Health Organization (1986): Codex maximum limits for pesticide residue, Rome, Codex Alimentaries Commissions. Food and Agriculture Organization of United Nation (CAC) Vol. XIII, ED -2.

Gadalla, M. N. (1999): Organochlorine pesticides residues in tissues of slaughtered animals Ph.D Thesis (Meat Hygiene) Fac. Vet. Med. Assiut University.

Gergis, A.F. (1983) pesticide residues in meat. M. V. Sc. Thesis Fac. Vet. Med. Cairo University, Egypt.

Hashim, M.F. (2002) Pesticide residues in local processed fish products J. Egypt. Vet. Med. Ass. 62 (6c): 7 – 13.

Hashim, M.F. and Salem, G.S. (2006): Studies on some pesticide residues in cultured and wild fish J. Egypt. Vet. Med. Assoc. 66 (4): 249 – 258.

Hassouba, M.M.; Hashim, M.F. and El-Maghraby, O.M. (2007): Hygienic status and prevelance of heavy metals and pesticide residues in frozen meat, chicken and their products in Luxor city. Assiut Vet. Med. J. 53 (114): 91 – 105.

Ize – Iyamu, O.K.; Abia, I. O. and Egwakhide, P.A. (2007): Concentrations of residues from organochlorine pesticide in water and fish from some rivers in Edo State, Nigeria. Int. J. Physical sci, 2 : 237 – 241.

Jayashree, R. and Vasudevan, N. (2007): Effect of tween 80 added to the soil on the degradation of endosulfan by pseudornonas aeruginosa. Int. J. Environ. Sci. Tech. 4 (2): 203 – 210.

Jurewicz, J. and Hanke W, (2008): Prenatal and Childhood Exposure to Pesticides and Neurobehavioral development: Review of Epidemiological Studies Int. 7 Occup med Environ. Health 21 (2): 121 – 132.

Kipcic, D.; Vukusic, J. and Sebecic, B. (2002): Monitoring of chlorinated hydrocarbon pollution of meat and fish in Croatia. Food Technol. 40 (1): 39-47.

Marsalek, P.; Weiss, V. and Koleika, J. (2004): Chlorinated hydrocarbon residues in fish from Nove Mlyny reservoirs along Dyje River, Czech Republic. ACTA Vet. Brno. 73: 275 – 281.

Ntow, W.J. (2001): Organochlorine pesticides in water, sediments, crops and human fluids in a farming community in Ghana. Arch. Environ. Contam. Toxicol, 40, 557 – 563.

Ntow, W.J. Gijzen, H. J. and Drechsel, P. (2006): Farmer perceptions and pesticide use practices in vegetable production in Ghana Pest Manage. Sci, 62 (4): 356 – 365.

Olea, N.; Pazos, p. and Exposito, J. (1998): Inadvertent exposure to xenoestrogens Eur J. Cancer Prev, 7: 17 – 23.

Ownby, D. R.; Trimble, T. A.; Cole K. A. and Lydy, M. J. (2004) Pesticide residues in water sediment and fish at the Sparta Il, USA National Guard Armony. Bull. Environ. Contam Toxicol. 73: 802 – 809

Pathuk, R.; Ahmed, R.s: Tripathi, A.K.: Guleria, K.; Sharma, C.S; Makhijani, S.D.; Banerjee, B.D. (2009): Maternal and cord blood levels of organochlorine pesticides: an association with preterm labor. Clin. Biochem. 42: 746 – 749.

Pesticide Analytical Manual (1978): Methods which Detect Multiple Residues Vol. 1, U. S. Deponent of health and human services. Food and Drug Administration.

Ralls, J. W. and Cortes A. (1972): Survey of food ingredient DDT reactions under thermal processing conditions J. Food Sci. 37: 760 – 765.

Saxena M. C.; Siddique, M. K.; Bhargava, A. K.; krishina, C. R. and kutty, D. (1981): Placenta transfer of pesticides in humans. Arch Toxicol., 48: 127 – 134.

Shrestha, S.K.; Aulakh, R.S.; Bedi, J.S. and Gill, J.P. (2009): Organchlorine pesticide residues in buffalo meat in Punjab, India. Pakistan. J. Zool. Suppl. Ser., 9: 135 – 137.

Therdteppitak, A. and Yammeng, K. (2003): Determination of organochlorine pesticides in commercial fish by gas chromatography with electron capture detector and confirmation by gas chromatography mass spectrometry. Science Asia, 29: 127 – 134.

WHO (1989): Pesticide residues in food, FAO plant protection paper, 157 – 159.

Winter, C. (1992): Dietary pesticide risk assessment. Rev. Environ. Contam. Toxicol, 127: 23 – 67.

Zasadowski, A.; Amarowiez, R.; Barsri, D. and Terleckam A. (1991): Residues of polychlorinated pesticides in fat, liver and brain of cattle and pigs from the region of Varnia and Mazuria (1981 – 1988) Bromatol. Chem. Toksykol . 24 (3 – 4): 317 – 322.

متبقيات المبيدات في اللحم البقري المجمد وأسماك البلطي الطازجة المتداولة في أسواق محافظة قنا

جيهان رجب محمد داود ، هناء محمد رجب حجازى* ، على معوض احمد **

قسم الرقابة الصحية على الأغذية – كلية الطب البيطرى – جامعة جنوب الوادي (قنا) - جمهورية مصر العربية
*** قسم الطب الشرعى والسموم - كلية الطب البيطرى – جامعة كفر الشيخ - جمهورية مصر العربية**
**** قسم الرقابة الصحية على الأغذية - جامعة قناة السويس - جمهورية مصر العربية**

الملخص العربي

تم في هذه الدراسة تقييم بقايا بعض المبيدات الحشرية(مركبات الكلورين العضوية) "د.د.ت، ألدرين، داى إلدرين وليندان" فى عدد ثلاثون عينة من اللحم البقرى المجمد وأخري من عينات السمك البلطى الطازج الذين تم تجميعهم من أسواق محافظة قنا وقد تم تحليل العينات باستخدام جهاز التحليل الكروماتوجرافى السائل ذو الضغط العالى ووجد أن القيم المتوسطة لبقايا الـ د.د.ت، ألدرين، داى إلدرين، ليندان فى عينات اللحم البقرى المجمد كانت٢ ± ٠,١٤٥، ٠,٤٨ ± ٠,٠٦٥، ٠,٥٢ ± ٠,٠٣٢، ١,٤٧ ± ٠,٠٦٤ ميكروجرام / كجم على التوالى بينما كانت القيم المتوسطة لهذه البقايا فى عينات سمك البلطى الطازج ٢,٥٦ ± ٠,٠٢٩، ٠,٢٦ ± ٠,٠٠٩، ٠,١٦ ± ٠,٠٠٦، ٠,٠٠٢٠ ± ٠,٠٠٠٨ ميكروجرام / كجم على التوالي.

وقد تم مقارنة النتائج بالمواصفات القياسية وقد وجد أن عينات اللحم البقرى المجمد كانت جميعها مطابقة للمواصفات القياسية طبقاً لمنظمة الصحة العالمية عام ١٩٨٩ وأيضاً عينات سمك البلطى كانت مطابقة لمواصفات الأغذية والزراعة / منظمة الصحة العالمية لعام١٩٨٧. وقد تم مناقشة الأهمية الصحية والتأثيرات الخطيرة لبقايا هذه المبيدات على صحة الإنسان والإجراءات الوقائية المتبعة للإقلال من بقايا المبيدات الحشرية فى اللحوم والأسماك.

A Study of Ultraviolet Irradiation at Qena, Upper Egypt

A.A. Hassan , S. M. El Shazly*, Kh. O. Kassan, E. El Nobi and Emad, A. A.
Physics Dept. Faculty of Science, South Valley University, Qena, Egypt

Abstract

Hourly data of global (G) and ultraviolet solar irradiation (UV & UV-B) for three years (2001-2003) were obtained from Egyptian Meteorological Authority at South Valley University station at Qena / Upper Egypt (26° 16` N, 32° 75` E and 78 m asl). Actual sky condition records were analyzed to study hourly, monthly and seasonally variations. Also the role of solar zenith angle (SZA) and clouds cover (C) on ultraviolet irradiation has been studied. The study revealed a small share of UV irradiation in the incoming G irradiation (UV/G =3.32 % and UV-B/G = 0.25 %). Also transmission of UV-B decrease as cloud cover increases, where the reduction in UV-B irradiation was about 27.7 % in case of 50 % cloud cover (4 Octas) and 45.7 % in case of cloud overcast condition (100 % clouds cover). Empirical formulas between the UV-B transmission and cloud cover have been given. Also empirical formulas have been deduced concerning the interrelation of global and ultraviolet irradiation. A very good correlation was found between them. It can be used to estimate the values of UV irradiation that are not usually available with the aid of the abundance G measurements. These formulas may be used at any nearby sites with acceptable accuracy.

Key words: global solar irradiation –Ultraviolet solar irradiation – hourly and monthly variations – Solar Zenith angle effect – cloud effect

*** Corresponding author:**

E-mail address: Hassan_xp58@yahoo.com

1- Introduction

Approximately 9.5 % of the incident solar energy at the top of the atmosphere lies in the UV part of the spectrum (McKenzie et al., 1995). UV - irradiation from the sun is an area of interest to both the scientific community and the general public. It has numerous useful applications but increased awareness and control of UV hazards are needed to prevent accidental overexposures. Environmental photo-biologists normally define the wavelength regions of ultraviolet irradiation as UV-C (200-280 nm), UV-B (280-320 nm), and UV-A (320-400 nm).

The earth surface receives only UV-A and UV-B while the UV-C component is removed by absorption through the protective ozone layer (O_3). UV-B is partially absorbed by the ozone layer while UV-A is transmitted (McKenzie et al., 1995). The beneficial and damaging effects of UV-A and UV-B irradiation on humans, the ecosystem, animals, plants, and materials are many (Parrish, et al., 1978, Biswas, 1979 and Giese, 1982). Adverse biological effects of UV irradiation on man include, among others, sunburn (erythema), conjunctivitis, and skin cancer (WMO, 2003).

Many previous studies are concerned for the variability of the level of ultraviolet irradiation reaches to earth's surface over some locations in Egypt (Robaa, 1999 and 2004; El-Metwalley, 2004; Trabea and Salem, 2001 and Shaltout et al., 1994). These studies did not include Qena, where the ultraviolet measurements were absent before year 2000.

Qena is a provincial capital location located in the south part of Egypt about 600 Km south of Cairo and 64 Km north of the tourist city Luxor at Latitude 26° 10′, Longitude 32° 43′ and elevation 78 meter above sea level(see Fig.1). Climate of Qena is very hot, dry in summer and cold in winter. It rarely rains. Also it receives a large quantity of solar irradiation especially in summer; of course it contains large percentage of ultraviolet irradiation. Accordingly, increased awareness must be taken to avoid its adverse effects in this region.

In the present study, hopefully, we could quantify ultraviolet irradiation at Qena, which is very important and benefit study for inhabitants and tourists as well. In this consideration the present work aims mainly to study the characteristics and behavior of global and UV - irradiation, particularly UV-B irradiation, over Qena Upper Egypt. The study includes the following:

1. **Variation of global (G) and ultraviolet (UV & UV-B irradiation in actual sky conditions.**
2. **Effects of both solar zenith angle and cloud covers on UV –B irradiation**
3. **Prediction of some empirical relationships (e.g. UV& G, UV-B & G and UV-B & UV irradiation) for computing UV irradiation using available data. Performance of these relationships has been done.**

2- Database and methodology

The database considered in this study contains hourly values of global - , UV- and UV-B - solar irradiation in wh/m2 as well as cloud cover in Octas in the period from 2001 to 2003. These data were obtained from the meteorological station in south valley university at Qena / Upper Egypt, which is one of the stations grids of the Egyptian Meteorological Authority. The last is a member of Word Meteorological Organization (WMO) and works according to its rules. All instruments used in the measurements are manufactured by "The Eppley laboratory, Inc" and "Yankee Environmental systems, Inc" (YES).

Global solar irradiation in Qena is recorded by the Eppley Precision Spectral Pyranometer (PSP) No16317IS. The accuracy of this Pyranometer corresponds to the first class according to the WMO classification (WMO, 1990). The instrument measures G in the spectral range 295 - 2800 nm with precision 3-4%, sensitivity 9 µ V /(W/m2) and cosine response ± 1 % from normalization 0-70˚ zenith angle. Ultraviolet irradiation is measured using an Eppley radiometer TUVR No. 31737. Its sensitivity and cosine response are approx. 150 µ V / (W/m2) and ± 3.5 % from normalization 0-70˚ zenith angle. The model UVB -1 Ultraviolet Pyranometer No. 960842, Yankee Environmental System INC (YES) is used to measure the global UV- irradiation from 280 to 320 nm (UV-B). The sensitivity of the measurements is 1.97 volt / (W/m2) of total UV-B irradiance and the cosine response is ± 5 % for 0 - 60˚ solar zenith angle. The instrument measurement technique uses colored glass filters and a UV-B phosphor to convert incoming UV-B – irradiation to green light, which is then measured by a calibrated solid state photo detector.

3-Result and Discussion

3.1 Global irradiation variability:

a- Hourly Variations (HG):

Fig. 2 represents the mean, maximum and minimum variations of the average hourly global solar irradiation (HG) at Qena city through the period from 2001 to 2003. The following points can be deduced:

1. **Mean values of hourly global solar irradiation (HG) range from 13.41 Wh/m2 (at 18 - 19 LAT) to 872.61 Wh/m2 (at 11- 12 LAT).**
2. **Maximum values of (HG) irradiation range from 32.5 Wh/m2 (recorded at 18-19 LAT) to 1137.5 Wh/m2 (recorded at 11-12 LAT), while the minimum ones range from 0.83 Wh/m2 (recorded at 5 - 6; 6 - 7 and 17- 18; 18 -19 LAT) to 286.94 Wh/m2 (at 11-12 LAT).**

b- Monthly variations (MDG):

Fig. 3 shows the mean, maximum and minimum variations of the monthly average of daily Global solar irradiation (MDG) expressed in Wh/m2 for the whole period (2001-2003). From this figure it can be concluded that the highest intensity values of global solar irradiation lie in June, July and August, while the lowest ones are in Dec. Jan and Feb. The figure shows that the mean value of MDG ranges from 3885.01 Wh/m2 (recorded in December) to 8204.97 Wh/m2. (recorded in Jun). Also, the maximum and minimum values of MDG through this period range from 4211.94 to 9081.64 Wh/m2 (at Dec and Jun) and from 2436.72 to 7253.89 Wh/m2 (at Nov and Jun), respectively.

c - Seasonal variation (SDG)

Fig. 4 shows the mean, maximum and minimum variations of the seasonally average of daily Global solar irradiation (SDG) expressed in Wh/m2 for the whole period (2001-2003). It is very clear that:

1-The mean values of SDG change in the following trend:

Winter <	**autumn**	**<**	**spring**	**<**	**summer**	
(Dec - Feb)	**(Mar – May)**		**(Jun -Aug)**		**(Sep - Nov)**	
4259.96	**<**	**5234.75<**	**7071.81<**	**7895.39**		

2-The ratios of mean seasonal daily dose (SDG) of global irradiation in autumn, spring and summer to its corresponding value in winter (as a reference) were 1.2, 1.7 and 1.9, respectively.

3.2 Ultraviolet irradiation (UV & UV-B) variations

a- Hourly Variations:

Fig. 5a,b represents the mean, maximum, and minimum hourly variations of ultraviolet irradiation (HUV & HUV-B) in Wh/m2 through the study period. The following points can be deduced:

1. **Mean values of HUV range from 0.73 Wh/m2 (recorded at 18-19 LAT) to 32.49 Wh/m2 (recorded at 11-12 LAT).**
2. **Mean Value of HUV-B ranges from 0.28 Wh/m2 (recorded at 17-18 LAT) to 2.87 Wh/m2 (recorded at 11-12 LAT).**
3. **The maximum values of HUV range from 1.39 Wh/m2 (at 18 -19 LAT) to 46.94 Wh/m2 (at 11-12 LAT), while the minimum ones range from 0.28 Wh/m2 (at 18 -19 LAT) to 11.11 Wh/m2 (at 11 -12 LAT).**
4. **The maximum values of HUV-B range from 0.28 Wh/m2 (at 17 -18 LAT) to 4.17 Wh/m2 (at 11 -12 LAT), while the minimum ones range from 0.27 Wh/m2 (at 17 – 18 LAT) to 1.11 Wh/m2 (at 11 12 LAT).**

b- Monthly variations

Fig 6a,b shows the mean, maximum and minimum variations of the monthly average of daily dose of UV and UV-B irradiation (MDUV & MDUV-B) in Wh/m2 through the study period. From this figure we can conclude that the highest intensity values of both UV and UV-B irradiation lie mainly in June, July and August, while the lowest ones are mainly in Dec. Jan and Feb. Maximum values are recorded in June and minimum ones are recorded in Dec. The figure clarifies the following:

The mean values of MDUV & MDUV-B lie in the ranges (130.95 – 306.67) and (7.67 -23.89) Wh/m2, respectively.

The maximum values of MDUV range from 149.96 to 307.45 Wh/m2, while its minimum values range from 87.59 to 225.91 Wh/m2.

The maximum values of MDUV-B change from 9.17 to 26.11 Wh/m2, while its minimum values range from 2.50 to 21.39 Wh/m2,

c- Seasonal variation

Fig. 7a,b represents the mean, maximum and minimum variations of the seasonal average of daily dose of UV and UV-B irradiation (SDUV & SDUV-B) expressed in Wh/m2 through the study period (2001 – 2003). It is very clear that the mean values of SDUV and SDUV-B vary in the following manner:

1-For UV irradiation

Winter <	**Autumn**		**<**	**Spring**	**<**	**Summer**
(Dec - Feb)	**(Mar – May)**			**(Jun -Aug)**		**(Sep - Nov)**
145.05	**<**	**181.02**	**<**	**237.10**	**<**	**253.70**

2-For UV-B irradiation

Winter	**<**	**Autumn**	**<**	**Spring**	**<**	**Summer**
(Dec - Feb)	**(Mar – May)**			**(Jun -Aug)**		**(Sep - Nov)**
8.92	**<**	**12.73**	**<**	**18.96**	**<**	**22. 85**

.If we take the winter's values as a reference, the ratio of each (SDUV and SDUV-B) in autumn, spring and summer, to its corresponding values in winter were 1.25, 1.63 and 1.74 for UV irradiation and 1.43, 2.13 and 2.56 for UV-B irradiation. It means that the solar irradiation component (UV and UV-B) are more intensive in summer and spring than winter and autumn

3.3 Percentages of UV/G, UV-B/G and UV-B/UV

Solar irradiation that incident at the top of our atmosphere contains approximately 8.5 % of UV band and 1.4% of UV-B band. In fact this percentage is reduced during its travel to the earth's surface. Ozone plays an important role, it absorbs UV-B irradiation consequently its percentage will reduce and becomes lower than 1.4. The percentages of UV/G, UV-B/G and UV-B/UV have been calculated for the selected period of study. Table (1) summarizes the monthly variations of these percentages. The following can be concluded:

In general, global irradiation includes a small share of UV and UV-B irradiation. The percentage of UV/G over the whole measurements period equals (3.32 %), while the percentage of UV-B/G equals 0.25 %.

The mean percentage of UV-B/UV through this period is equal to 7.68 %. It means that the most UV irradiation which reaches earth's surface is UV-A irradiation. Fortunately it is less energetic than UV-B.

.The ratios of UV/G and UV-B/G at Qena city are characterized by slight monthly and seasonal variation during the study period. This means that there are no remarkable atmospheric conditions have an obvious effect on either ultraviolet or global irradiation.

3.4 Comparison with measured values at other Locations

To illustrate the potential of solar irradiation components at Qena in comparison with other locations, differ in their latitudes, some corresponding daily average values of global solar irradiation at the same study period (2001 -2003) at Mersa Matrouh, Al - Arish, Cairo, Kharga, and Aswan are introduced (Trabea and Shaltout,2000). Their corresponding latitudes are 31o 52\, 31o 07\, 30o 08\, 25o 45\ and 23o 97\, respectively. Fig. 8 shows these values at these locations. The following can be concluded:

1. **Mean values of global solar irradiation at Aswan, Qena and Kharga through this period are 6231.8, 6115.48 and 6141.2 (Wh/m2), respectively. It is clear that they are the nearest to equator (Aswan is the nearest one).**
2. **Al - Arish and Matrouh lie at the north direction of Egypt and are the farthest locations to equator. So, they received less values of global irradiation (5438.8 and 5256.9 Wh/m2, respectively.**
3. **Cairo is heavy populated city at the latitude 30o 05\ N. However, it does not show high potential of global irradiation (5277.8 Wh/m2) compared with other locations. This is a result of the large quantity of pollutants emitted into the atmosphere from different man activities to the large numbers of vehicles of various kinds, which in turn is working on the attenuation of the amount of radiation reaching the earth's surface.**

In addition some available data for monthly UV irradiation at Aswan (Egyptian Meteorological Authority) and Cairo (Robaa, 2004) are used for comparison with our data as shown in Fig. (9). It is clear that the mean values of UV irradiation at Qena and Aswan Cities are greater than its corresponding values at Cairo at all months . The mean values of UV solar irradiation at Cairo, Qena, and Aswan were 224.35, 238.22 and 242.56 Wh/m2, respectively. This variation may be explained by the same manner of global irradiation.

3.5 Site consideration

The level of ultraviolet irradiation that reaches the earth's surface can vary by temporal, geographical and meteorological factors. The most important factors are stratospheric ozone, aerosol, clouds, and solar zenith angle. The effects of cloudiness conditions and solar zenith angle, only, have been considered in the present study. This is owing to the comparatively low variability of stratospheric ozone and aerosol at Qena and the non available accurate data of them in the present time

3.5.1 Solar zenith angle effect

Solar Zenith angles (Z) are calculated during the time from 6hr to 18hr over the whole period of study. Fig. 10 clarifies the mean hourly variations of UV-B irradiation (Wh/m2) and solar zenith angles (Z) in degree at the different seasons during this period. Regression formulas between the two parameters are included in this figure. The following can be deduced:

Both of UV-B and solar zenith angle vary in a reverse manner in all seasons and over the whole year, viewing similar distribution patterns during the four seasons (winter, spring, summer, autumn as well as the whole period). This behavior may be explained in terms of the path of the sun's rays through the earth's atmosphere. At noontime the sun is positioned high in the sky having shorter path than that in the early morning and late afternoon. Consequently, less solar irradiation is attenuated and more solar irradiation reaches the earth's surface at noontime, low SZA (ϴz). The reverse occurs in early morning and late afternoon, high SZA (ϴz).

3.5.2 Clouds effect

The study consists of two parts. In the first part, the cloudiness conditions of the Qena atmosphere have been introduced. In the second part the effect of clouds on UV-B irradiation have been discussed under the cloudiness conditions of the Qena atmosphere. The meteorological parameters, we used in this study, which describe cloudiness conditions is cloud cover (C, Octas)

and types. The cloud observations are carried out visually each hour at all standard meteorological stations in Egypt.

3.5.2.1 Clouds cover

The cloud cover is classified into four classes on the basis of cloud amount. Table 2 illustrates their mean percentages in different seasons in the study period. It is clear that:

1. **Percentages of class I range from 62.7% (in winter) to 94.8 % (in summer) and class II from 5.2 % (in summer) to 16% (in spring), while percentages of class III range from 0 % (in summer) to 13.2 % (in winter) and class IV from 0 % (in summer) to 4 % (in spring).**
2. **In general, the sky is clear in summer where the effective cloud classes III and IV represent 0 %.**
3. **More effective clouds (class III and IV) are recorded in spring and winter, where it represent (12.4%, 4.0%) and (13.2%, 1.8%), respectively.**

3.5.2.2 Cloud types

Seasonal percentages of cloud types are calculated and tabulated in Table (3) From this table one can see that the prevailing types of clouds are Cirrus (high level clouds) and stratocumulus (low level clouds). They represent about 39.35% and 38.86 % of the total cloud cover, respectively. At the same time, the occurrence percentages of both cumulus (1.96%) and cumulonimbus (0.65%) types are very small compared to stratocumulus and Cirrus

3.5.2.3 Clouds Transmission of UV-B Irradiation (T_c)

The clouds transmission (Tc) of UV-B irradiation is defined as the percentage between the UV-B irradiation at cloudy (UVBc) and cloudless (UVBo) sky conditions. Previous studies have focused empirical cloud relationships of transmission as a direct function of cloud cover (Bais et al., 1993; Blumthaler et al., 1996; Nemeth et al., 1996; Kuchinke et al., 1999; and Ilyas, 1987). The present study aims to examine this topic by producing detailed estimates of cloud transmission for UV-B irradiation at Qena atmosphere. To calculate the UV-Bo irradiation empirical formulas are developed between it and the length of its path in the atmosphere, expressed by solar zenith angle (Foyo–Moreno et al., 1999) at cloudless sky conditions. Fig. 11a relates the hourly values of UV-Bo radiation versus cos (θz) during the selective period (2001-2003). The increase of UV-Bo irradiation values with decreasing the solar zenith angle is obvious. It is possible to parameterize the dispersed data in Fig.11a by Fig.11b. The regression analysis of the maximum values of UV-Bo with solar zenith angle leads to the following empirical formula:

$$UV - B_0 = 4.506 \ (\cos \theta_z)^2 + 0.39 \cos \theta_z$$

With R =0.9855 (1)

The clouds transmissions of UV-B irradiation (Tc) was then calculated for different cloud cover amount C (Octas). It is concluded that the transmission of UV-B irradiation decrease as cloud cover increases. The average reduction in UV-B irradiation was about 27.7 % in case of 50 % cloud cover (4 Octas), while it was 45.7 % in case of cloud overcast condition (100 % clouds cover). Fig.12 represents the relation between Tc and cloud cover averaged over the whole study period. Regression analysis between the both parameters has been done using all the calculated data and forced to a transmission of 1 for conditions of no apparent cloud cover (i.e. C = 0). The following polynomial equation was found:

$$T_c = 0.0051 C^2 - 0.0948 C + 1 \quad (2)$$

As mentioned above in section 3.5.2.1 and 3.5.2.2, 77.9% of the sky conditions are cloudless and 39.35% of the observed clouds are cirrus (high level clouds). Consequently it has a weak effect on the incoming solar radiation and permits to large extent its transition to the earth's surface.

3.6 Empirical Relationships between UV&G, UV-B&G and UV-B&UV

Construction of the relationships between daily values of UV&G, UV-B&G and UV-B&UV has been started by plotting scatter diagrams between them, as shown in Fig. (13). Different regression formulas are tested for prediction the relationships between them. All these formulas provided quasi the same efficiency in describing these relationships (Table 4). The following linear relationships were considered in the study region:

$$UV = a_0 G + a \quad (3)$$

$$UV - B = b_0 G + b \quad (4)$$

$$UV - B = c_0 UV + c \quad (5)$$

The small variations in the value of Column ozone support the using of these relations. The linear relationship between ultraviolet and global irradiation has been found by many authors inside and outside Egypt particularly in the region of moderate to low G values (e.g. Koronakis et al., 2002; Ilyas et al., 1999; Trabea, 2006; Trabea and Salem, 2001; Robaa, 2004). The coefficients a_0, a, b_0, b, c_0 and c were determined using the known least mean square method using the daily dose data (Wh/m2). Values of these coefficients and their statistical analysis are given in Table (5). From this table one can see the following:

1. **The standard deviations (Sdv's.) of the calculated coefficients are too small value compared with the values of coefficients themselves, reflecting the good accuracy of the determination.**
2. **The large values of T-ratio reflect the good contribution and higher certainty of the coefficients. Also, the T-Value shows that slop parameters of fitting lines (a0, b0 and c0) have greater contributions, in fitting, than the intercept parameters (a, b and c).**
3. **The F- test is high compared to its critical value (254.3) which means that the calculated coefficients in the present equations have significant effects in the regression analysis.**
4. **The high values of R reflect the good fitting.**

Accordingly, the Eqs. (3, 4 and 5) become in the following form (must be changed to exponential equations)

$$UV = 0.0311G + 11.78 \quad (6)$$

$$UV - B = 0.0036G - 6.172 \quad (7)$$

$$UV - B = 0.113UV - 7.053 \quad (8)$$

These equations represent empirical models from which we can compute the ultraviolet irradiation intensity (UV & UV-B) during the day time if we have the values of global irradiation. It should be noted that these empirical equations should only be applied at Qena because total ozone amount, cloud types, aerosol content will be different at other sites in Egypt or other countries.

3.6.1 Model Verification

To check the efficiency of the above equations, they have been used to calculate UV and UV-B values over new period (Jan 2004 – Sep 2004). The relations between the calculated and measured values of UV and UV-B as well as the percentages of relative deviation errors of its calculated values from the measured ones are plotted in Figs. (14) and (15) for daily and monthly average dose, respectively.

From both the figures, it is clear that the empirical equations 6 and 7 provide best estimates for each of UV and UV-B irradiation either daily or monthly. It can be seen that the calculated values of both UV and UV-B are in an acceptable agreement with the measured data. Also, the majority of points of the relative deviation of the calculated daily UV and UV-B irradiation from the measured ones lie in the range up to ±10% and fewer points have values more than this percentage (fig. 14), while all the points lie in the range up to ±10% for average monthly values (fig. 15). In view of that, it is concluded that the constructed model is successful and useful to calculate the values of UV and UV-B irradiation with the aid of global irradiation records.

As a try to use Eq. 6 and 7 in calculating these parameters in other nearby locations, equation 6 has been used to calculate the daily and monthly mean of UV at Aswan / Upper Egypt, a city with similar weather conditions with the aid of available measurements of G during the same period (2001-2003). Comparing the calculated values (UVc) with measured ones (UVm), relations between them are illustrated in Fig. 16a, b. From this figure, it can be seen that the calculated values of UV solar irradiation are in a reasonable agreement with its measured ones whereas the ratio of UVc/UVm was about 0.8. This gives us the impression that the present deduced empirical relationship (Eq. 7) could be used also to a rough calculate the UV-B irradiation at Aswan with a sensible accuracy.

4- Conclusion

The study leads to the following important conclusions:

1. **A significant correlation between G and UV irradiation has been found, where both G and UV irradiation have similar pattern.**
2. **The average monthly daily doses of global and ultraviolet irradiation vary from month to month. The maximum values were recorded in Jun while the minimum ones were in December.**
3. **The mean ratio of UV/G was found (3.32 %), while UV-B/G was (0.25 %).These ratios point out for the small share of UV irradiation in the incoming G irradiation.**
4. **The transmission of UV-B decrease as cloud cover increases. The reduction in UV-B irradiation was about 27.7 % in case of 50 % cloud cover (4 Octas); while it was 45.7 % in case of cloud overcast conditions (100 % clouds cover). The relationship between the transmission of UV-B T_c and sky cloud cover C is expressed mathematically by**

$$T_c = 0.0051 C^2 - 0.0948 C + 1 .$$

5. **Good empirical relationships existed between each of UV-B and UV irradiation with global (G) irradiation which may help in the estimation of UV-B or UV using the available measurements of G irradiation.**
6. **Future study should include more attention on the effect of different parameters such as surface ozone, aerosol and cloud type on the UV irradiation reaching the earth's surface. This needs more precise data for long time.**

5- References

Bais A. F. Zerefos C.S., Meletie C., Ziomas I.C., Tourpali K., 1993. Spectral measurements of solar UV-B radiation and its relations to total ozone, So2 and clouds. J.Geophys.Res.98,5199-5204.

Biswas. A.K., 1979. The Ozone Layer. Vol. 4. Pergamon Press. Oxford.

Blumthaler M., Ambach W., Cede A., Staehelin J., 1996. Attenuation of erythemal effective irradiance by cloudiness at low and high altitude in the alpine region. Photochemistry and Photobiology, 63 (2), 193-196.

El-Metwally M., 2004. Simple new methods to estimate global solar irradiation based on meteorological data in Egypt. Atmospheric Research 69, 217–239.

Giese A. C., 1982. Living with our suns' ultraviolet rays, Plenum Press New York.

Ilyas M., 1987. Effect of cloudiness on solar ultraviolet radiation reaching the earth's surface. Atmospheric Environment 21, 1483-1484.

Ilyas M., Pandy A., Hassan S.I., 1999. UV-B radiation at Penang. Atmospheric Research 51, 141-152.

Koronakis P. S., Sfantos G.K., Paliatsos A.G., Kaldellis J.K., GarofalakisJ.E. and Koronaki I.P., 2002. Interrelations of UV-global/global/ diffuse solar irradiance components and UV- global attenuation on air pollution episode days in Athens, Greece. Atmospheric Environment 36, 3173- 3181.

Kuchinke C., and Nunez M., 1999. Cloud Transmission Estimates of UV-B Erythemal Irradiance. Theor. Appl. Climatology 63,149-161.

Mckenzie R.L., Blumthaler M., Booth C.R., Diaz S.B., Frederick J.E., Ito T., Madronich S., Seckmeyer G., 1995. Surface ultraviolet irradiation. In: Scientific Assessment of Ozone Depletion. WMO Global Ozone Research and Monitoring Project Report No. 37, 9, 1-9. 22.

Nemeth P., Toth Z., Nagy Z., 1996. Effect of weather conditions on UV-B irradiation reaching the earth's surface. J. Photochemistry and Photobiology 32 (3), 177-181.

Nunez M., Chen D., 1998. A comparison of cloudless sky erythemal ultraviolet irradiation at two sites in southwest Sweden. Int. J. Climatology 18, 915-930.

Parrish J.A., Rox Arderson R., Urbach F., Pitts D., 1978. UV-A. Plenum Press, New York.

Peak M. J. and Peak J. G., 1986. Molecular photobiology of UVA. Biological Effects of UVA Irradiation ed F Urbach and R W Gange (New York Praeger) pp 42-52.

Robaa S., M 2004. A study of ultraviolet solar irradiation at Cairo urban area, Egypt. Solar Energy77, 251-259

Robaa S.A., 1999. Impact of urbanization on meteorology and human comfort in Greater Cairo, Egypt. Ph.D. Thesis, Astronomy and Meteorology Department, Faculty of Science-Cairo University.

Shaltout. M.A., Ghonim. M.M., Trabea A.A., Allam H., 1994. Ultraviolet solar irradiation over Egypt. World Renewable Energy Congress–III, Reading Univ., UK 5 (2), 1506–1509.

Trabea A.A. and Shaltout M. A., 2000. Correlation of global solar radiation with meteorological parameters over Egypt, Renewable Energy, 21,297-308.

Trabea A. A., 2006. Erythemal Ultraviolet – B Radiation over Egypt. Egyptian Meteorological Authority – Meteorological Research Bulletin 21, 82-92.

Trabea A. A and Salem A. I., 2001. Empirical Relationship for Ultraviolet Solar Irradiation over Egypt, Egypt .J. Sol., 24, 123-132.

WMO 2003. Scientific Assessment of Ozone Depletion: 2002. Global Ozone Research and Monitoring Project. WMO Report 47, Geneva.

WMO 1990. Guide to Meteorological Observations Methods. Tn-8, Geneva, Switzerland, WMO Secretariat, Chapter 9, 925–932.

LIST OF TABLES

Table Captions

Table 1: Monthly variations in percentages (%) of UV/G; UV-B/G and UV-B/UV.

Table 2: Mean percentages of the cloud classes in different seasons in the study period.

Table 3: Seasonal percentages of the cloud types in the study period.

Table 4: Different regression formulas for describing the relations between UV&G and UV-B&G at the study region.

Table 5: Statistical analysis of the coefficients of the linear relationships between UV&G; UV-B&G and UV-B&UV.

Table 6: Comparison between the measured and calculated monthly average values of UV and UV-B radiation at Qena in a new period (Jan – Sep. 2004)

Table 1

Month	UV/G	UV-B/G	UV-B/UV
Jan.	3.47	0.20	5.87
Feb.	3.46	0.23	6.77
Mar.	3.40	0.25	7.43
Apr.	3.36	0.27	8.15
May	3.31	0.28	8.35
Jun.	3.25	0.29	8.97
Jul.	3.22	0.29	8.95
Aug.	3.21	0.29	8.92
Sep.	3.17	0.28	8.84
Oct.	3.25	0.25	7.63
Nov.	3.36	0.22	6.41
Dec.	3.34	0.20	5.92
Winter	3.40	0.21	6.15
Spring	3.35	0.27	8.00
Summer	3.21	0.29	9.01
Autumn	3.46	0.24	7.03
Mean	3.32	0.25	7.68

Table 2

Cloud Class	Cloud Condition	Cloud Cover (Octas)	Percentage (%)				
			Winter	Spring	Summer	Autumn	Whole Period
Class I	Cloudless Sky	0	62.7	67.6	94.8	79.9	77.9
Class II	Few clouds Sky	1- 3	22.4	16.0	5.2	13.6	13.1
Class III	Cloudy Sky	4 - 6	13.2	12.4	0.0	6.3	7.6
Class IV	Overcast	7 - 8	1.8	4.0	0.0	0.2	1.3

Table 3

Type	Percentage (%)				
	Whole Period	Winter	Spring	Summer	Autumn
Cirrus	39.35	35.70	32.04	45.71	43.93
Cirrostratus	6.04	4.74	14.99	2.14	2.31
Altostratus	2.94	9.17	2.58	0.00	0.00
Altocumulus	10.21	5.40	12.40	8.57	14.45
Stratocumulus	38.86	41.43	32.56	42.14	39.31
Cumulus	1.96	3.57	2.84	1.43	0.00
Cumulonimbus	0.65	0.00	2.58	0.00	0.00

Table 4

Variables	Equations	R2	Corr
UV & G	UV= 0.0311G + 11.785	0.977	0.988
	UV = 0.0328G	0.974	0.986
	UV = -3E-07G2 + 0.035G	0.940	0.969
	UV = 9E-07G2 + 0.0196G + 46.145	0.962	0.980
	UV = 0.0558G0.9398	0.975	0.987
	UV = 73.329e0.0002G	0.961	0.980
UV-B & G	UV-B = 0.0036G - 6.1723	0.958	0.978
	UV-B = 0.0027G	0.890	0.943
	UV-B = 2E-07G2 + 0.0015G	0.932	0.965
	UV-B = 1E-07G2 + 0.002G - 1.4117	0.939	0.969
	UV-B = 5E-05G1.4406	0.956	0.977
	UV-B = 3.2225exp0.0002G	0.944	0.971

Table 5

Variables	Coefficients		Sdv.	T- ratio	F-test	F-critical	R2	Corr
UV & G	ao	0.0311	0.0002	203.95	41594.62	254.314	0.98	0.99
	a1	11.785	0.98	11.96				
UV-B & G	bo	0.0036	0.00002	147.81	21849.01		0.96	0.99
	b1	- 6.1723	0.1569	-39.34				
UV-B & UV	co	0.1134	0.001	111.83	12505.02		0.93	0.96
	c1	- 7.0536	0.2153	-32.76				

Table 6

Month	Ultraviolet Irradiation (Wh/m2)					Ultraviolet-B Irradiation (Wh/m2)				
	UVm	UVc	RMSE	MBE	MAE	UV-Bm	UV-Bc	RMSE	MBE	MAE
Jan.	134.91	133.04	0.54	0.16	0.16	7.28	7.86	0.17	-0.05	0.05
Mar.	217.36	210.50	1.98	0.57	0.57	16.91	16.83	0.02	0.01	0.01
Apr.	239.80	227.64	3.51	1.01	1.01	19.63	18.81	0.23	0.07	0.07
May	264.51	240.78	6.85	1.98	1.98	22.08	20.33	0.50	0.15	0.15
Jun.	273.03	255.74	4.99	1.44	1.44	23.69	22.07	0.47	0.14	0.14
Jul.	261.43	246.70	4.25	1.23	1.23	22.40	21.02	0.40	0.12	0.12
Aug.	247.61	236.59	3.18	0.92	0.92	21.18	19.85	0.38	0.11	0.11
Sep.	234.06	212.92	6.10	1.76	1.76	18.19	17.11	0.31	0.09	0.09

List of Figures Captions

Fig. 1: Map of the study area

Fig. 2: Variations of the average hourly global solar irradiation (HG) in Wh/m2 through the period (2001-2003).

Fig. 3: Variations of the average monthly of daily global solar irradiation (MDG) in Wh/m2 through the period (2001-2003).

Fig. 4: Variations of the average seasonally of daily global solar irradiation (SDG) in Wh/m2 through the period (2001-2003).

Fig. 5: Variations of the average hourly ultraviolet irradiation (HUV&HUV-B) in Wh/m2 through the period (2001-2003).

(a) HUV (b) HUV-B

Fig. 6: Variations of the average monthly of daily ultraviolet solar irradiation (MDUV&MDUV-B) in Wh/m2 through the period (2001-2003).

(a) MDUV (b) MDUV-B

Fig. 7: Variations of the average seasonally of daily ultraviolet solar irradiation (SDUV&SDUV-B)) in Wh/m2 through the period (2001-2003).

(a) SDUV (b) SDUV-B

Fig. 8: Daily average values of Global solar irradiation at different locations in Egypt in the period (2001-2003).

Fig. 9: Monthly variations of ultraviolet solar irradiation at different locations in Egypt in the period (2001-2003).

Fig.10: Diurnal variations of UV-B irradiation (Wh/m2) and Solar Zenith angles (deg) in different seasons in the period (2001-2003).

Fig.11: Variation of UV-B0 versus the solar zenith angle.

Fig.12: Relation between clouds transmission (Tc) and cloud cover (Octas) averaged over the study period (2001-2003).

Fig.13: Scatter diagrams between daily UV&G, UV-B&G, and UV-B&UV.

Fig.14: Comparison between the calculated and measured daily averages of UV and UV-B as well as the relative deviations errors of their calculated values from their measured ones (%) at the period (Jan 2004 – Sep 2004).

Fig.15: Comparison between the calculated and measured monthly averages of UV and UV-B as well as the relative deviations errors of their calculated values from their measured ones (%) (Jan 2004 – Sep 2004).

Fig.16: Comparison between measured values of ultraviolet solar irradiation (UVm) at Aswan with that calculated (UVc) using global irradiation measurements applying eq. 6.

(a) Daily (b) Monthly

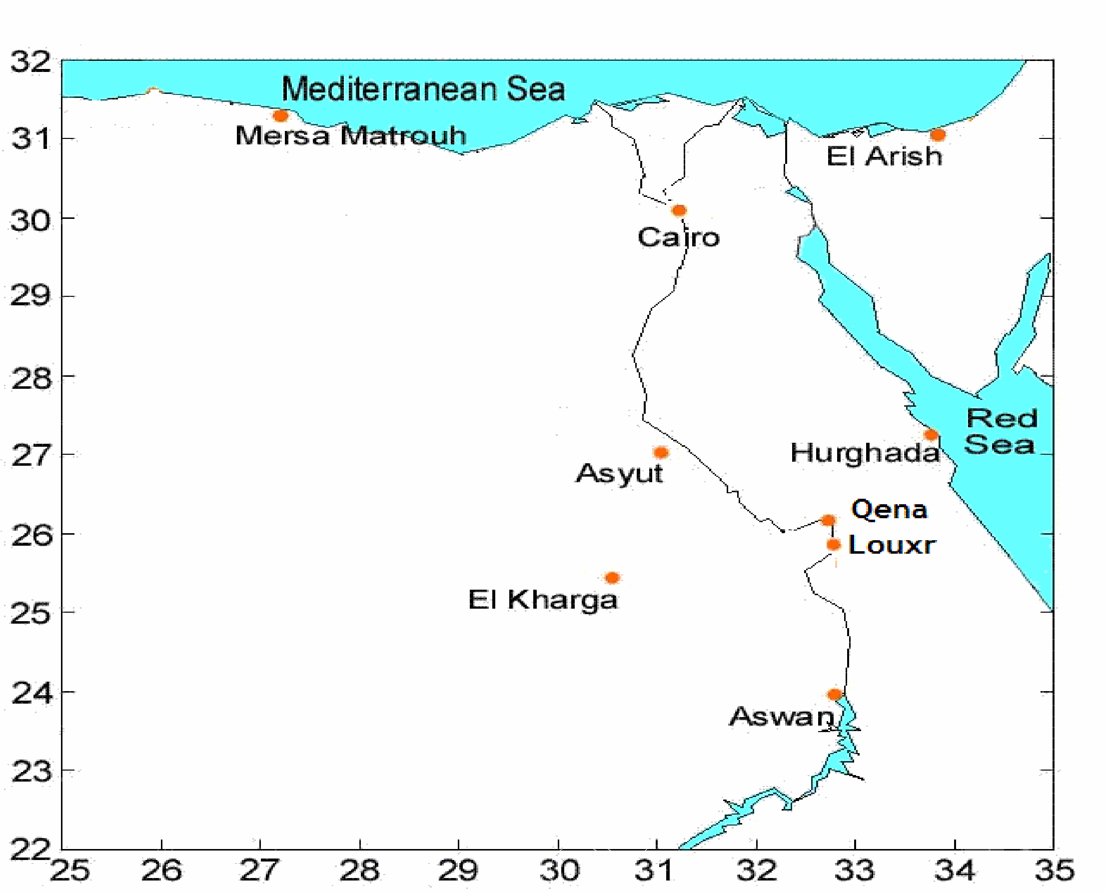
Mediterranean Sea
Mersa Matrouh
El Arish
Cairo
Red Sea
Hurghada
Asyut
Qena
Louxr
El Kharga
Aswan
32
31
30
29
28
27
26
25
24
23
22
25
26
27
28
29
30
31
32
33
34
35

Fig. 1

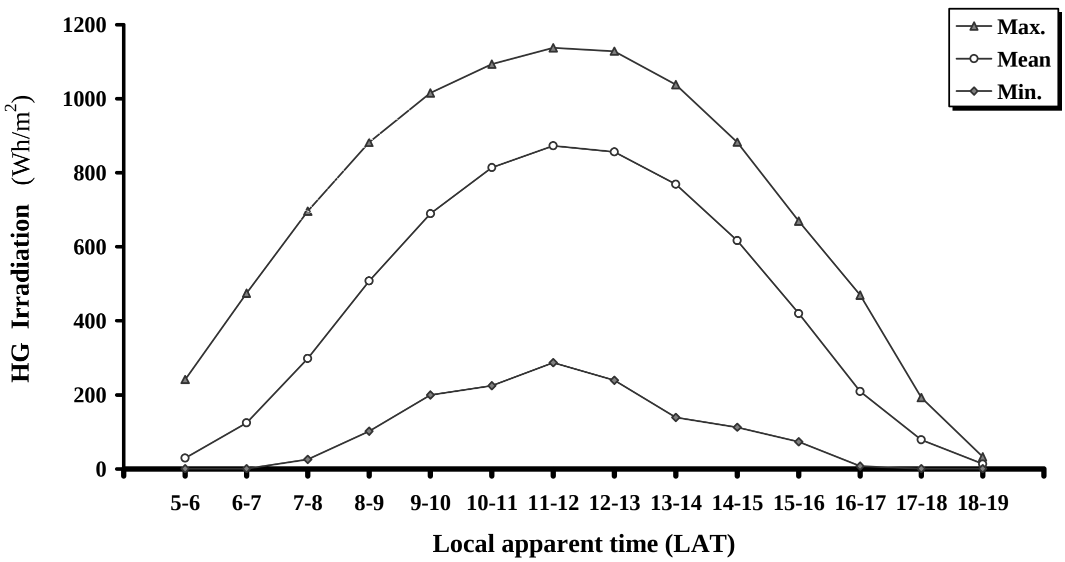
Max.
Mean
Min.
HG Irradiation (Wh/m2)
1200
1000
800
600
400
200
0
5-6
6-7
7-8
8-9
9-10
10-11
11-12
12-13
13-14
14-15
15-16
16-17
17-18
18-19
Local apparent time (LAT)

Fig. 2

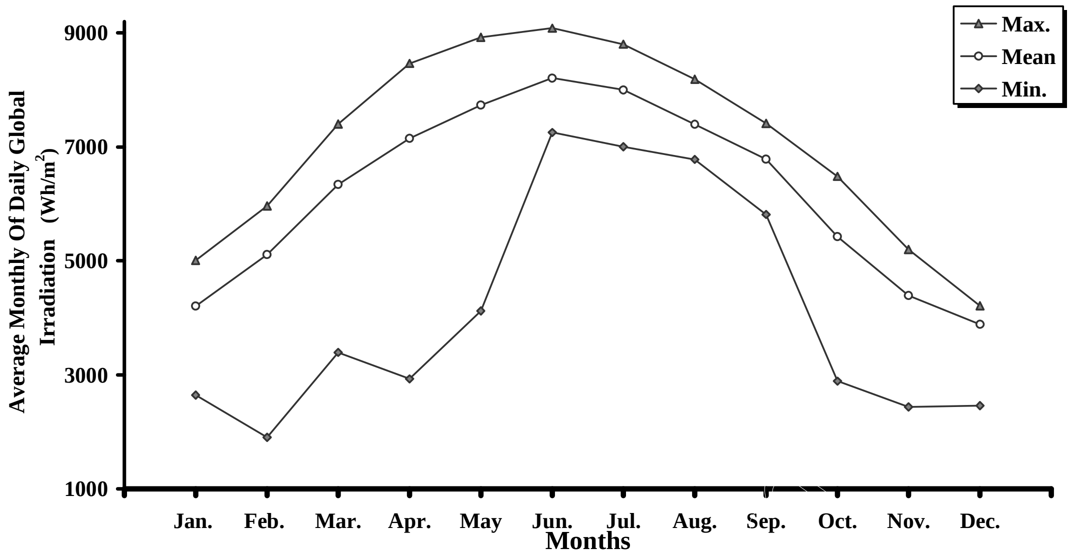
Max.
Mean
Min.
Average Monthly Of Daily Global Irradiation (Wh/m2)
9000
7000
5000
3000
1000
Jan.
Feb.
Mar.
Apr.
May
Jun.
Jul.
Aug.
Sep.
Oct.
Nov.
Dec.
Months

Fig. 3

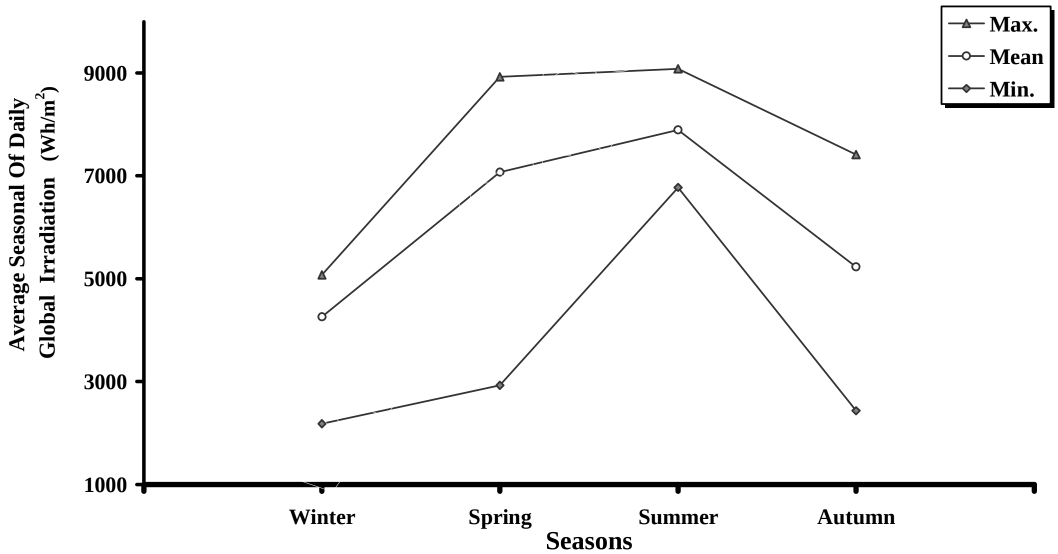
Max.
Mean
Min.
Average Seasonal Of Daily Global Irradiation (Wh/m2)
9000
7000
5000
3000
1000
Winter
Spring
Summer
Autumn
Seasons

Fig. 4

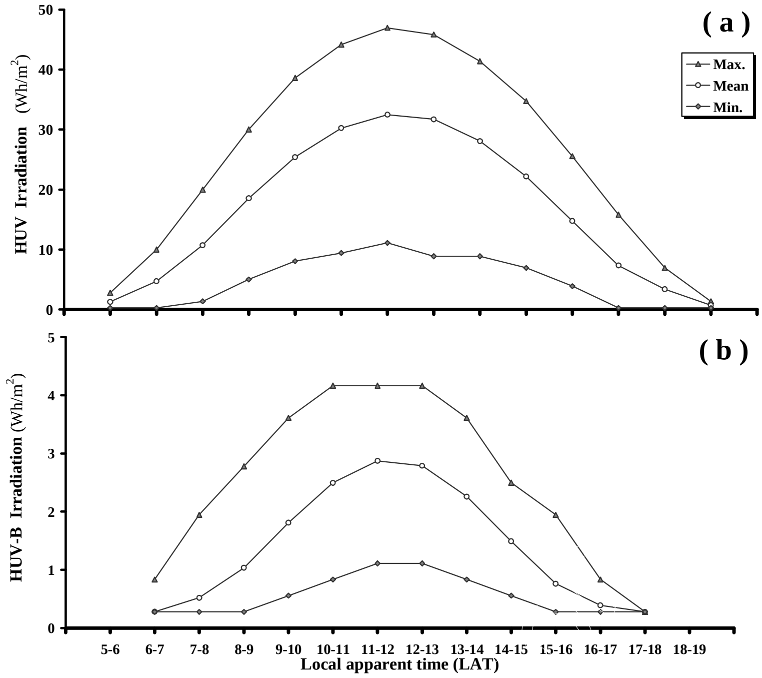
(a)
Max.
Mean
Min.
HUV Irradiation (Wh/m2)
0
10
20
30
40
50
(b)
HUV-B Irradiation (Wh/m2)
0
1
2
3
4
5
5-6
6-7
7-8
8-9
9-10
10-11
11-12
12-13
13-14
14-15
15-16
16-17
17-18
18-19
Local apparent time (LAT)

Fig. 5

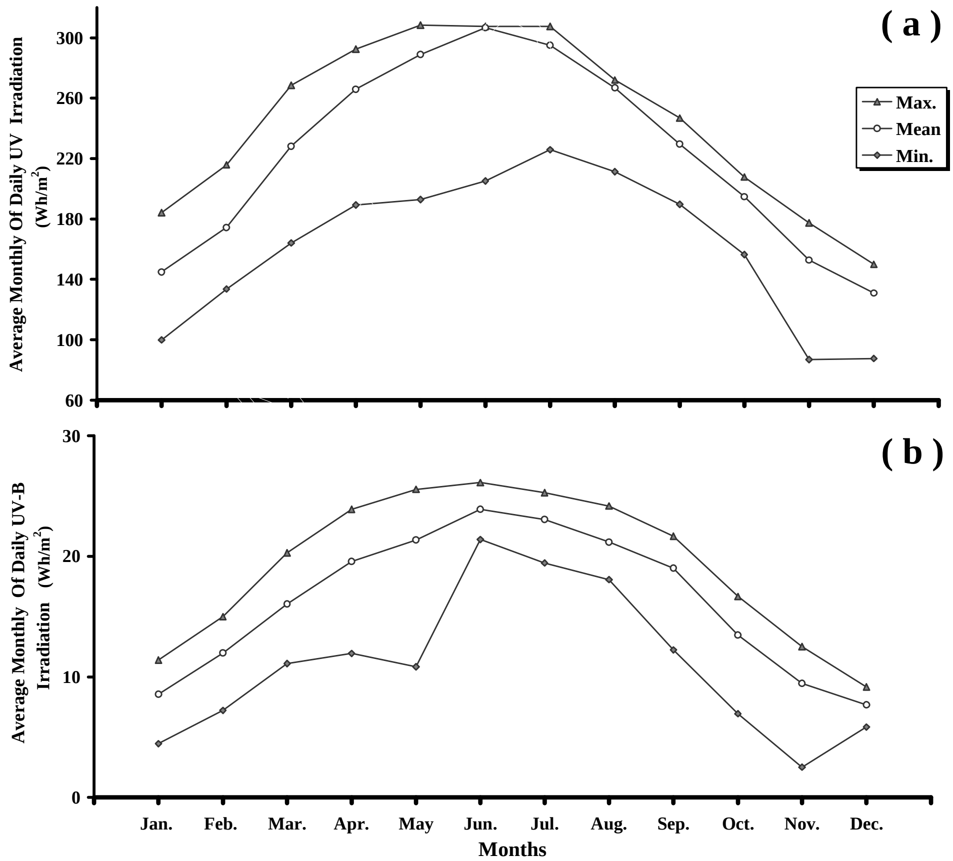
(a)
Max.
Mean
Min.
Average Monthly Of Daily UV Irradiation (Wh/m2)
60
100
140
180
220
260
300
(b)
Average Monthly Of Daily UV-B Irradiation (Wh/m2)
0
10
20
30
Jan.
Feb.
Mar.
Apr.
May
Jun.
Jul.
Aug.
Sep.
Oct.
Nov.
Dec.
Months

Fig. 6

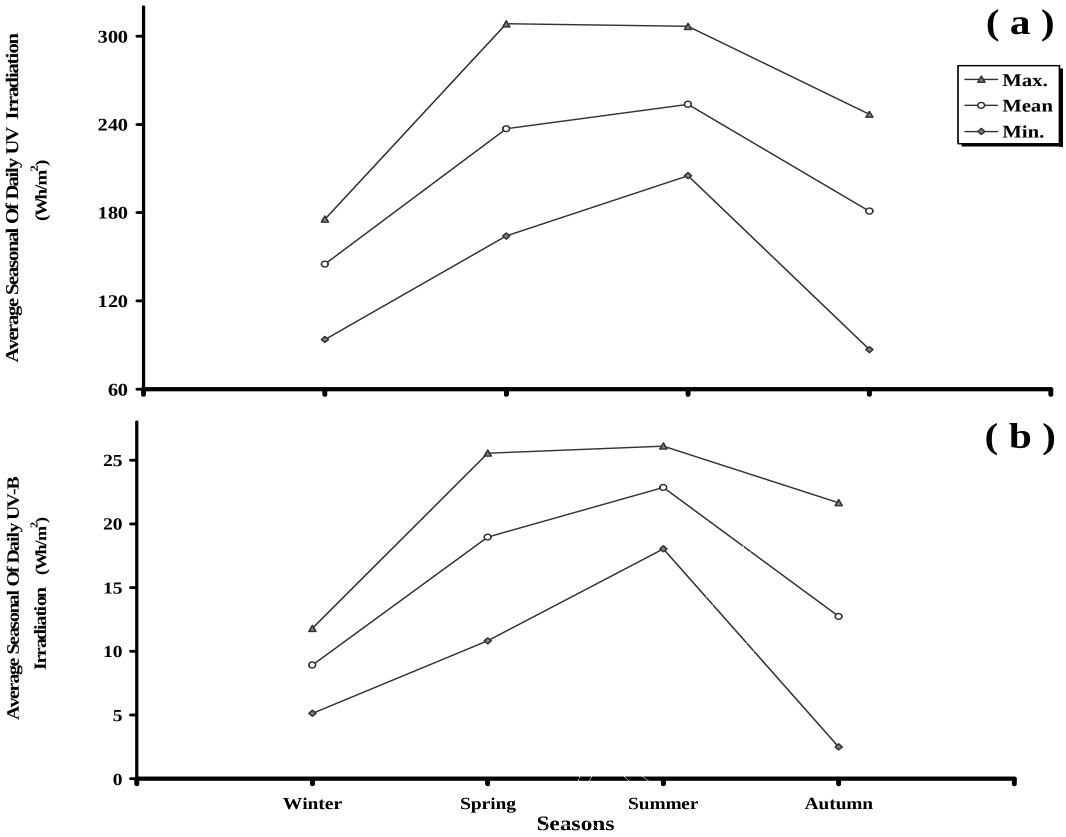
(a)
Max.
Mean
Min.
Average Seasonal Of Daily UV Irradiation (Wh/m^2)
300
240
180
120
60
(b)
Average Seasonal Of Daily UV-B Irradiation (Wh/m^2)
25
20
15
10
5
0
Winter
Spring
Summer
Autumn
Seasons

Fig. 7

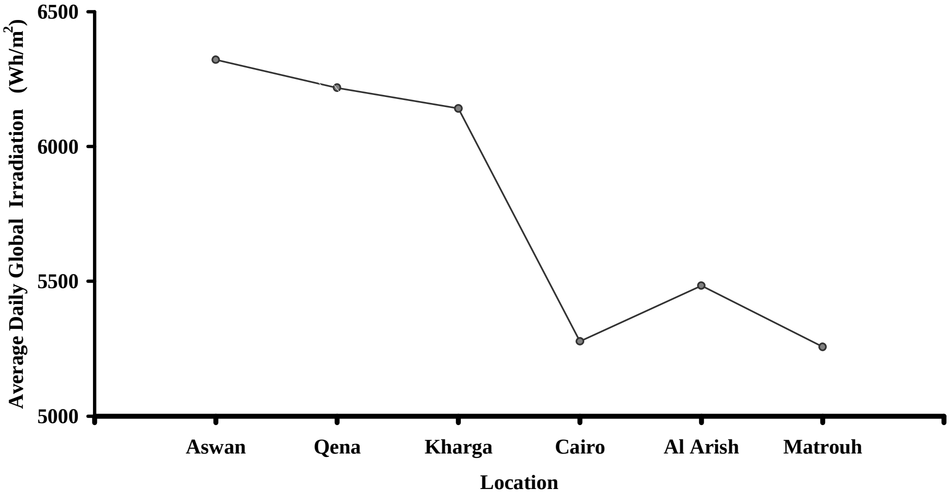
Average Daily Global Irradiation (Wh/m^2)
6500
6000
5500
5000
Aswan
Qena
Kharga
Cairo
Al Arish
Matrouh
Location

Fig. 8

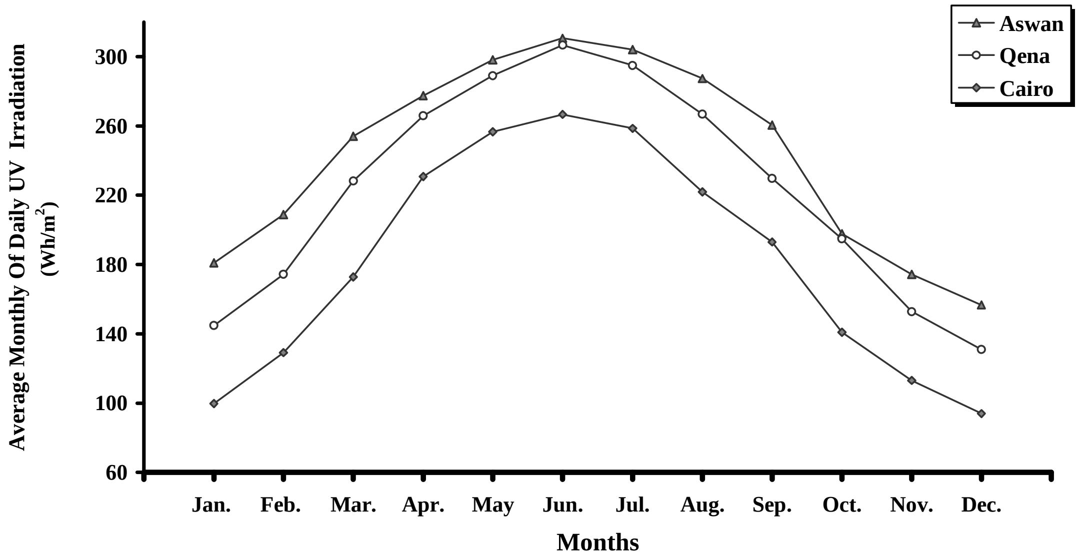

Fig. 9

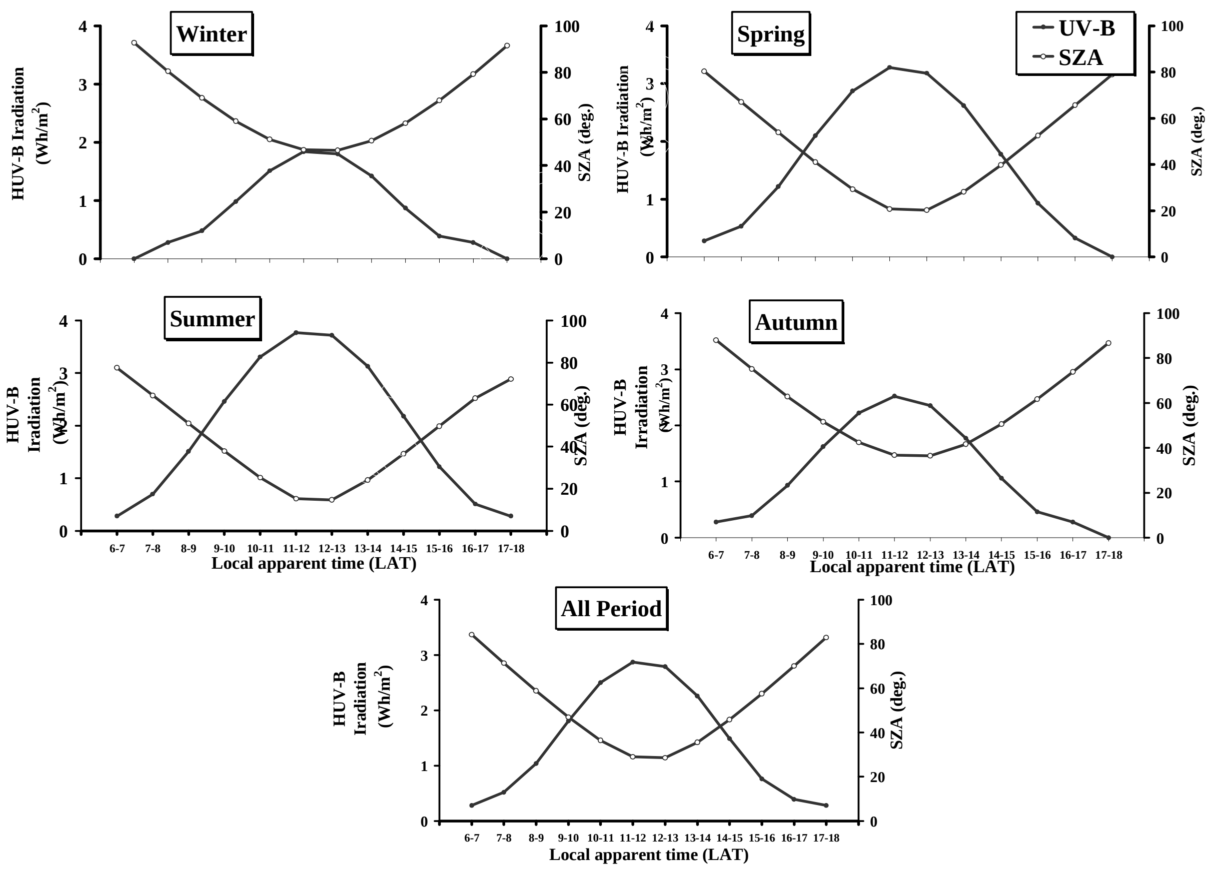

Figure (10)

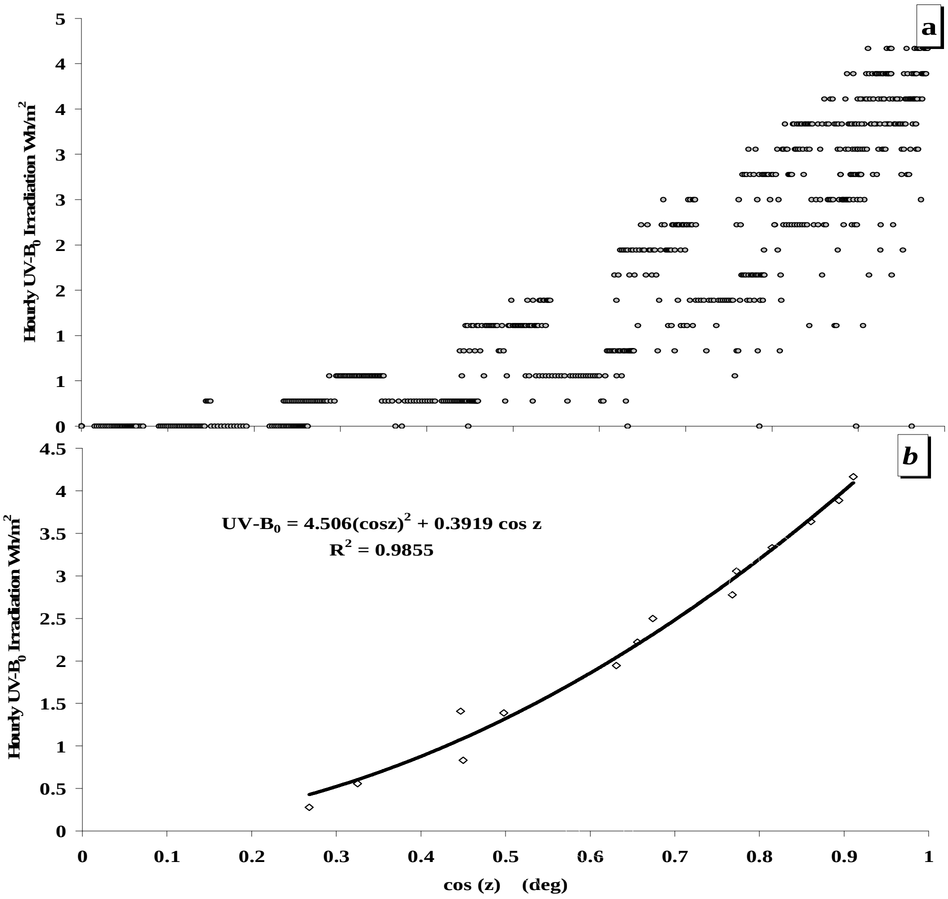

Figure (11)

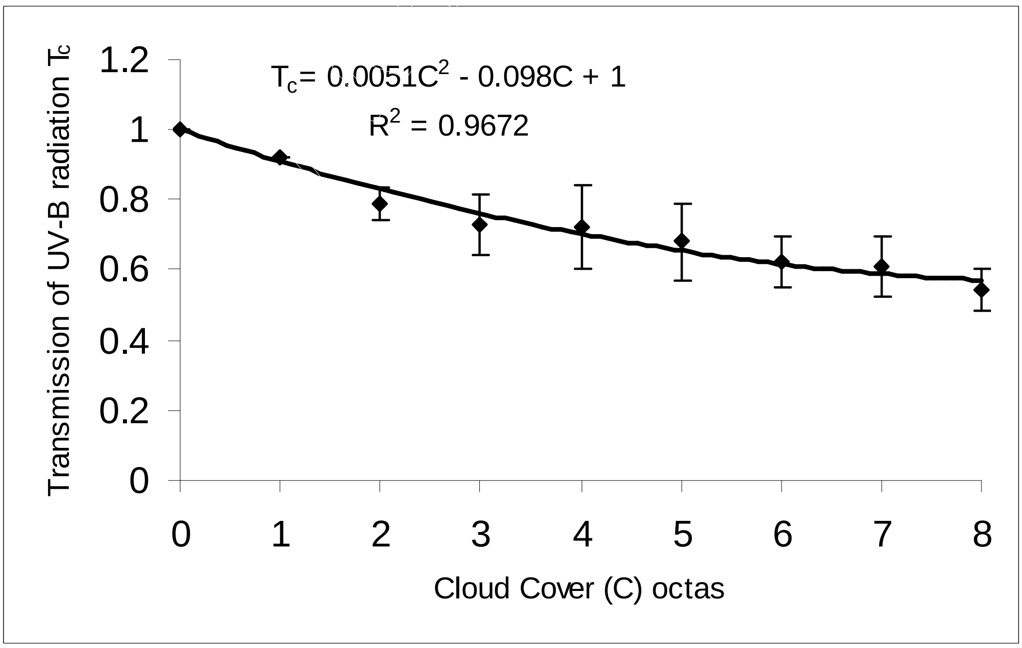

Fig. 12

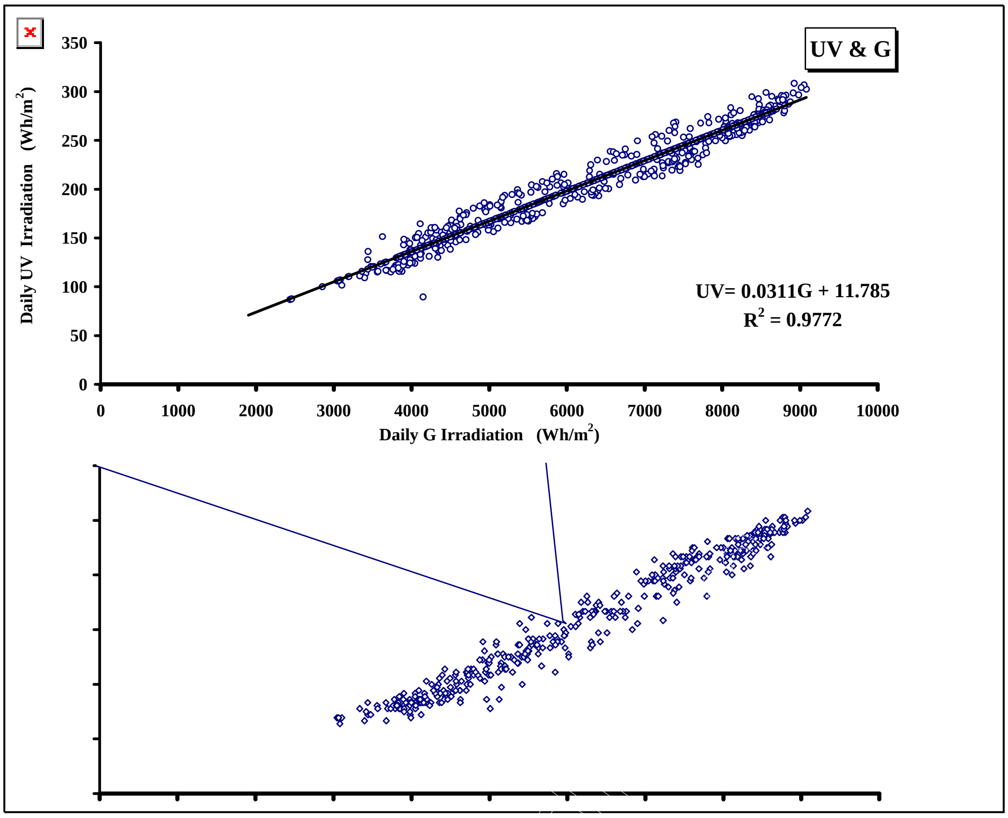

Fig. 13

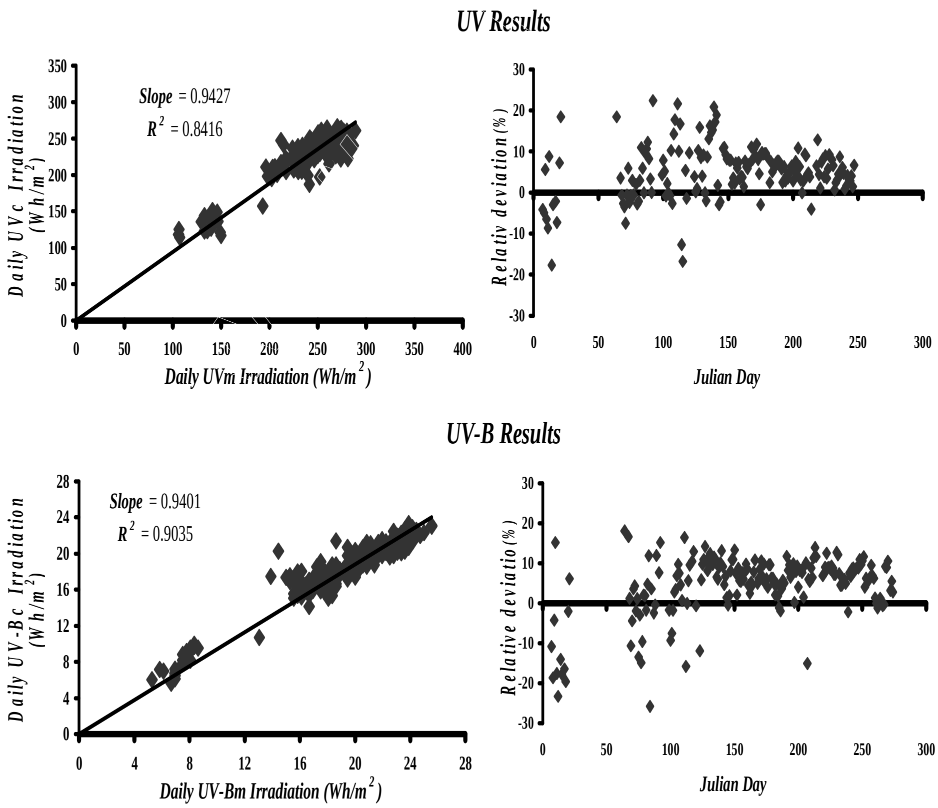

Figure (14)

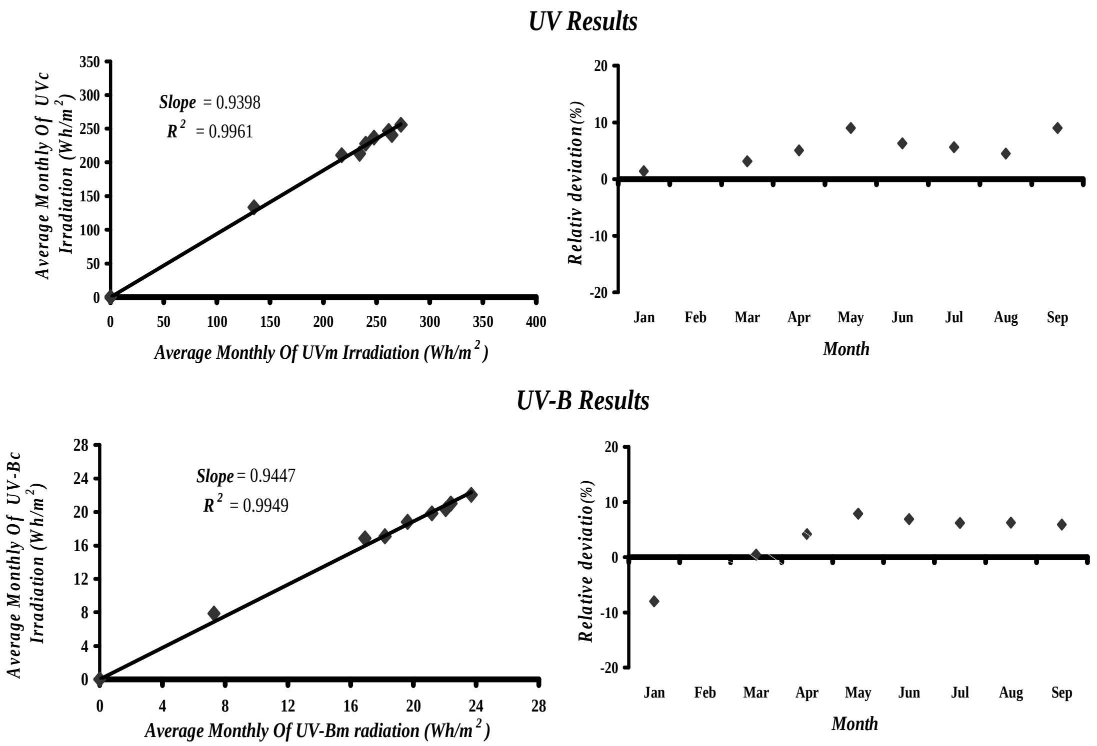

Figure (15)

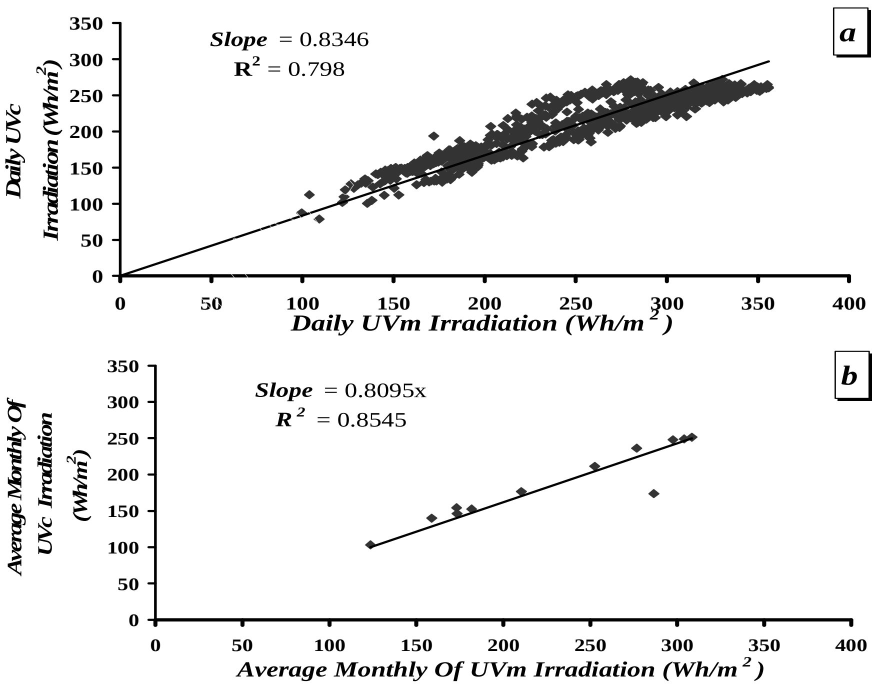

Figure (16)

الملخص العربي

فى هذا البحث تم دراسة وتحليل تغيرات كلا من كمية الاشعاع الشمسى الكلى (G) والأشعة الفوق بنفسجىة(UV) الساقطة على مدينة قنا فى الفترة ما بين ٢٠٠١ .دور بعض العوامل التى تؤثر فى تغير كمية الأشعاع الساقط مثل زاوية السمت وكمية السحب قد أخذت فى الأعتبار عند الدراسة. كما تم وضع العلاقة بين كمية الأشعاع الشمسى الكلى وكمية الأشعة الفوق بنفسجية فى أطار معادلة وضعية .

الدراس تشير الى أن: ((UV-B/G = 0.25 %) (UV/G =3.32% وان هناك ارتباط قوى بين كمية الاشعاع الشمسى الكلى (G) والأشعة الفوق بنفسجىة(UV) .

Diurnal and seasonal variations of surface ozone in Cairo and Alexandria, Egypt.

Kassem, Kh. O; S. M. Elshazly; Masaaki Takahashi
*: M. EL-Nouby Adam: A. A. Hassan:A. A. Emad
Department of Physics, Faculty of science at Qena, South Valley University, Qena, Egypt.
*** Center for climate system research, the university of Tokyo , Japan.**

Abstract:

Diurnal and seasonal variations of surface ozone have been studied in Cairo and Alexandria, Egypt, during the period 2001-2003. Diurnal variation of surface ozone in Cairo is characterized by high values in afternoon and low values at night and early morning hours. This behavior reflects photochemical production and consumption of surface ozone. In Alexandria, diurnal variation of surface ozone is characterized by negligible fluctuation. It represents background station. Summer season values of surface ozone are higher than that in winter season in the two cities. Surface ozone diurnal variation shows positive correlation with that of temperature and negative correlation with that of relative humidity in Cairo. In Alexandria, these correlations are not so clear. Analysis of autocorrelation function for the hourly average values of surface ozone in Cairo and Alexandria has been done. The results indicate that transported ozone is more effective in Alexandria than that in Cairo and in winter than that in summer in both cities.

1. Introduction

Ozone is found in the two lower parts of the atmosphere, about 90% of its concentration is found in the stratosphere and the remained 10% is found in the troposphere. Surface ozone is a secondary pollutant formed in the lower troposphere through the photochemical reactions of nitrogen oxides NOx (NO + NO2) and volatile organic compounds VOCs with the presens of solar radiation (Angle et al, 1989; Cheng et al, 1997; Solomon et al, 2000).

The ozone concentration changes near the ground depend on many agents, mainly on NOx concentration, temperature, solar radiation, wind velocity and direction [Warneck, P. (1987), Guicherit R. (1988)].

High values of surface ozone concentrations are known to have adverse health effects. (Mauzerall et al, 2001; Dorion et al., 2000). Where, It can irritate the respiratory system, causing coughing, threat irritation, and an uncomfortable sensation in the chest. Also, it can aggravate asthma (U. S. Environmental Protection Agency (Jul 27th, 2004) Web document URL: http://www.epa.gov/airnow/). Within the lung itself, there is damage to the ciliated cells (Griffin, 2007). As well as it can cause significant damage to agricultural crops. (Fumagalli et al, 2001 ; Heck et al, 1983, Mauzerall et al, 2001; and Heath, 1994: Britvec et al 2001). The high reactivity of ozone causes it to react with walls and contents of buildings.

In the present work, an attempt is made to give an account about atmospheric pollution with respect to surface ozone in two cities in Egypt, Cairo and Alexandria, during winter and summer seasons of the period 2001-2003. In this direction, the followings have been done:

1- **Comparison between diurnal and seasonal variations of O_3 values in the two cities to investigate the characteristics of the two cities with different nature.**
2- **Analysis of autocorrelation function for the hourly values of O_3 in the two cities to investigate the effect of transported ozone on the measured values.**

2. Meteorology and data collection

Egypt is located in the northeast of Africa (Figure 1). The warmest period in the year can be occurred in June and July. While the coolest month is generally January. Precipitation concentrated

mainly in the north coast during winter and autumn seasons. It varies from 25-50 mm in January to 10 mm in October with total annual value of about 194 mm in Alexandria.

The annual sunshine amount in the north coast varies from relatively low value in winter, about 150-200 h in January, to higher amount in summer, about 350 h in July. While, South of Egypt enjoys about 400 h in July. (Martyn, 1992)

Cairo city (30.10^o N, 31.29^o E, 34 m) is located north of Egypt, about 120 km south of the Mediterranean Sea coast, between two hills of about 200 m height forming a valley through which the Nile River flows. The valley may affect the prevailing northerly wind by channeling it along the north south axis (Gusten et al, 1994). The total area of the city is about 250 km^2. The meteorological situation of Cairo is largely determined by the vast surrounding desert; the west and the east deserts. Cairo city is highly populated; its inhabitances are more than 15 millions. About 52% of the industries and about 40% of electrical power stations in Egypt are found in it (Khoder, 2007). It characterized with narrow streets and high buildings, more than 1.5 million cars with the industrial regions represent the main sources of air pollution.

Alexandria 31.21^o N & 29.92^o E is a costal city located in the north west of the delta. Its population is about 5 millions people. It represents the main port and the second industrial city in Egypt.

Fig.(1): Map of Egypt

In Cairo and Alexandria, the data have been monitored by Egyptian Environmental Affairs Agency, Environmental Information & Monitoring Program EEAA-EIMP during the period 2001-2003. In Cairo we used data of O_3 values in El Abbassyia station, which is located at one of the buildings of the Meteorological Authority near Abbassyia. Instruments are located in a shelter on the top of 3 floors building. Air intake is 1m from the wall, about 16-m above the street level. The area is considered as regional residential area. It is normally up-wind from Cairo city center, but down-wind from the Shoubra industrial area and Shoubra urban area. In addition to regionally exposed, it is influenced by local automobile exhausts as main local source of air pollution. So, this station is considered as representative for regional urban area. O_3 is measured by UV-Photometric Absorption instrument model TEL M 49 C. Meteorological parameters are measured by Automatic Weather Station (AWS).

In Alexandria, The monitoring station is located in a small shelter on the top of 7 floors building in Alexandria university. There are local sources of air pollution represented in some traffic but the station is high above the street, emissions have no great effect on the measured O_3. This station represents background ozone. O_3 is measured by UV-Photometric Absorption instrument model TEL M 49 C; air intake is about 30 m above the ground. Meteorological parameters are measured by automatic weather station.

3. Results and discussion

3.1. Diurnal and seasonal variation of surface ozone

Figure (2) represents diurnal variation of O_3 in Cairo during winter and summer seasons in the period 2001-2003. Upper and lower pares of the rectangle represent third and first quartiles(q_3 and q_1), respectively.

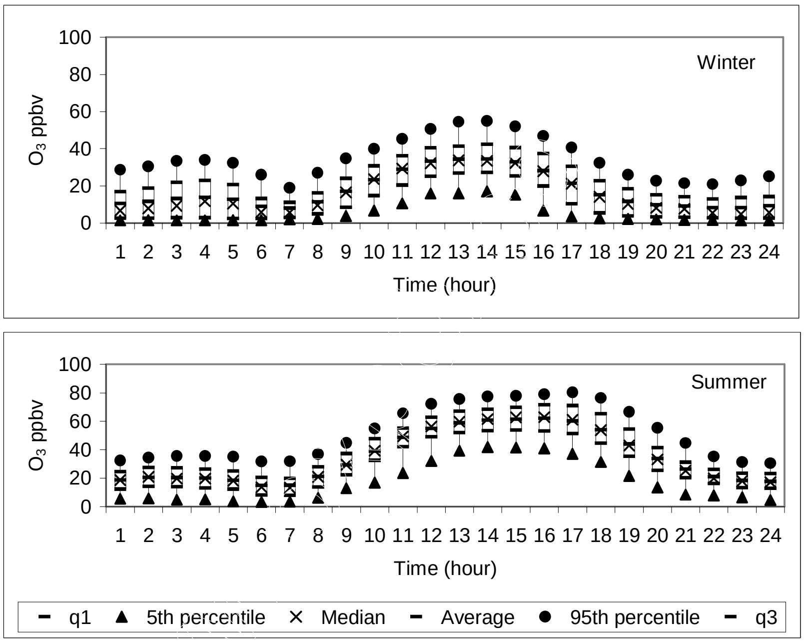

Fig.(2): Diurnal variations of O_3 (ppbv) in Cairo during winter and summer seasons of the period 2001-2003.

From the figure we can conclude the following:

(i) In general, O_3 diurnal variation has the same pattern in the two seasons: Relatively low average values during night hours and relatively high average values during day-light hours are observed. This behavior is common in the urban atmospheres and reflects the dominant titration of O_3 (reaction 3) during night hours due to increased values of NO concentration as a result of nocturnal inversion. While during day light hours, increased values of O_3 is resulted from dominant photochemical generation (reaction 2), as well as O_3 transport from the residual layer, which maintains the same O_3 concentration as in the well mixed layer air, after the disappearance of the nocturnal boundary layer (El-Hussainy et al, 2003).

Ozone is produced by photolysis of Nitrogen dioxide NO_2:

$$NO_2 + h\nu \rightarrow NO + O \qquad \rightarrow 1$$

The oxygen atom (O) rapidly recombines with molecular oxygen (O_2) to produce (O_3).

$$O_2 + O + M \rightarrow O_3 + M \qquad \rightarrow 2$$

Where, M is a third molecule such as N2 for stabilization of the reaction.

Normally, reaction (1-1) is counterbalanced by the reaction of NO with ozone:

$$NO + O_3 \rightarrow NO_2 + O_2 \qquad \rightarrow 3$$

(ii) The maximum average value during winter season occurs after noon at 13 and 14 hrs (34 ppbv). Time of maximum value delays in summer season in comparison with the case during winter season, where it occurs at 16 hr in summer with a value 62 ppbv. This phenomena may be a result of increased values of solar radiation intensities during summer as well as the long sunshine duration.

(iii) Minimum values of O_3 (8 ppbv) occur at morning and midnight at the hrs 7, 22, 23 in winter. During summer season, these values occur at morning hours with 15 ppbv at 6 and 7 hrs. This may be a result of corresponding increased values of NOx during both morning and night hours as a result of increased traffic intensities at morning hours as well as the decreased values of mixed layer during both night and morning hours.

(iv) O_3 patterns during winter has lower values than that during summer season. This may attributed to: firstly the relatively high values of NOx during winter season in comparison with its values during summer season. Secondly, relatively low values of solar radiation during winter in comparison with its values during summer. The last two factors may lead to low generation process during day light hours and more titration process during night hours.

(v) Seasonal average values vary from 17 ppbv during winter to 35 ppbv during summer season. This may be resulted from the relatively high photochemical production during summer season as a result of more solar radiation intensities, and increased values of mixing height, as well as less values of NOx concentration in comparison with the case during winter season.

Figure (3) represents diurnal variation of O_3 in Alexandria during winter and summer seasons in the same period. The following can be concluded:

(i) In general, O_3 diurnal variation has the same pattern in the two seasons: Low diurnal variation during the two seasons has been observed. This may be attributed to the low generation process of O_3 during day-light hours and low destruction process during night hours. Low generation process during day-light hours is owing to low temperature and high relative humidity, where, maximum average temperatures not exceed 19, 28 ^oC during winter and summer respectively. Also average values of relative humidity are not less than 75%, 83%, during winter and summer respectively. Low destruction of O_3 during night hours may be resulted of the relatively strong winds (of the dominant north west and western winds) that may disturb the vertical stability and may account for O_3 uniform diurnal profile in all seasons and the expected transported O_3 within these wind sectors from west Europe.

(ii) Seasonal average values of O_3 vary from 22 ppbv during winter to 35 ppbv during summer season, respectively. The relatively low seasonal averages during winter season may be attributed to the relatively low received solar intensities during this season in comparison with the case in summer season.

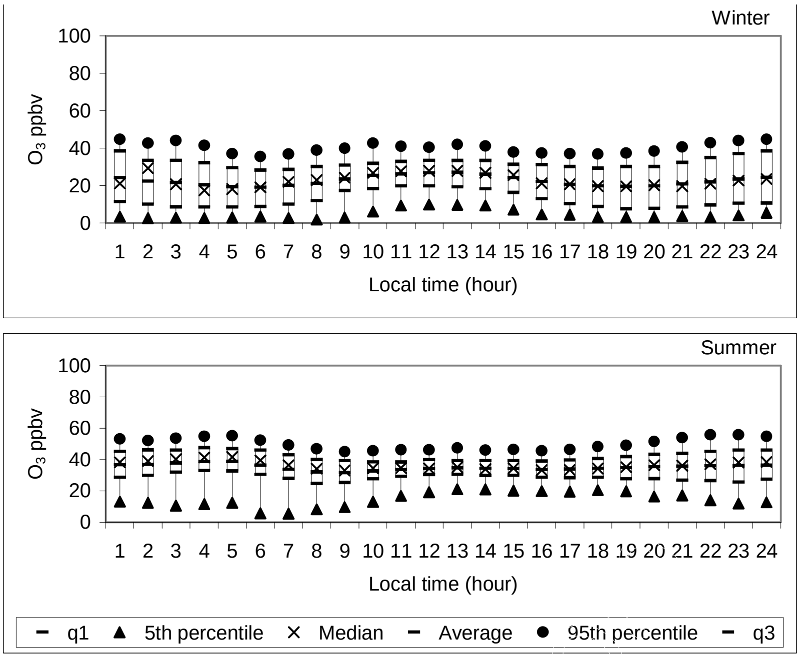

Fig. (3): Diurnal variation of O_3 (ppbv) in Alexandria during winter and summer seasons of the period 2001-2003.

3.2. Analysis of Autocorrelation Function

Figure (4) illustrates the autocorrelation function for the hourly surface O_3 values in Cairo and Alexandria during winter and summer seasons in the period 2001-2003. The following can be concluded:

There is no complete periodicity in the autocorrelation function within 24 hours, where, Autocorrelation function values decreased after 24 hours to be 0.74 and 0.87 in winter and summer, respectively in Cairo. While it decreased to be 0.51 and 0.60 in winter and summer, respectively in Alexandria.

This result leads us to suggest that there may be portions of surface O3 has been transported (Klasinc et al, 1996) to the two cities and that these portions are more effective in Alexandria than that in Cairo, and in winter than that in summer in the two cities. Transported O3 is mainly coming from the northern and northwestern wind sectors as will be illustrated in details in another contribution using air mass trajectory analysis

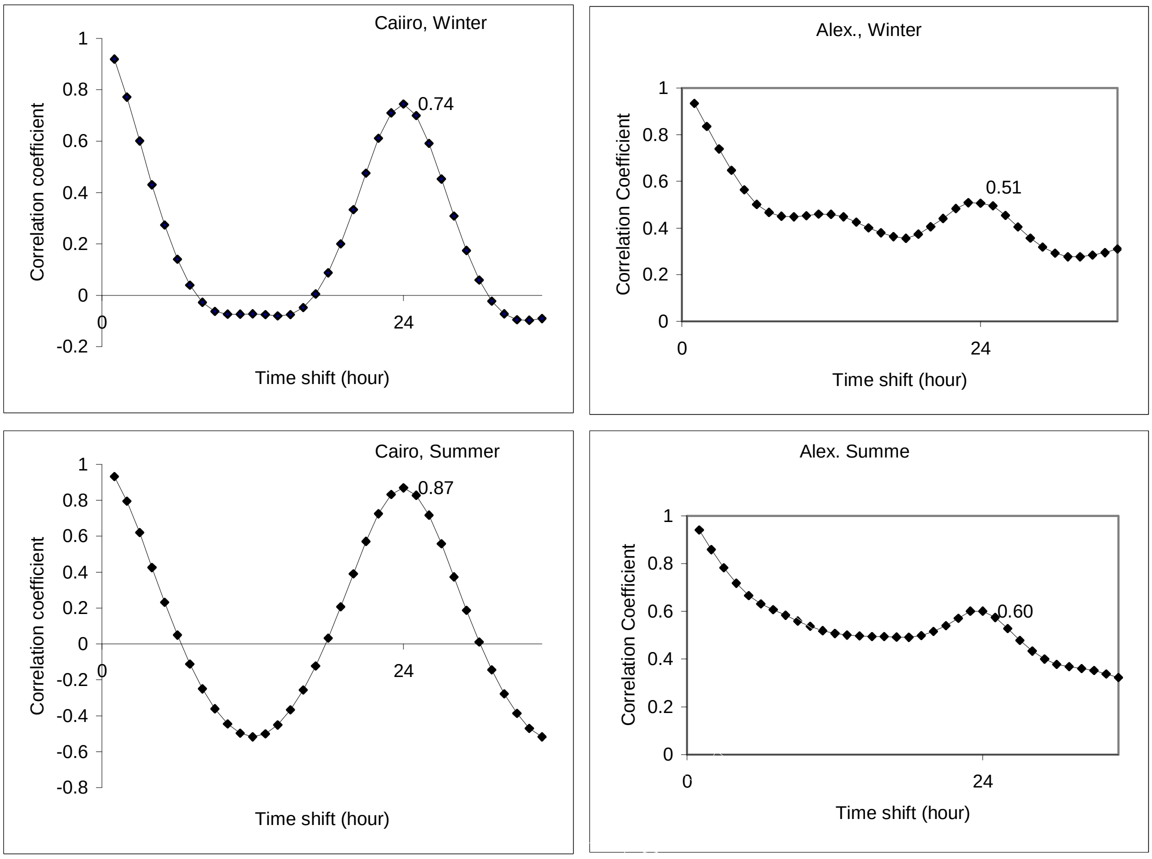

Fig. (4): Autocorrelation function for surface ozone in Cairo and Alexandria during winter and summer seasons of the period 2001-2003.

3.3. Effect of relative humidity (RH) and temperature (T)

a) In Cairo

Figure (5, A) illustrates diurnal variation of O_3 ppbv, T ^oC and RH % during winter and summer seasons in Cairo. We can notice that:

(i) Diurnal variation of T is approximately in similar to that of O_3 especially during summer season. Minimum average values of T (12 ^0C) occur at morning at the time period 5-6 hrs during winter. This value increased to (25 ^0C) at the hour (6) during summer season.

(ii) Maximum average values (24 ^oC) occurred afternoon at 13-15 hrs during winter. While this value increased to (39 ^0C) at (14-16 hrs) during summer season. The correlation coefficient between daily average values of temperature and global solar radiation in Cairo during the period 2001-2002 was 0.77. So T may be considered as an indicator of the intensity of solar radiation. It is well known that high value of T encourages the photo-oxidation processes leading to the highest value of O_3. The photochemical response driven to change in temperature is driven by several factors, including the reaction rate of Peroxy-Acetyl Nitrate (PAN), the emission rate of biogenic VOC, photolysis rates, and H_2O concentrations (Sillman et al, 1995)

(ii) RH diurnal variation occurs in a reverse manner with that of both O_3 and T. Minimum average values of RH% (45%) occur afternoon at the hrs (14,15) during winter. During summer season this value (45%) occur at the hrs (14, 15).

Maximum average value (79%) occurs at early morning at the hrs (4,6) in winter, while maximum value (91%) occurs at the hr (6) during summer season. We can notice that O_3 average values reached to their maximum value when humidity values were minimum. This can be relatively attributed to the enhanced decrease in the effective photo dissociation of ozone. This may be in agreement with the finding of (Hamdy, 2005), (Ooy et al, 1995) who found strong negative

correlation coefficient between ozone and relative humidity. Also the findings of Ma et al, 2000, who stated that the fraction of excited oxygen atoms that react with water vapor (fa) according to the reaction

$$O(^1D) + H_2O \rightarrow 2OH$$

can be determined from the relation:

$$f_a = q_v/(q_v + 82),$$

where: (q_v) is the specific humidity (g/kg).

So that increasing of water vapor leads to increasing the fraction of excited oxygen atoms that react with it and consequently decreasing the probability of the O_3 formation reaction

$$O(^1D) + O_2 \rightarrow O_3$$

In addition, ozone loss occurs through the HOx (=OH + HO_2) catalytic cycle

$$HO_2 + O_3 \rightarrow OH + 2O_2$$

$$OH + O_3 \rightarrow HO_2 + O_2$$

This implies the importance role of water vapor in the effective photo dissociation rate coefficient of ozone. So, decreasing of relative humidity leads to decreasing of ozone loss.

b) In Alexandria,

(i) The station in Alexandria is representative for a coastal site, about 1.5 km from the Mediterranean Sea coast, It is down wind from the Mediterranean sea most of the day and night hours, so there is slight diurnal variation in T and RH (Figure (5, B)) in comparison with the case that occurred in Cairo.

(ii) T values are strongly lower than that in Cairo while RH values are strongly higher than that in Cairo.

(iii) Diurnal variation of T is so week in comparison with that in Cairo. It varies from minimum average values 14, 26 ^oC in winter and summer seasons, respectively to maximum values 19, 28 ^oC in winter and summer seasons respectively. Low temperature values may make the atmosphere of Alexandria not photo-chemically active. Also the small difference in temperature between day and night hours may lead to small difference in mixing height in the two periods.

(iv) RH has in general high values in comparison with that in Cairo. It varies from minimum average values 75%, 83% in winter and summer seasons, respectively to maximum average values 90%, 92% during winter and summer, respectively. This relatively high values of RH may lead to small O_3 homegrown generation as stated above.

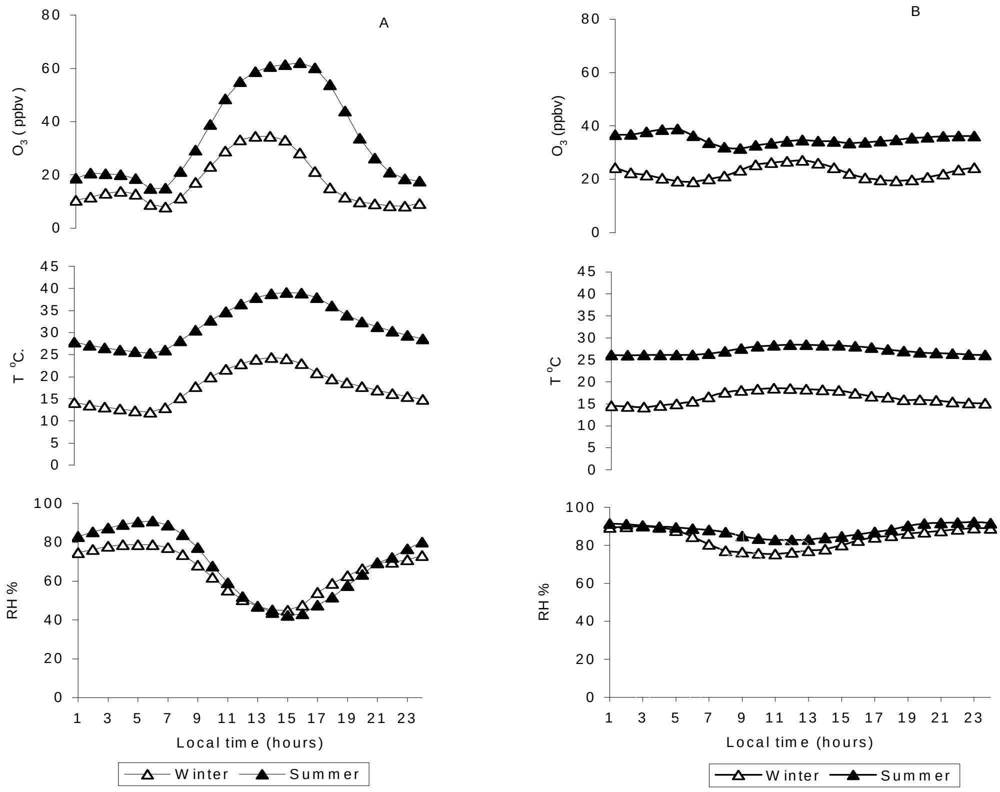

Fig. (5): Diurnal variation of O_3 ppbv, T °C and RH % during winter and summer seasons in Cairo (A) and Alexandria (B) during the period 2001-2003.

3.4. Frequency distribution of surface ozone at day and night hours.

To illustrate the generation and titration effects during day and night hours, frequency distributions of O_3 hourly average values during day and night hours in winter and summer seasons are illustrated in Figures (6 and 7) in Cairo and Alexandria, respectively. It is clear that in Cairo, the maximum frequency distribution of O_3 occurs at low concentration at night hours in comparison with that at day hours in the two seasons. Where, In winter, maximum frequency (27%) is in the interval range 20 – 30 ppbv during day-light hours, while during night hours maximum frequency increased to a value (57%) and the interval range decreases to 0 -10 ppbv. Also in summer, maximum frequency (23%) is in the interval 50 – 60 ppbv during day-light hours while at night hours it increased to a value (55%) and the interval decreased to 20 – 40 ppbv. As we can notice there is increasing in the frequency value and decreasing in its concentration interval as we move from day to night. This may be results from increasing the effect of surface ozone titration by NOx at night hours in comparison with that at day hours.

In Alexandria., maximum frequencies (30%) in winter day hours are located in the O_3 interval values 20-30 ppbv. While during night hours the maximum frequencies (28%) became in the lower interval 0-10 ppbv as a result of relatively high values of NOx concentrations during night hours in this season. The situation is different in summer, where, maximum frequencies occur at the same O_3 intervals during day and night hours (30-40 ppbv). But during day hours, maximum frequencies are (48%), while during night hours maximum frequencies decreased to (38%). This phenomena is attributed to the weak production rate during day hours and weak destruction rate during night hours as a result of planetary boundary layer disturbance as mentioned above. It is clear that the

photochemical generation of surface ozone during day hours and its titration during night hours is so clear in Cairo in comparison with that in Alexandria

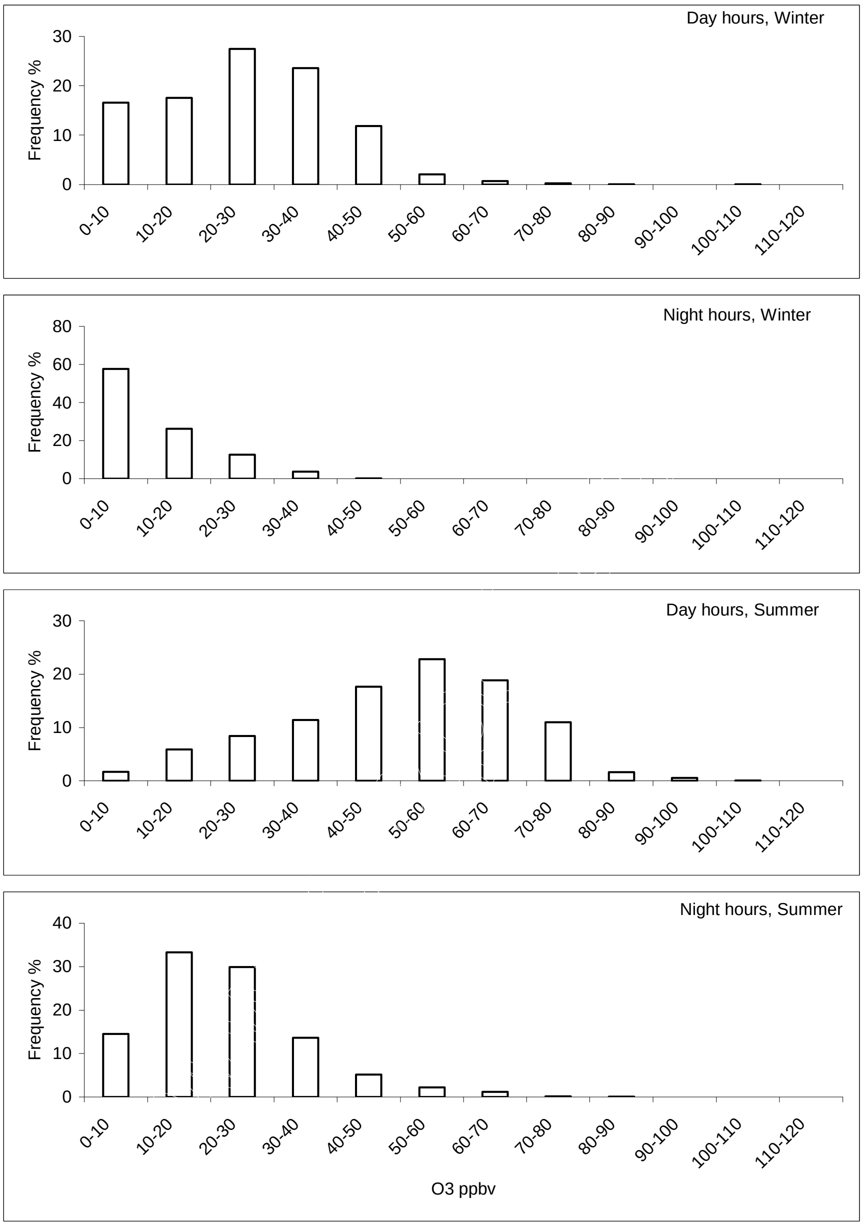

Fig. (6): Frequency distribution of O_3 at night and day hours during winter and summer seasons of the period 2001-2003 in Cairo.

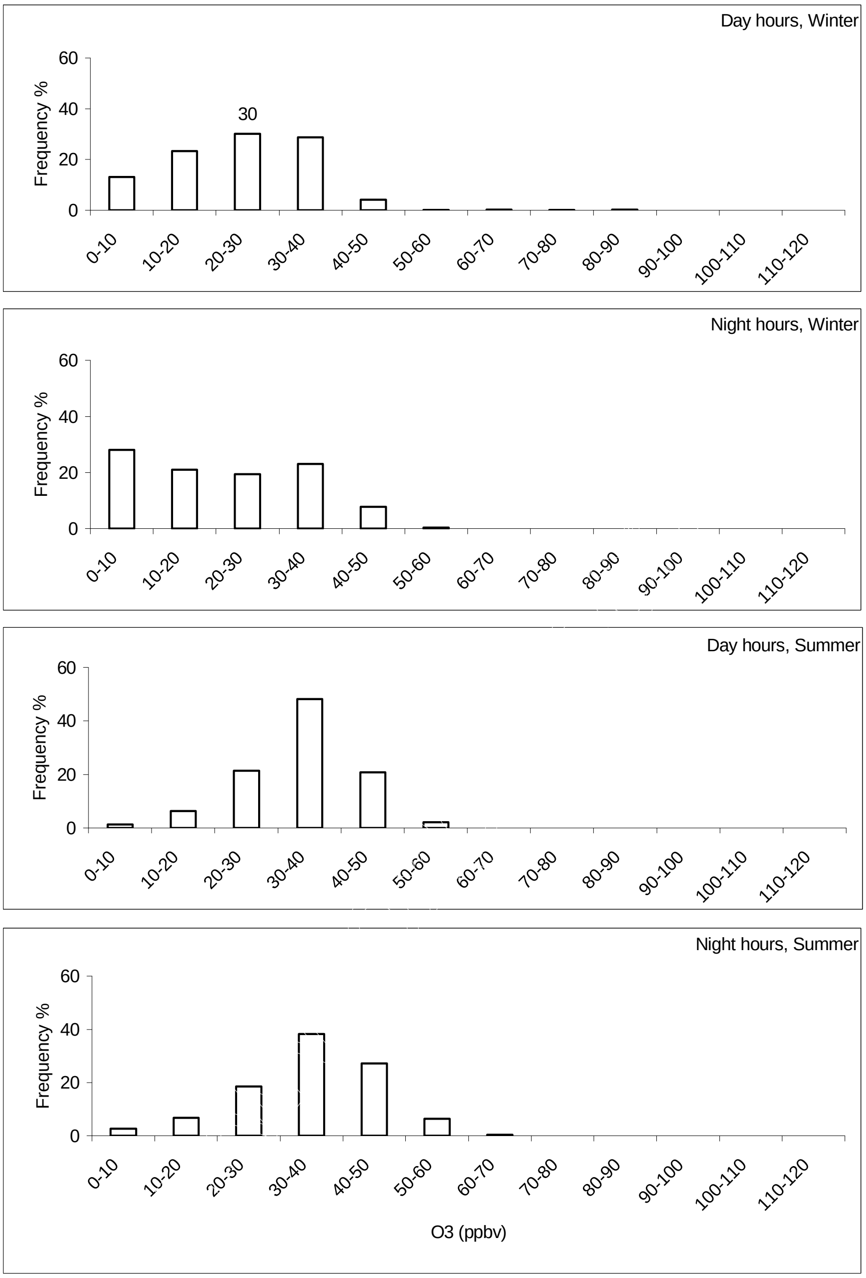

Fig. (7): Frequency distribution of O_3 in day and night hours during winter and summer seasons of the period 2001-2003 in Alexandria.

4. Conclusion

This study leads to the following conclusions:

1- Diurnal variation of surface ozone in Cairo, as an urban site, is different from that of Alexandria which is characterized as regional background station.

2- In Cairo, relatively strong production of O_3 during day hours may be resulted of photochemical production.

3- Diurnal variation of O_3 is in forward proportion with that of temperature as it can enhance photochemical production, and in backward proportion with that of relative humidity as it can relatively prevent O_3 production from one hand and can destroy it in the other hand.

4- Summer average values of O3 in Cairo and Alexandria are similar, 35 ppbv. Although there is much production during day hours in Cairo, it compensated with the much distraction during night hours .

5- Winter average values of O3 in Cairo 17 ppbv are less than that in Alexandria 22 ppbv as a result of increased values of NOx values in Cairo in comparison with that in Alexandria.

6- Seasonal variation of O_3 in Cairo is characterized by relatively high values during summer and relatively low values during winter. Which may be attributed to the difference in solar radiation intensities and temperature in the two seasons. As well as the differences in NOx concentrations.

7- In Alexandria, negligible diurnal variation of surface ozone has been observed and may attributed to relatively low temperatures and high relative humidity with low fluctuation in both of them during day and night hours.

8- Titration effect of O_3 by NOx during night hours is much pronounced in Cairo in comparison with that in Alexandria in all seasons.

9- Analysis of autocorrelation function indicated that transported ozone is more effective in Alexandria than that in Cairo and in winter than that in summer in the both cities.

10- Further discussion on the effect of long ranged transported surface ozone to the two stations will be done in next paper.

Refferences:

Angle, R. P., Sandhu, H. S., 1989. Urban and rural ozone concentrations in Alberta, Canada. Atmos. Environ. 23, 215 – 221.

Britvec, M., Reichenauer, T., Soja, G., Ljubesic, N., Eid, M., Pecina, M., 2001. Ultrastructure changes in grapevine chloroplasts caused by increased tropospheric ozone concentrations. Biologia, Bratislava, 56/4: 417 – 424.

Cheng, L., Fu, L., Angle, R. P., Sandhu, H. S. January 1997. Seasonal variation of volatile organic compounds in Edmonton, Alberta. Atmos. Environ. Vol. 31, No. 2, 239-246.

Dorion-S. M., Stieb, D., Raizenne, M., Brook, J., Dales, R., Leech, J., Cakmak, S., Krewski, D., 2000. Association between ozone and hospitalisation for acute respiratory diseases in children less than 2 years of age. American Journal of Epidemiology 153, 444–452.

El-Hussainy, F. M., Sharobiem, W. M., Ahmed, M. D., 2003. Surface ozone observations over Egypt. Quarterly Journal of the Hungarian Meteorological service. Vol. 107, No. 2, April-June 2003, pp. 133-152.

Fumagalli, I.., Gimene, B. S., Velissariou, D., Temmerman, L. D., Mills, G., 2001. Evidence of ozone – induced adverse effects on crops in the Mediterranean region. Atmospheric Environment 35, 2583 – 2587.

Griffin, R. D., 2007. Principals of air quality management. Second edition, Taylor & Francis Group, Boca Raton London New York.

Guicherit R. 1988. Ozone on an urban and regional scale with special reference to the situation in the Netherlands. Tropospheric Ozone Ed. By Isaksen I. S. A., D. Reidel Publ. Com. P. 49 – 62.

Gusten, H., Heinrich, G., Weppner, J., Abdel-Aal, M.M., Abdel-Hay, F. A., Ramadan, A. B., Tawfik, F. S., Ahmed, D. M., Hassan, G. K. Y., Cvitas, T., Jeftic, J., Klasinc, L., 1994. Ozone formation in the greater Cairo area. The Science of the Total Environment 155, 285-295.

Hamdy, K. Elminir, 2005. Dependence of urban air pollutants on meteorology. Science of the total Environment 350, 225 – 237.

Heath, R., 1994. Plant Responses to the Gaseous Environment. Chapman & Hall, London.

Heck, W. W., Adams, R. M., Cure, W. W., Heagle, A. S., Haggested, H. E., Kohut, R. J., Kress, L. W., Rawlings, J. O., Taylor, O. C., 1983. A reassessment of crop loss from ozone. Environmental Science and technology. 17, 572A – 581A.

Khoder, M. I. 2007. Ambient levels of volatile organic compounds in the atmosphere of Greater Cairo. Atmospheric Environment 41, 554-566.

Klasinc, L., Cvitas, T., 1996. The photosmog problem in the Mediterranean region. Marine Chemistry 53, 111 – 119.

Ma, J., Weele, M. V., 2000. Effect of stratospheric ozone depletion on the net production of ozone in polluted rural areas. Chemosphere: Global change science 2, 23-37.

Martyn D, 1992. Climate of the world: ELSEVIER, PWN-Polish-Scientific-Publishers, pp199-220.

Mauzerall, D. L., Wang, X., 2001. Protecting agricultural crops from the effects of tropospheric ozone exposure: reconciling science and standard setting in the United States, Europe and Asia. Annual Reviews of Energy and Environment, 26, 237 – 168.

Ooy, D. J. V., Carroll, J. J., 1995. The special variation of ozone climatology on the western slope of the Sierra Nevada. Atmospheric environment, vol. 29, No. 11, pp. 1319-1330.

Sillman, S., Samson, P. J., 1995. Impact of temperature on oxidant photochemistry in Urban, polluted rural and remote environments. Journal of Geophysical Research, Vol. 100. No. D6, Pages 11,497-11,508, June 20.

Solomon, P., Cowling, E., Hidy. G., Furiness, G., 2000. Comparison of scientific findings from major ozone field studies in North America and Europe, Atmos. Environ. 34, 1885 – 1920.

U. S. Environmental Protection Agency, Jul 27th, 2004. Web document URL: http://www.epa.gov/airnow/.

Warneck P ،.1987 .Chemistry of the natural atmosphere. Int. Geophys. Ser. 41, Acad. Press, London.

Deterioration and conservation of Dioritic Relief in The Queen Hathepsut's chapel at Temple of Karnak

Dr. Nabil Ahmed Abed El-Tawab

Conservation dep., Faculty of Archaeology, South Valley University, Qena , Egypt.

Abstract :

The Queen Hathepsut's chapel is considered as an important part at the temple of Karnak , The chapel is adjacent to and immediately north of the Main Sanctuary of the Karnak temples. It is includes the most beautiful sunk relief which had been engraved in Diorite stone which had been used in many important Ancient Egyptian monuments during the heights of ancient Egyptian civilization . This chapel suffer from a lot of deterioration factors due to local variability of atmospheric condition (temperature, relative humidity, wind, chemical weathering , salts pressure) , Diorite decomposition takes place mainly by loosing grain by grain which leads to loss a lot of relief from mural painting. Diorite samples which it had fallen from the Queen Hathepsut's chapel were studied by X-ray diffraction (X.R.D), X-ray florescence, Petrographical examination, and scanning electron microscope (S.E.M). Physical and mechanical properties were determined before and after treatment with five different polymers.The results were confirmed by S.E.M, and showed that the co-polymer (paraloid B66, diluted at 5% in Acetone + Wacker VB132) is the best material to consolidate disintegrated Diorite. Four kinds of mortar were studied to show a suitable mortar for the conservation of the missing part of Diorite relief. It was found that the mortar consists of the (Diorite crushing to 5 mm, dark sand, glass powder and Wacker VB132+ Acryloid B-72) , is the best one for the weather Diorite.

Key words: Diorite, chapel, Temple of Karnak, deterioration, atmospheric condition, conservation, Wacker, mortar.

Corresponding author, E. mail: drnabil_bader@yahoo.com

1. Introduction:

The temple of Karnak in Luxor is a record of the history and civilization of Egypt from New Kingdome (Remises III) to the reign of the Ptolemy, it is often understood as the Precinct of Amun-Re only. The Karnak holy earth was included beside the major temple of Amun-Re other temple to other goddess like Precinct of Mut . No doubt that the development stage of this great temple of the Precinct of Amun-Re was determined by the kings and queen of New Kingdome to Precinct of Amun-Re who is the donor victory, So all the kings were desiroused to erection edifice or obelisk or pillar hall …etc. So Queen Hathepsut had some changes in the temple construction, she had built two obelisks and some chapels at the two sides of the sacred boat . One of these chapels, which can be reached it from the north Diorite entrance and had the most beautiful sunk relief, represent Queen Hathepsut with Precinct of Amun-R. Thtmoess III removed most of this relief which represented Queen Hathepsut with the aim of revenge, figure(1d,e).

This Diorite chapel suffer from several deterioration factors which lead to loss a lot of this relief.The characteristics of the deterioration of the sunk relief at Queen Hathepsut's chapel takes the following forms :

- **loss of a lot of parts from mural painting which represents the Hathpsut offering to Amun-Re.**
- **Mechanical exfoliation detachment and falling of Diorite surface.**
- **Change in mineral composition (color & type of minerals).**
- **Degradation of the minerals characteristized by a spontaneous granules of the Diorite stone.**
- **Cracks takes the form in all relief.**
- **Original surface takes a Brown & orange color.**
- **Some parts in Façade ornament are particularly damaged.**

-

-


A
B
C
D
E
F
J
H
I

2. Experimental & results:

2.1. Materials studied:

Diorite samples were taken from removing the fragments removed from Hathepsut's chapel and Karnak temple which is exposed to the same deterioration phenomenon. The deterioration processes go through chemical and mineralogical via X-Ray diffraction (XRD), X-ray fluorescence (XRF), textural and mineralogical via Polarizing microscope and Scanning electron microscope dispersive X-ray analysis (SEM-EDX), The physical & mechanical properties were investigated through laboratory measurements, The Diorite samples were treated with several different polymers, the results were confirmed by S.E.M.

2.2. X-ray fluorescence analysis

The results of the X-ray fluorescence analysis indicate a high silicate (Si-47.14%), Fe (18.25), Al(12.09), Ca(9.79), low Potassium(4.42),Mg(3.14),Ti(2.44) and minor of Sodium(1.36),S(1.04), Mn(0.36 and less minor of Chloride.

Table (1) Shows major Chemical composition (%)of the Diorite samples :

Element	Weight %
Na_2O	0.7014
MgO	4.9043
Al_2O_3	8.3237
SiO_2	49.4750
Cl	2.62
K_2O	3.3480
CaO	8.2466
TiO_2	3.1895
MnO	0.3641
Fe_2O_3	20.4464

2.3. X-ray Diffraction analysis (XRD):

X-ray diffraction analysis (fig.3) indicates that mainly quartz (SiO_2), Na-feldspar Albite ($NaAlSi_3O_8$) K-feldspar -Orthoclase($KAlSi_3O_8$), mica group Muscovite $KAl_2(AlSi_3O_{10})$ (OH)2, and traces amount of Hematite (Fe_2O_3) and Kaolinite Si_4 Al_4 O_{10} $(OH)_8$.

Table (2) Shows the results of XRD of the Diorite samples.

Mineral name	Chemical Structure	Cart. No	Specie.
Quartz	SiO_2	5-0490	Major
Albite	Na Al Si_3O_8 Sodium Aluminum Silicate	10-393	Minor
Muscovite	$H_2KAl_3Si_3O_{12}$ Potassium hydrogen Aluminum Silicate	2-55	Minor
Orthoclase	$KAlSi_3O_8$ Potassium Aluminum Silicate		Minor
Hematite	Fe_2O_3 Iron Oxide	13-534	Trace
Kaolinite	Si_4 Al_4 O_{10} $(OH)_8$ Al. Silicate Hydroxide Hydrate		Trace

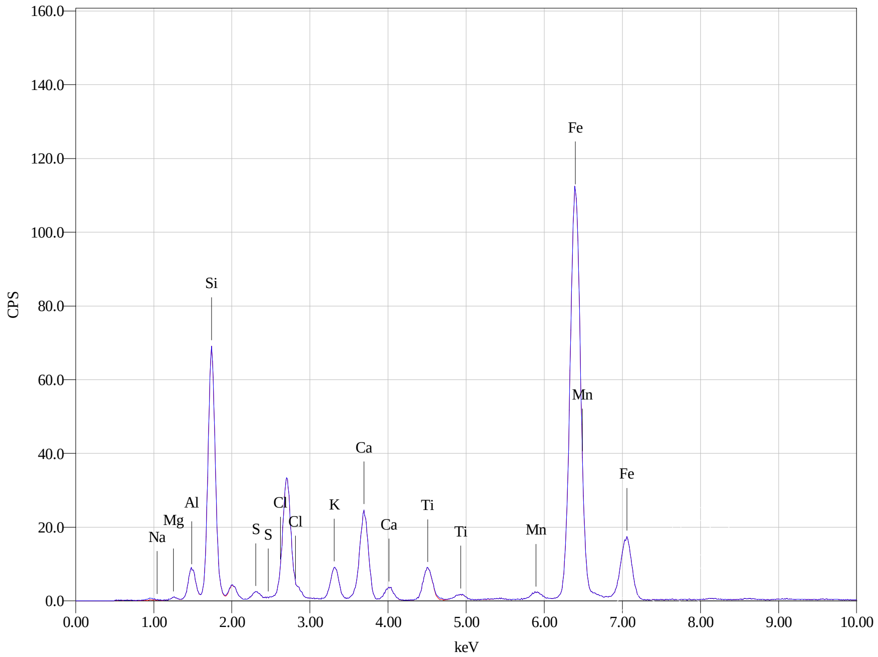

Fig, (2) shows elemental composition by X-ray fluorescence.

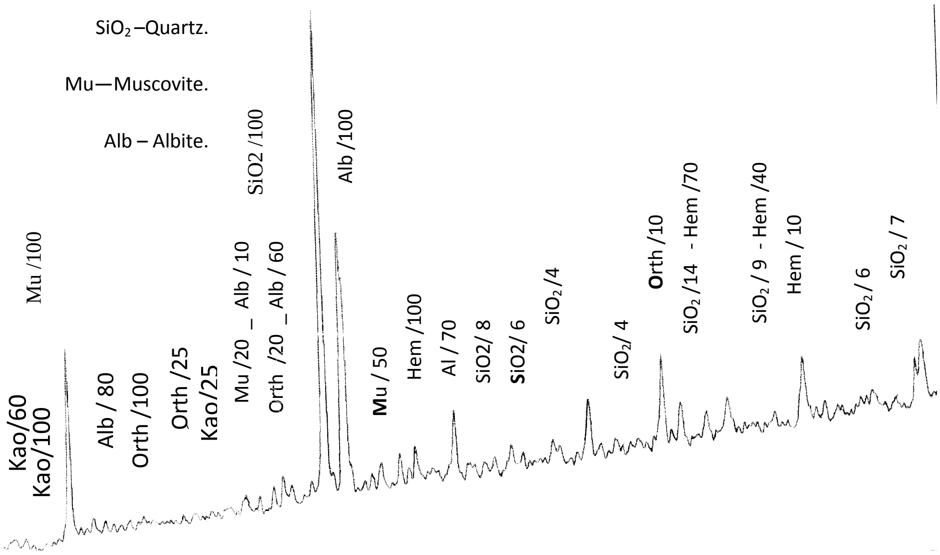

Fig.(3) X-ray diffraction pattern of Diorite Sample, Hathepsut's chapel, temple of Karnak ,Major, Quartz ,Albite ,Minor :Muscovite ,Orthoclase, Traces: Hematite .

2.4. Petrographic characteristic of Diorite (thin section analysis):

The investigated diorite samples are composed essentially of Plagioclase, Biotite and Hornblende together with minor of Quartz. K- Feldspar, Apatite, Muscovite and Iron oxide are presented as accessories, whereas Chlorite and clay minerals are secondary constituents. Plagioclase, occurs as euhedral to subhedral moderately to completely altered crystal. Biotite crystals are moderately altered to chlorite and contain Abatite crystals and Muscovite as inclusions. Quartz occurs as rounded to subrounded embayed grains within plagioclase and Biotite .Abatite occurs as short prismatic crystals included within Biotite and feldspar minerals.

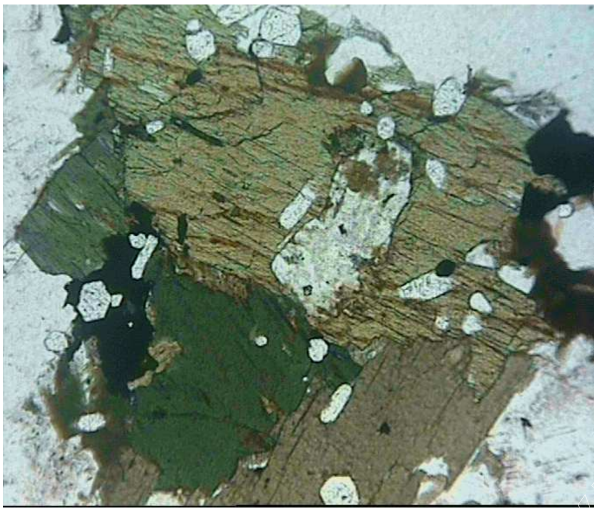

Fig.(4): shows altered Biotite , Hornblende, Quartz , plagioclase(X=25 under polar light).

Fig.(5): shows Biotite partly altered to chlorite , also contained Hematite which to dye the other place . (X= 63 under polar light).

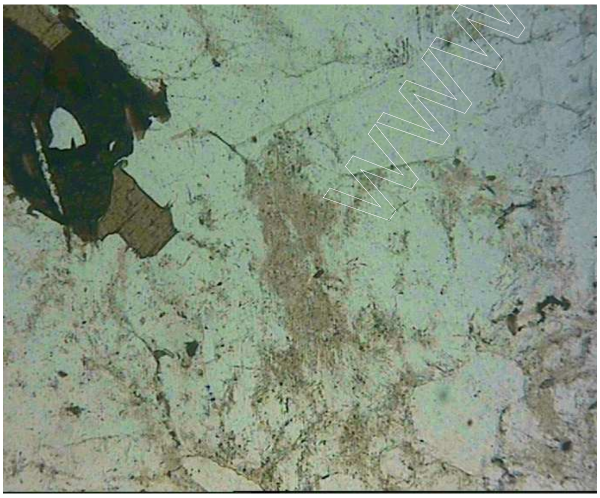

Fig.(6):shows completely altered Feldspar to clay minerals(X= 60 under PPL).

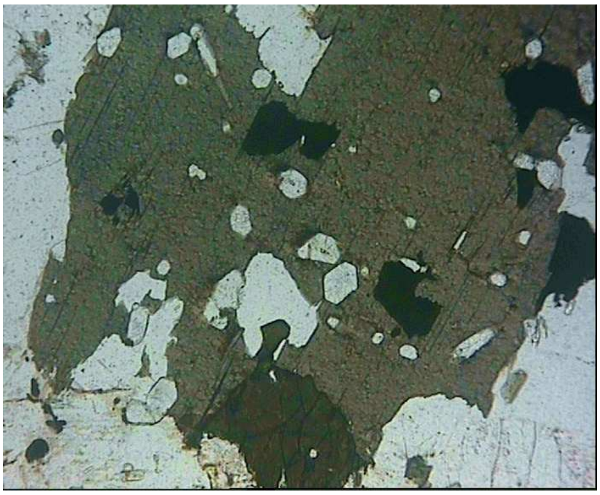

Fig.(7):shows Biotite mineral carry Abatite with white color(X= 60 under PPL).

3. Consolidation :

for this study, four products of conservation were tested ,three of Acrylic resin , one of organosilicic type .

Table (3)shows the consolidant polymers & there solvents .

consolidant polymers	Chemical composition
Acryloid B-72 dissolved in Acetone (5%)	Acrylic resin , Ethyl methacrylate co -Polymer
Acryloid B-66 dissolved in Toluene (5%)	an isobutyl methacrylate polymer. It is an alkyd-compatible acrylic ester
Acryloid B-82 dissolved in Toluene (5%)	methyl methacrylate copolymer
Wacker VB132(ready to use)	Ethyl silicate: (TEOS) tetraethox silane
Wacker VB132 and Solution of 5% Acryloid B-82	Acrylic resin + Ethyl silicate (TEOS)

3.1. Application of the consolidant to the stone samples :

Diorite samples which were taken from the removal of fragments around Hathepsut's chapel and Karnak temple, were cut into cubes (4cm^3), slabs (7× 7 ×3.5 thickness) ,columns (10‹L›×4‹h›×4‹t›), the samples were cleaned, dried at (105º C).But the samples which were treated with organosilicon were wetted and left in the air until the water content was 0.2gm. This procedure favors the polymerization of organosilicon products (Rosario&Others1996)

$$H_2SiO_2 + H_2O \rightarrow SiO(OH)_4 \qquad [1]$$

$$Si\,(OH)4 \rightarrow SiO2 + 2H_2O \qquad [2]$$

Samples impregnation were performed by immersion, the same treatment was repeated after 24 hours, All the samples were kept at the atmospheric circumstances of the room for at least 30 days to allow the polymerization process to take place. Several properties were measured on samples before and after the treatment to evaluate the effects of polymers on improvement of Diorite properties.

3.2.Physical properties:

Visual evaluation of the color doesn't show any color difference between the treated and untreated samples. The degree of penetration was assessed by low magnification scanning electron microscope. Bulk density, Water absorption and Porosity of the treated and untreated samples were determined, table 4 & fig.8.

3.4. Mechanical properties:

Compressive strength was determined for treated and untreated samples, table 5 Fig. 9. The untreated samples had an average value of 148 kg/cm^2 , the samples treated with TEOS + 5% Acryloid B-66 in toluene gave the highest value. 328 kg/cm^2.

Indirect Tensile strength measuring show that the average values for treated and untreated sample , The value for the untreated sample was 11.5 whereas those for the treated samples with TEOS + 5% Paraloid B-66 in toluene gave the highest value. 15.9 .

For testing successful extension for consolidation materials to protect the relief and granting it mechanical power to struggle the sandy wind, The Abrasion Strength test was determined, Some Diorite samples were cut into square slabs(7 x 7 × 3.5cm thickness). Mechanical brushing had been applied to clean the samples, after drying in an oven at 105ºc for 24 hours, then weighed, the slabs were consolidated with chosen polymers. After 30 days the slabs samples were put in testing machine with Corporundum. The table (4) show the loosing weight in Diorite samples after abrasion, The value for the untreated sample was 15.6 gm , whereas those for the treated samples with TEOS + 5% Acryloid B-66 in toluene gave the less value. 2.65 gm losing.

Table (4) : shows the Physical properties to untreated & treated Diorite samples.

Physical properties	untreated	B-72	B-66	B-82	Wacker VB132	B- 66+ VB132
Bulk density (gm / cm^3)	2. 54	2 . 63	2. 67	2. 59	2. 62	2.69
Water absorption (%)	2. 4	1. 84	1. 66	2. 05	2. 23	1. 85
Porosity (%)	4. 87	3. 23	2. 88	3. 54	3. 58	2. 76

Table (5) : shows the mechanical properties to untreated & treated Diorite samples.

Mechanical properties	untreated	B-72	B-66	B-82	Wacker VB132	+ B-66 VB132
Compressive strength (gm /cm^2)	148	278	310	235	227	328
Tensile strength N/mm^2	11. 5	14. 3	15. 8	13. 6	13. 40	15. 9
Loosing by Abrasive (gm)	15. 6	3. 6	2. 88	3. 8	4 . 20	2. 65

3.5. Artificial weathering:

In order to obtain the most suitable polymer to give the best consolidation which can outlast in front of different weathering factors the experimental condition used for the purpose of artificial weathering were far more severe than natural condition .The test was carried out by wet-dry cycles and salt crystallization weathering according to(ASTM Designation C88 – 56 T) . The results were determined after 30 cycles. Physical & mechanical properties were determined; the results were confirmed by S.E.M.

Table (6) : shows the Physical properties to untreated & treated Diorite samples after artificial weathering.

Physical properties	untreated	B-72	B-66	B-82	W acker VB132	B- 66+ VB132
Bulk density (gm / cm^3)	2. 54	2 . 59	2. 64	2. 57	2. 60	2.66
Water absorption (%)	2. 4	4.54	3.78	4.76	3.04	2.44
Porosity (%)	4. 87	8.75	5.34	7.67	4.85	4.23

Table (7) : show the mechanical properties to untreated & treated Diorite samples after artificial weathering.

Mechanical properties	untreated	B-72	B-66	B-82	Wacker VB132	+ B-66 VB132
Compressive strength (gm /cm^2)	148	210	295	190	218	298
Tensile strength N/mm^2	11. 5	12.8	13.8	12.5	12.95	14.87
Loosing by Abrasive (gm)	15. 6	8.4	5.22	7.56	6.12	4.78

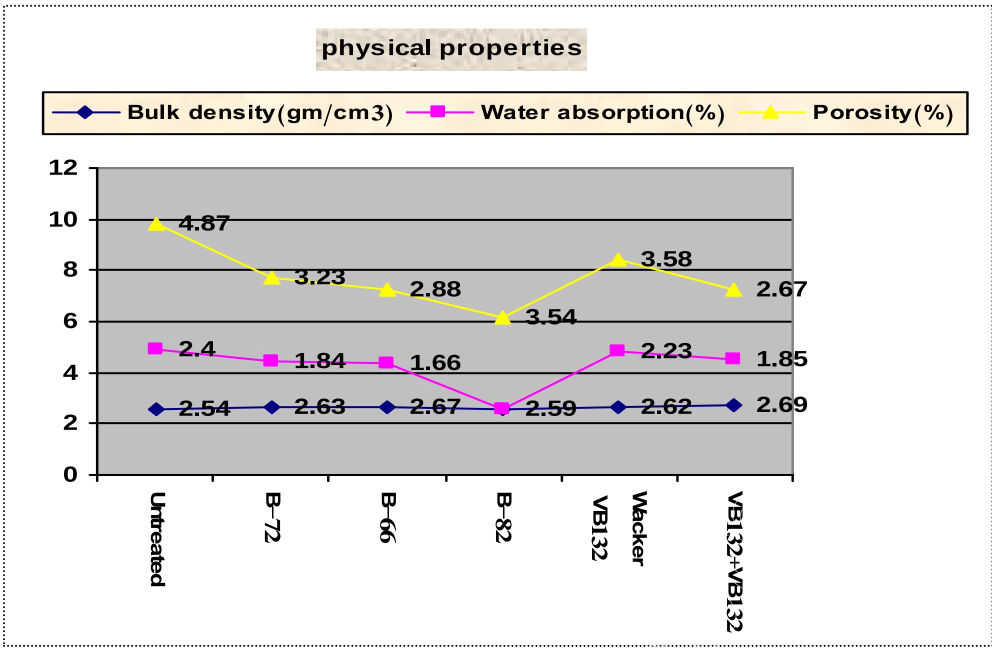

Fig. (8) shows the Physical properties to untreated & treated Diorite samples .

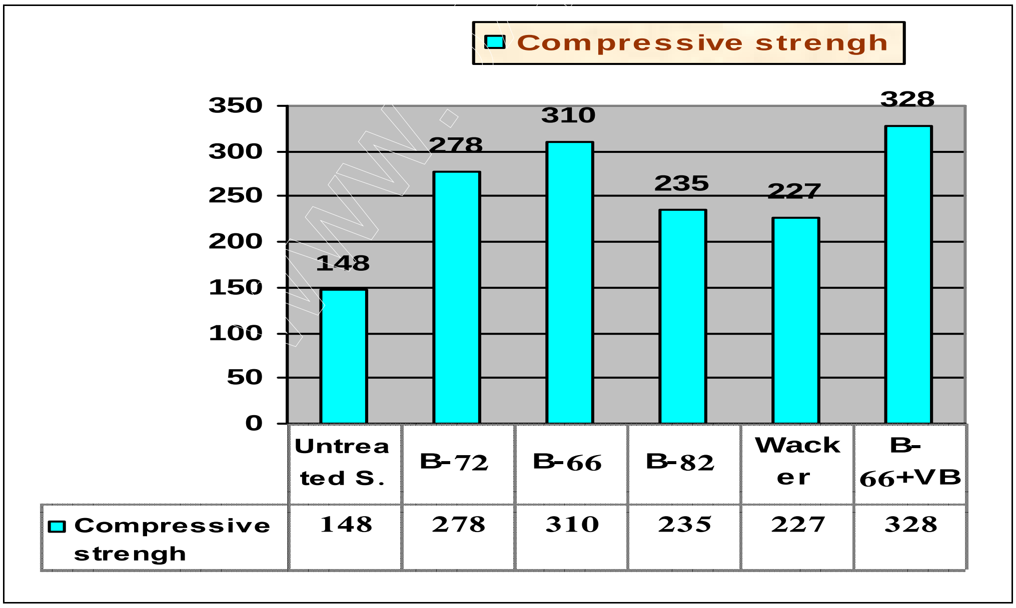

Fig.(9) shows the Mechanical properties(Compressive strength) of untreated & treated Diorite samples .

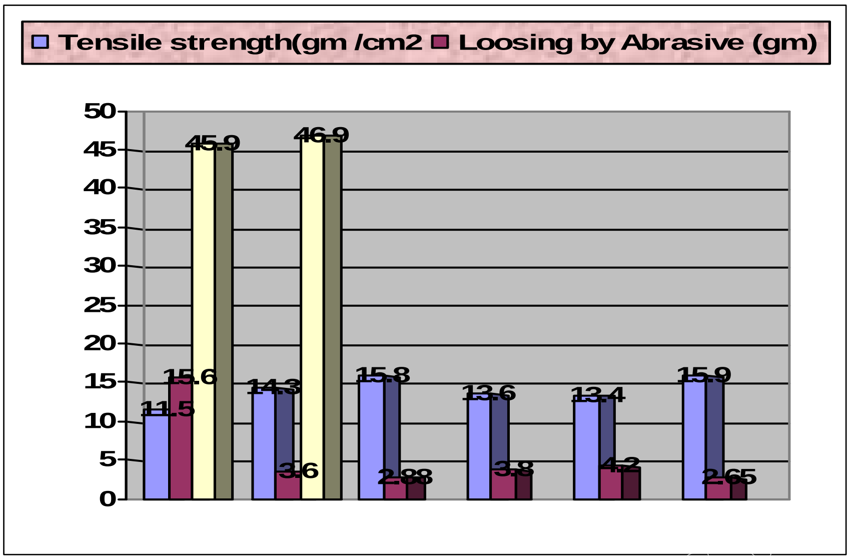

3.6. Scanning electron microscopy (SEM).

Investigation with SEM was used for examination of the untreated samples and aimed at establishing the location of the penetrated samples as it was expected, and the possibility of the linking with consolidants materials used in the treatment of Diorite. The SEM micrographs of the untreated sample, Plate (1) show the patches of the fine-grained quartz mineral, obliteration of the characterized igneous textures, fractures in the minerals, the volume and distribution of the pores, and the binding material which contains salt and Kaolinite crystals.

SEM micrographs of the sample treated with 5% Acryloid B-72 in toluene, Plate (2) had a network of polymer and the consolidant were deposited around Diorite grains.

The sample treated with Acryloid B-66 dissolved in Toluene 5% ,Plate(3) shows that the massive coating was deposited around Diorite grains , the polymer was found on the surface of the Diorite grains . The sample treated with Acryloid B-82 dissolved in Toluene 5%, Plate (4) shows the coating of the consolidant material on Diorite grains was observed the sporadic network of the polymer. The sample treated with Wacker-Silicone VB1321 diluted with turpentine, Plate (5) shows perfect penetration, The network structure of consolidant can be seen dispersed between the grains and through the pores. The sample treated with Wacker VB 1321 and after that treated with 5% Paraloid B-66 (mixture between the silicon resin & the acrylic resin) Plate(6) shows unsuccessful results because a thin layer of the polymer has been formed but this network structure has failed to fill fine cracks .

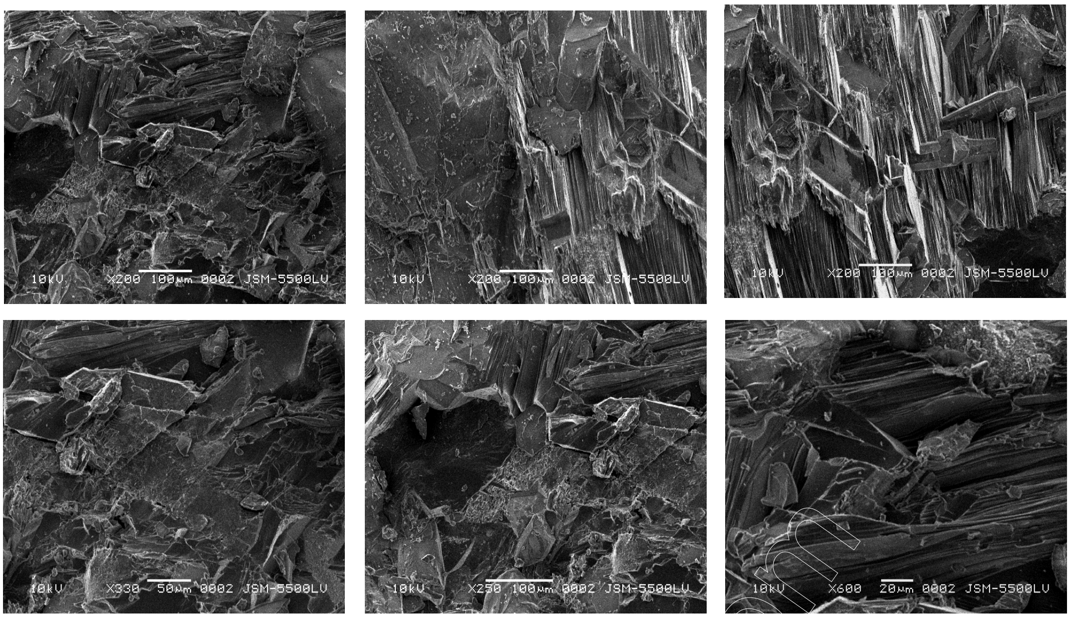

Plate 1 : SEM micrographs showing the untreated Diorite sample .

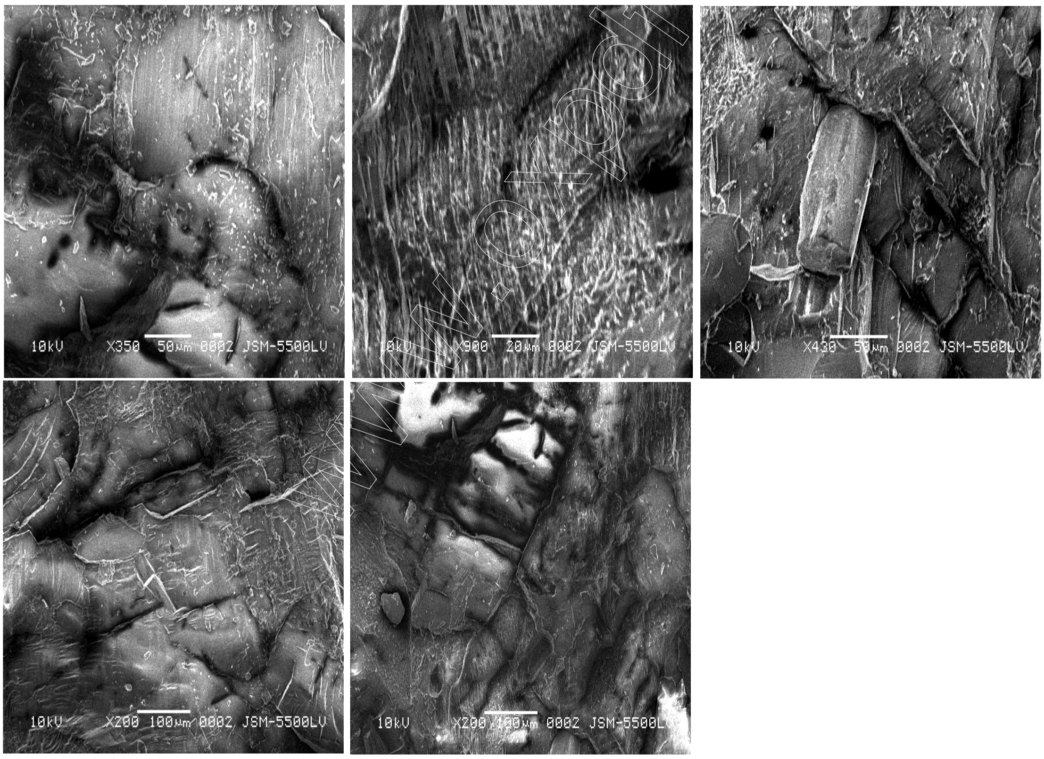

Plate 2: SEM micrographs showing the Diorite sample treated with 5% Acryloid B-72 in Acetone

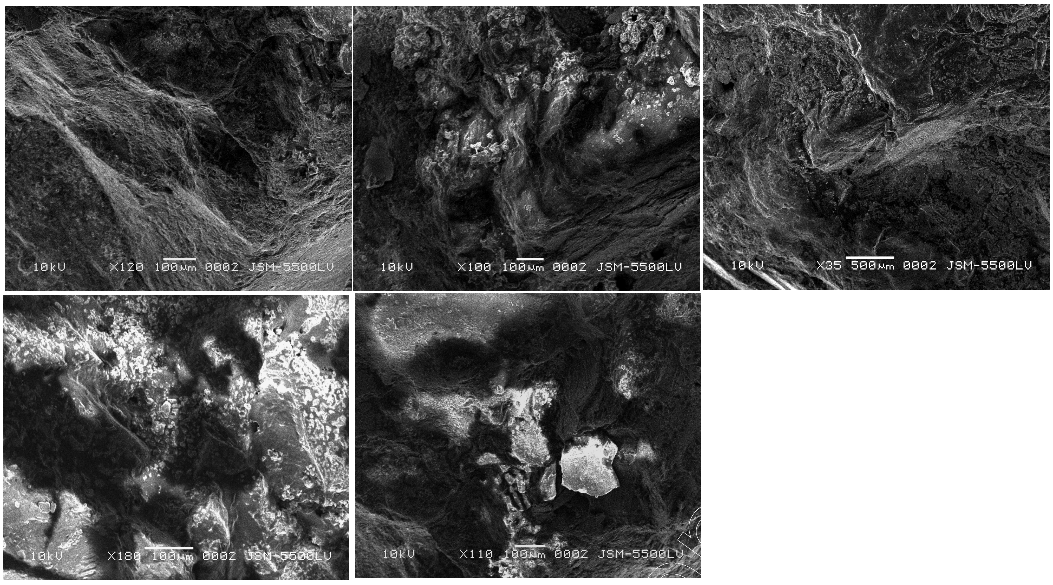

Plate:3 SEM micrographs showing the Diorite sample treated with 5% Acryloid B-66 in Toluene

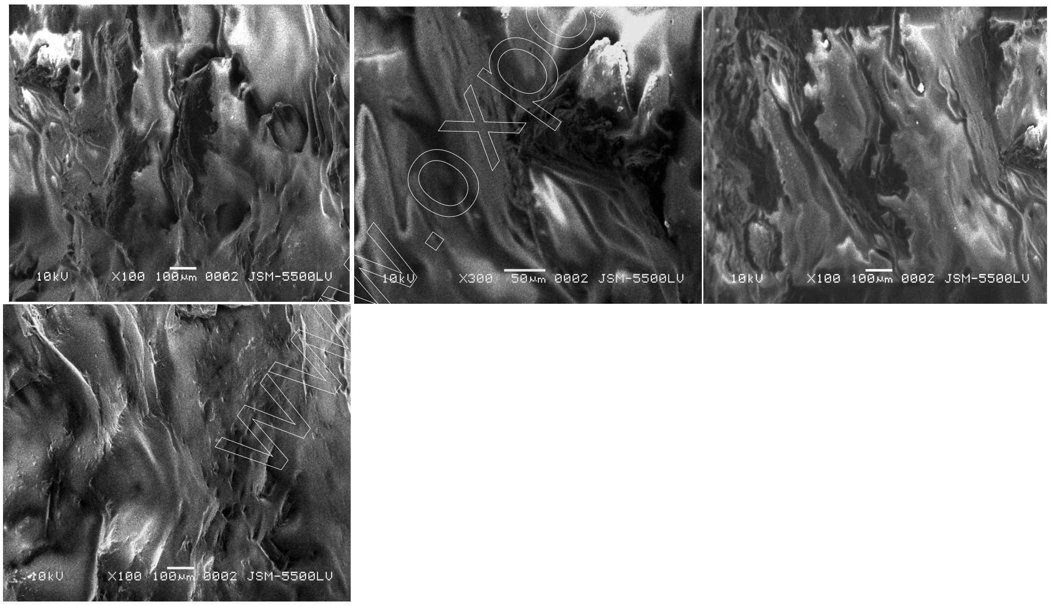

Plate4: SEM micrographs showing the Diorite sample treated with 5% Acryloid B-82 in Toluen

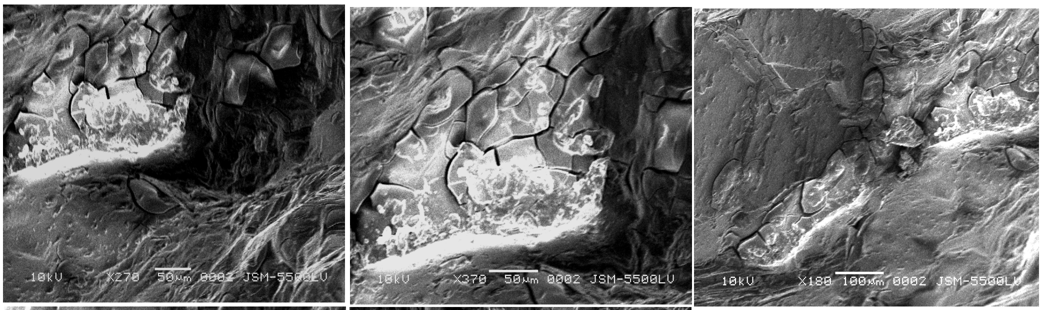

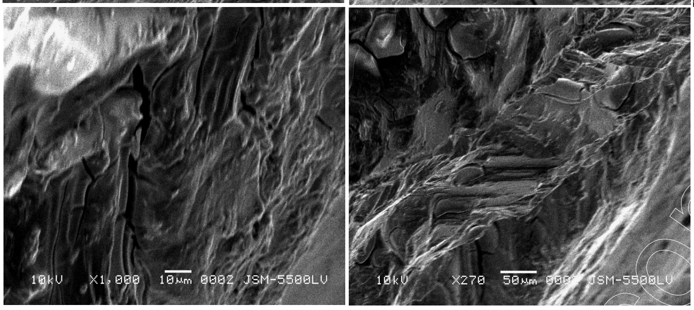

Plate 5 : SEM micrographs showing the Diorite sample treated with Wacker VB1321.

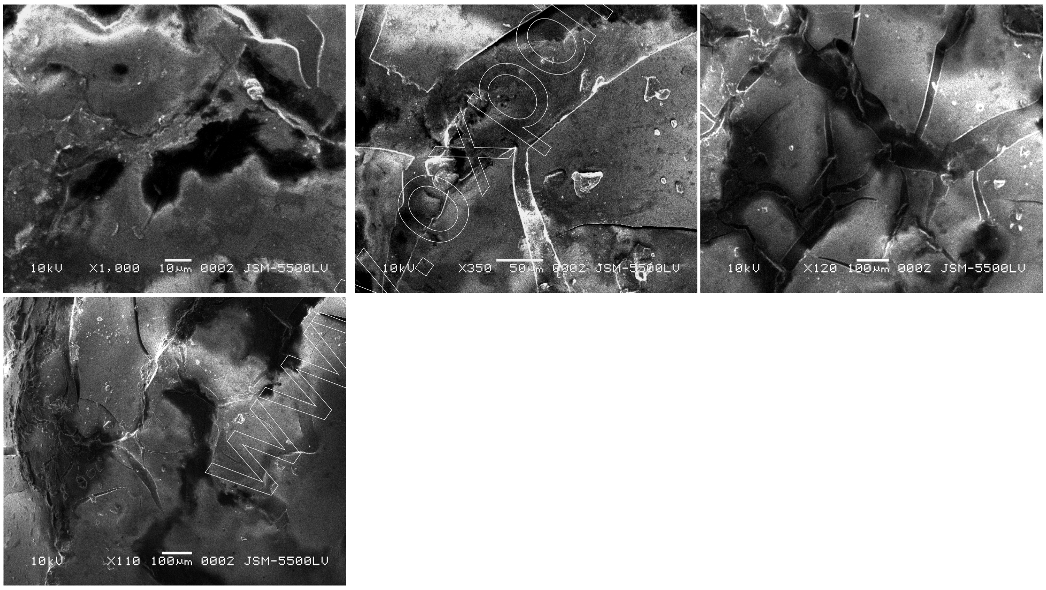

Plate 6 : SEM micrographs showing the Diorite sample treated with Solution of 3% Paraloid B-782 dissolved in Wacker OH 100.

4. Evaluation of Mortars:

The purpose of this study is to experience the durability and the characteristics of the suitable mortars used in conserving missing part of Diorite reliefs, it is often necessary to apply mortar which look like the original Diorite stone to fill fissures or for small conservation. In addition to that, five types of mortars were used in this study. The raw materials utilized for producing the mortar are :

mixtures consisted of Diorite crushing under 5 mm , glass powder (The role of the glass powder is to fill the space between the particles of crushed Diorite, It makes also the application much easier , by thickening the mixture, dark sand, to fill the empty volumes in the crushed Diorite- glass powder, Araldite 1092. Cold Setting Resins (Epichlorohydrin + A- Bisphenol), Wacker VB1321 + Acryloid B72 , Primal Ac33 (Acrylic resin) , Senorox grout (production of CMB), Eucotan DM (production of Swiss chemical company)

Samples have been prepared :

1- **The first (M1) containing Diorite crushing under 5 mm ,dark sand and Araldite 1092.**
2- **The second (M2) containing Diorite crushing under 5 mm ,dark sand, senorox grout and Primal AC33.**
3- **The third (M3) containing Diorite crushing under 5 mm ,dark sand ,glass powder, and Wacker VB132+ Acryloid B-72.**
4- **The forth (M4) containing Diorite crushing under 5 mm ,dark sand , and senorox grout and Eucotan DM.**

Table (8) The compositions of the mortars studied

Composition	M1	M2	M3	M4
Diorite crushing (gm)	500	500	500	500
dark sand(gm)	250	250	250	250
glass powder(gm)	~~~~~	~~~~~	150	~~~~~
Eucotan DM (Liter)	~~~~~	~~~~~	~~~~~	½
senorox grout(Kg).	~~~~~	½	~~~~~	1
Primal AC33(20%)(Liter)	~~~~~	½	~~~~~	~~~~~
Araldite 1092 (Gm)	500	~~~~~	~~~~~	~~~~~
Wacker VB132+ Acryloid B-72	~~~~~	~~~~~	500mm	~~~~~

- Samples preparation :

For the preparation of the mortars all materials were measured by volume and the following procedure was followed , sand and Diorite crushing were mixed with water to remove any salts , The mixture was vibrated and compressed into moulds in order to obtain samples were cubic with 5cm and then were stored at 50-60% RH , temperature (20-25 °C) for one month. To complete drying .

4.1. Accelerated ageing:

For the durability determination of all mortars against various decay agents, the samples were subjected to accelerated ageing cycles with wet-dry cycles, soluble salts and acid attack:

- **Samples drying at 105°c for 20 hours.**
- **Samples were left two hours at room temperature**
- **Samples were left one hour immersion in soluble (NaCl) .**
- **Samples were left one hour immersion in acid (HCl 5%).**
- **Samples drying at 105°c for 22 hours .**
- **The results were measured after 20 cycles.**

The results from the study of the physical and mechanical properties of the mortar samples after ageing cycles show at Fig. (11,12).

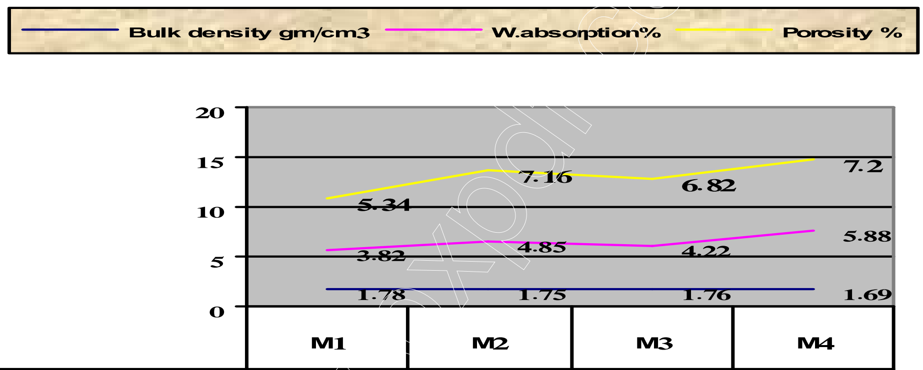

	M1	M2	M3	M4
Porosity %	5.34	7.16	6.82	7.2
W.absorption%	3.82	4.85	4.22	5.88
Bulk density gm/cm3	1.78	1.75	1.76	1.69

Fig. (11)Shows the results from the study of the physical properties of the mortar Samples after ageing cycles.

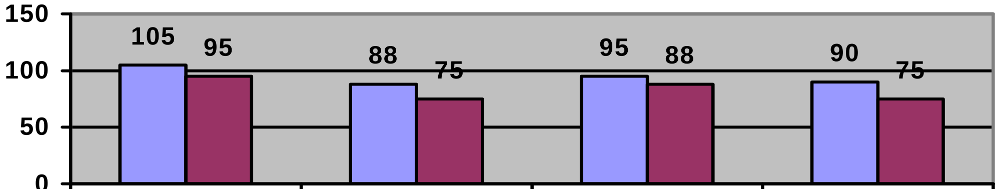

	M1	M2	M3	M4
Dry	105	88	95	90
Wet	95	75	88	75

Fig. (12)Shows the results from the study of the mechanical properties of the mortar Samples after ageing cycles .

5. Discussion :

This study of the diorite used in the Queen Hathepsut's chapel at Temple of Karnak shows some of the reasons for the deterioration of the stone like mechanical exfoliation & disintegration detachment and falling of Diorite surface due to the arid climate of the region and continuous changes between day, night and seasonal changes in temperatures are considered very important participating factor in physical weathering.

the surface layers of Diorite relief on the sunny sides often reach much higher temperature in July 41°c and relative humidity- 50% RH in December (Marie H.,H.,2004) and this causes serious deterioration and decomposition of Diorite stones, Chemical weathering processes , change ferrous iron to ferric ions of the minerals constituents, this alteration produces cracks and weakness which cause granular disintegration into minerals of Diorite and coloration (Sulovsky, Peter, et al 1996). Relative humidity variation and saline salts also plays a role in Diorite decomposition, many rocks show a significant strength decrease with increasing moisture content,(Hoek & Brown) A more probable cause of this type of degradation is the infiltration of soluble salts into the rock pores and crystallization of the salts therein. Salts are the most powerful weathering agents. Efflorescing salts improve the esthetic value. Honeycomb weathering and pitted features, the salts present crystallized. Pressures on the microspores of the rock due to the crystallization of the salts, would have likely caused its deterioration. Under natural conditions surrounding minerals, which is enough to crack most rocks common to Diorite (Jonna, M., Carlanec,R ., et al 1982), also the ground water assists in the weathering of Plagioclase and Biotite and other minerals.

Thin-section analysis showed the alteration of potassium feldspar minerals (orthoclase to kaolinite) This confirmed the role of chemical weathering like mainly moisture and air pollution (mainly SO_2 gas which its concentration in Luxor reaches 23 µg/m^3)(Marie H.,2004) in the deterioration of the Structure of the stone.

$2KAlSi_3O_8 + 2H^+ + SO_4^{2-} + H_2O \rightarrow Al_2Si_2O_5(OH)_4 + 2K^+ + 4SiO_2 + SO_4^{2-}$ (Sulovsky 1996).A traces of Sodium chloride (Halite) salts were found between grains which are considered most strongly influencing the level of stone degradation ,the salt pressure crystallization of Sodium chloride between the grains cause main stone exfoliation (Garcia and others 1996).

Mechanical action promoted by atmospheric agents, fundamentally wind erosion participated on removal of sunken relief . All these deterioration factors which lead to the wastage

of a lot of part of the relief in Queen Hathepsut's chapel. It was necessary to study some consolidation products to choose one of them which give the best degree of penetration, make a linking between separated grains, and replace the natural grain cement destroyed by weathering on the stone's surface.(Earhard ,M. 1997). Some acrylic products, silicone and mixture of the both were evaluated as follow , naked-eye investigation, study of physical & mechanical properties, study with S.E.M. after artificial aging [included cycles of heating & cooling, salt weathering] showed that the [wacker VB1321 + Paraloid B-66] is the best material to consolidate the weakness of Diorite relief.

From the evaluation of the results of mortars compressive strength, durability against wetting and drying showed differences between mortars . It can be concluded that mortar (code M1) containing Diorite crushing under 5 mm ,dark sand and Araldite 1092 , showed the highest values for compressive strength due to Araldite 1092, but this highest value isn't suitable for the weakness of Diorite relief .Mortar (code M2) containing Diorite crushing under 5 mm ,dark sand, senorox grout and Primal AC33 showed a high influence by moisture and it gives a high porosity and water absorption . Mortar (code M3) containing Diorite crushing under 5 mm ,dark sand , glass powder, and Wacker VB132+ Acryloid B-72showed that a suitable values for compressive , the deference between values for compressive in dry and wet was less than signifying that the mortar isn't influenced by moisture . Mortar (code M4) containing Diorite crushing under 5 mm ,dark sand , senorox grout and Ediobond materials showed high values for compressive strength on dry state , but in wet test the properties of the samples showed less value than signifying that and senorox grout and Eucotan DM gave a hard mortar but doesn't withstand against moisture.

6. Conclusion:

- **This study showed that the important causes of deterioration of Dioritic Relief at The Queen Hathepsut's chapel at Temple of Karnak due to environmental process property changes in temperatures and relative humidity between day and night .This phenomenon leads to disintegration and decomposition of diorite, so a lot part of relief were removed .**
- **Diorite samples of studied area showed that : Bulk density = 2. 54 gm/cm5) , Porosity = 4.87% ,Water absorption = 2.4% ,Dry – compressive strength = 148 kg/m2. , Tensile strength = 11.5 kg/m2 , Loosing by abrasive = 15.6 gm.**
- **The Petrographic study showed that decomposition of K-Feldspars into Clay minerals, cleavage planes of Biotite .**
- **To obtain the most consolidants, Some acrylic products, silicone and mixture of the both were investigated Before and after artificial aging . It showed that the paraliod B66 (diluted at 5% in Acetone is the best material to consolidate disintegrated Diorite**
- **To Evaluate suitable Mortar to complete the missing part , Four types of mortars were used in this study and it was found that the mortar (code M3) which consists of containing Diorite crushing under 5 mm ,dark sand, and Wacker VB132+ Acryloid B-72 is the best one for weather Diorite.**

References

1 Adamo, P. and Violante, P., Weathering of rocks and neogenesis of minerals associated with Lichen activity. In Applied Clay Science 16, Elsevier science, 2000, pp. 229-256.

2 Adiab,S., Encyclopedia of old Egyptian civilization , Elaraby for publishing and disruption , Egypt, 2000 ,pp.675-680 .

3 Brian M.,and Kennan P., Petrology and geochemistry of the Drogheda Granite, Irish Journal of Earth Sciences, Vol. 20 (2002), pp. 53-60

4 Cook , R. U. Geomorphology in Environmental Management , an introduction , London , 1988 – P. 291.

5 Earhard M. Winkler; Springer , V., Stone in Architecture: Properties and Durability , New York ,1997

6 Gracia,M.,Molera,J.,Vendrell,M., Main induced deterioration in the gothic cloister of "Palau de la generalitat" Spain , In International congress on deterioration and conservation of stone .V.2, 1996 , pp.61:67.

7 Hoek, E., and Brown E.T., Practical estimates of rock mass strength Published in the International Journal of Rock Mechanics and Mining Sciences, Vol 34, No 8, 1997, pages 1165-1186

8 Ismail,B.M.,El-Habaak,G.H., Durability characteristics of some Diorite and Granodiorite monumental , South Valley Univ.1996

9 Jesus,Gaitan,I.,Ortega,O.,Rosario, Previous studies for the restoration of the Cordoba door of carmona .Spain, In International congress on deterioration and conservation of stone .V.2,pp.1001-1007.

10 Jonna, M., Carlanec,R ., Wilson,Y.I, Dedyo, S, The mechanisms of the physicochemical reactions in diorite used in the construction of ancient royal Egyptian statues ,1982

11 Julia,H.,Valentin,T., Consolidation effect of Wacker-silicone on the properties of Sandy Limestone .In International congress on deterioration and conservation of stone .V.2, 1996 , pp.1195-1201

12 Marie H., H., Scientific Evaluation of Treatment strategy of painted plaster layers applied on stone supports – applied on one of the New kingdom Nobles Tombs – Western Bank Luxor , A Thesis Presented to Restoration and Conservation Department , Faculty of Archaeology , Cairo University, 2004.

13 Reinhold E. S., On Diorite , Proceedings of the Academy of Natural Sciences of Philadelphia, Vol. 34, No. 1 (Jan. -Apr., 1982), p. 59

14 Rosario,V.,Lourdes,M.,Jose,V.P.,Angel,B.M.,Manuel,A.M.,Characterization and conservation of the stone used in the Cathedral of Almera (Spain) , In International congress on deterioration and conservation of stone .V.2, 1996 , pp.89:98.

15 Saleh,A.S.,Helmi,F.M,Kamal,M.M,and El-Banna,A., Study and consolidation of Sandstone temple of Karnak .Luxor. Egypt, studies in con. V.37,N.2,1992

16 Sulovsky, Peter, Gregerova, and Miroslava, Mineralogical study of stone decay in Charles Bridge , Prague, In International congress on deterioration and conservation of stone .V.2,1996 ,pp.29-36

17 Wakizaka, Y., Ichikawa, K., Nakamura, Y. and Anan, S., Deterioration of concrete due to specific minerals. Proc. Aggregate 2001 –Environment and Economy, Vol.2, 331-338.

18 Rolland,O.,Floc,P.,H., Silica bound mortars for the repairing of outdoors Granite sculptures, In 9th International congress on deterioration and conservation of stone .V.1, 2000 , pp.307-315.

Erythemal dose in Qena, Upper Egypt based on solar UV-B measurements from UVB-1 pyranometer and its deviation from EP/TOMS satellite

S. M. El Shazly*, A.A. Hassan, Kh. O. Kassem, Emad A. A and E. F. El nobi

Atmospheric Physics Group, Department of Physics, Faculty of Science, South Valley University, Qena, Egypt

Abstract

Biologically active solar Ultraviolet irradiation is monitored in Qena, Upper Egypt (26° 16\ N, 32° 75\ E, 96 m asl) using a UVB-1 pyranometer for the period of 2001-2005. Cloud free condition records of erythemal UV were analyzed to study daily, monthly and seasonally variations. Results shows noontime one-hour average CIE (Commission International d'Eclairge) weighted dose rate can reach up to 285 mW m^{-2} (UV index =11 at solar zenith angle, SZA= 10° - 12°). Comparisons of ground-based measurement with TOMS satellite derived data have been examined. The examination revealed an overestimation of UV indices by TOMS, within the period of measurement, on average by 23±11 %.

Keywords: Erythemal UV; UV index; TOMS

*** Corresponding author: S. M. El Shazly**

E-mail address: sayedelshazly@yahoo.com

1. Introduction

The energetic solar UV irradiation is monitored with different ground and satellite based instruments. In addition, different extensive model calculations are used to analyze the UV irradiance especially the UVB in the wavelength range of 280 to 315 nm (Blumthaler et al., 1994; Kylling et al., 2000; WMO, 2003).

The effectiveness of UV of different wavelengths in producing erythema has been determined repeatedly in a number of studies over the past 70 years (Diffey, 1982). The technique is to determine the MED doses of UV at a series of wavelengths necessary to produce a minimally perceptible redness 8 or 24 hr after irradiation. The reciprocal of the MED is plotted against wavelength and the curve normalized to unity at the most effective wavelength. The MED at a given wavelength in a group of fair-skinned subjects are distributed lognormally. Studies in 254 normal subjects in the North East of England gave the median MED at 300 nm to be 34 mJ/cm^2 with a 95% confidence interval of 14-84 mJ/cm^2 (Diffey and Farr, 1989).

Although the action spectra determined by various workers have shown differences, particularly in the spectral region 250-300 nm, there is good agreement that at wavelengths greater than 300 nm the effectiveness drops very rapidly, falling to efficiency at 320 nm of about 1% of that at 300 nm. Parrish et al., 1982 and Gange et al., 1986 have extended determination of the erythema action spectrum up to 400 nm and have shown that the erythemal effectiveness of UV decreases with increasing wavelength through the UV spectrum, although the rate of change of effectiveness is much less from 330 to 400 nm, than from 300 to 330 nm. .

Although it can be seen from figure (1) that UV-A irradiation is much less erythmogenic than UV-B irradiation broadly speaking by a factor of 1000, the much higher UV-A irradiance (6.5 %) present in sunlight means that in summertime UV-A irradiation contributes about 15-20% to

the sunburn reaction. It is important to say here that of the global UV irradiation at the ground 94 % is UV-A and 6 % is UV-B. However, 17 % of the erythemal UV irradiance is UV-A and 83 % is UV-B.

The UVB irradiation leads to serious adverse effects such as: sunburn, skin ageing, cataracts in humans, reduction in yield and unnecessary growth in certain terrestrial as well as aquatic plants (Grant and Heisler, 2000). Therefore it is important to monitor and follow up carefully the short and long term variations of surface UV dose rate at any place. However, observational data on surface is lacking in the developing countries in the lower latitude where UV dose is expected to be higher and is significant for its adverse effects.

The spectral irradiance at the surface of the earth depends on different factors such as: irradiation from the sun, optical properties of the atmosphere, position of the sun given by the solar zenith angle (SZA), mean sun earth distance and the reflecting property of the surface (Madronich 1993; Dahlback, 1996; Kylling et al.,1998; Kerr, 2003). Among the optical properties of the atmosphere, cloud and aerosols are the complicated factors affecting UV, which are still not very well understood (Ilyas, 1987; Thiel et al., 1997; Grant and Heisler, 2000; Kylling et al., 2000; Kerr, 2003).

Two important parameters must be taken in account when monitoring UV irradiation and considering its effect on the human skin, namely UV index (erythemal UV index) and UV dose. The UV Index is a parameter introduced by the scientist that can be used as an indicator of the UV exposures. It is related to the known erythemal effects of solar UV irradiation on human skin and has been defined as an estimation of the UV levels that are important for the effects on the human skin, where 1 unit equals 25 mW/m^2. It is usually given for local solar noon, when the sun is highest in the sky, and it is valid for clear sky conditions (i.e. effects of cloud shielding part of the UV irradiation are not taken into account). The UV Index can range from 0 (when it is night time) to 15 or 16 (in the tropics at high elevations under clear skies). as shown in Table (1).

UV Index definition has later been standardized and published as a joint recommendation by the World Health Organization (WHO), the World Meteorological Organization (WMO), the United Nations Environment Program (UNEP) and the International Commission on Non-Ionizing Irradiation (ICNIRP). The UV Index is recommended as a way to raise the public awareness about the potential detrimental effects on health from solar UV exposure and to alert people of the need to adopt protective measures. Even for very sensitive fair-skinned people, the risk of short-term and long-term UV damage below a UVI of value 2 is limited, and under normal circumstances no protective measures are needed. If sun protection is required, this should include all protective means, i.e. clothing and sunglasses, shade and sunscreen. The Environmental Protection Agency (EPA) has devised general guidelines to UV index, as shown in Table (2).

The UV index is an artificial quantity derived from the erythemal irradiance, which is an integration of the UV irradiance at the ground weighted by the Commission International de l'Eclairage (CIE). The CIE action spectrum is a model for the susceptibility of the Caucasian skin to sunburn (erythema) as proposed by McKinlay and Diffey (1987) and adopted as a standard by CIE.

The "Minimal Erythemal Dose” MED is used to describe the erythemal potential of UV dose irradiation. MED is defined as the effective UV dose that causes a perceptible reddening of previously unexposed human skin. CIE erythemal action spectrum is recommended for use in assessing the skin damaging effect UV irradiation. However, because human individuals are not equally sensitive to UV irradiation due to different self-protection abilities of their skin (pigmentation), 1 MED varies among the population within the range of between 200 and 500 J/m^2 as shown in Table (3)

The main aim of this paper is to present the EUV irradiation in Qena, Upper Egypt,_see figure (2), and to find out its deviation from satellite data. .This deviation is useful when the observational data on surface is lacking.

2. Instrument and methods

2.1. Ground-based EUV measuring instrument

Hourly values measurements of UV-B at the horizontal surface was carried out by UVB-1 Pyranometer ''No. 960842, Yankee Environmental Systems Inc. (YES) was used to measure the total irradiance from 280 to 320 nm''. The instrument was installed on the roof of south vally meteorological station, of South Valley University in Qena, see figure (3). It was manufactured by the hourly values of UV-B were recorded by Combilog Data logger (No. 1020, TH. Friedrichs & CO.''Germany''). These values were used to calculate the EUV through the period of this study (2001–2005), as below.

For example, Suppose you take one UVB-1 instrument voltage reading (V) every k minutes and a total of N readings during the day. If the instrument has a calibration coefficient of C, The total daily MED dose, as defined by the Diffey erythemal action spectrum. Is given by the following

$$\text{MED dose} = \frac{1}{201} \sum_{i=1}^{N} C*0.0716*60k*V_i$$

Where …

The factor C*0.0716 convert the measured voltage to erythemal (Diffey) W/m^2
The factor 60*k converts the W/m^2 to erythemal J/m^2
The factor 201 convert the erythemal J/m^2 dose to MED unit (Parrish et al,1982), where the standard definition of the MED unit is 201 J/m^2

2.2. Satellite EUV data

The erythemal noontime irradiance data was measured by the Total Ozone Mapping Spectrometer (TOMS) installed on board of NASA's Earth Probe satellite. The Total Ozone Mapping Spectrometer (TOMS), installed on board of NASA's Earth Probe Satellite, measures the Total Ozone Column by an indirect way through the mapping of the Ultraviolet light emitted by the Sun and scattered by the Earth's atmosphere back towards the satellite (London, 1985). Data were obtained through TOMS/NASA webpage (http://jwocky.gsfc.nasa.gov).

Earth Probe Total Ozone Mapping Spectrometer (EP/TOMS) was launched July 2, 1996 and the first full day of data file generation began on July 25, 1996. The Earth Probe instrument has provided continuous data from that time until present, with the exception of a few days in Dec 1997 during which the satellite orbit was boosted from 500km to 750km, and a period in late 1998 when the instrument was in Safe hold. (see ftp://toms.gsfc.nasa.gov/pub/eptoms/earthprobe_data_coverage.txt/).

Earth Probe EP/TOMS was launched into a 500 km sun synchronous orbit on July 2, 1996. The first EP/TOMS Earth scan data were taken during orbit 216 on July 16, 1996. Normal science operations began during orbit 339 on July 24, 1996. Orbits prior to 7903 (December 4, 1997) were at the initial 500 km altitude. Orbits after 8037 (December 13, 1997) were at 740 km altitude after an orbit boosting maneuver This interface is designed for visualization and analysis of the Earth Probe TOMS Daily Global 1.0°x1.25° Products.

The erythemal noontime irradiance data in mW/m^2 from EP/TOMS have been used for the analysis of the data recorded from UVB-1 pyranometer. Also the data are collected from this site (ftp://toms.gsfc.nasa.gov/pub/eptoms/data/erythemal/) is divided by a conversion factor of 25 and rounded to the nearest whole number. This result in a number that usually ranges from 0 (where there is no sun light) to the mid teens. This value is the UV index.

Example: If EUV at noon =319.6 mW/m^2 then UVI = 319.6 /25 = 12.78 UVI = ~ 13

3. Results and discussions

3.1. Ground EUV climatology

Noontime average EUV irradiation in Qena for the period from 2001- 2005 during clear days, showed a decrease in EUV level in January followed by an increase from March reaching the maximum value in summer months followed by decrease again to December, see Figure (4). Maximum noontime EUV irradiation measured during the study period was 285 mW/m^2 (UV index 11) at solar zenith angle 10°-12°, on 25 July 2001 and 11, 30 June 2005. Noontime UV indices double from December to March.

3.2. Comparison between ground-based and satellite Observations

The linear fit of one-hour average noontime UV indices obtained from UVB-1 pyranometer and TOMS noontime indices showed that TOMS values were higher than measured UV indices at ground (Figure 5). The average percentage difference is (23±11%) as shown in (Figure 6).

Deviation between satellite and ground-based measurements can be explained by the fact that there are differences in spatial resolution between the two methods. The field of view of TOMS measurement is about 100 km (Arola et al., 2004), while the ground based instrument has a smaller field of view. Temporal differences can also occur because of difference in timing as TOMS data are from the time of direct overpass of the location, while ground-based measurements are one-hour averages values around satellite overpass time. Averaging ground-based measurements will reduce effects of rapid changing cloud cover. Effects of clouds are not fully taken into account in the UV index retrieval from the satellite (B.K. Bhattarai et al, 2007).

In addition Arola et al. (2004) has found that the factor between TOMS UV and ground-based measurement in Thessaloniki, Greece could reach as high as 4 in dusty environment. Also B.K. Bhattarai et al, (2007) show that frequent dusty events in the atmosphere could also be another cause of higher TOMS UV levels than ground based measurement in Kathmandu. High aerosol content influences the ground-based measurements and is not taken fully into account in the TOMS algorithm for UV index (Krotkov et al., 1998; Arola et al., 2005). This might be the reason for a systematic difference between the data. Finally differences in instrument calibration might be another factor for this discrepancy.

3.3. Variability of UV Index (UVI)

Figures (7) summarize the mean monthly variation of Ground UV index and EP/TOMS UV index. In general, Monthly mean increases from January crossing February, May, showing maximum values at June, July and August then fall down to December . From ground data, we can conclude the following:

- **The maximum mean value of UVI (11) was found at spring and summer months (May, June, July and August). According to the EPA general guidelines, as illustrate in table (1), this value is very high and advise to use protective clothing, sun glasses and avoid being in the sun.**

- **The minimum mean value was found at autumn and winter months (November, December and January). This value range from 4 to 5 and it is corresponding the low and moderate categories according to the EPA classification, see table (1).**

From satellite EP/TOMS data, we can conclude the following:

- **The maximum mean value of UVI (12) was found at spring and summer months (May, June, July and August). According to the EPA general guidelines, as illustrate in table (1), this value is very high and advise to use protective clothing, sun glasses and avoid being in the sun.**
- **The minimum mean value was found 5 at December, it is corresponding the moderate categories according to the EPA classification, see table (1).**

4. Conclusion

The study leads to the following important conclusions:

1. **For most of the days, the UV index at local noon exceeds 4**
2. **Through all the period, it is clear that the maximum values of UV indices are recorded at summer months while the minimum ones are recoded winter months**
3. **The maximum value of UV index, at local noon, was 11 while the minimum one was 4**
4. **Comparison of ground-based UV with TOMS satellite derived data reveals an overestimation on average by 23±11 %.**
5. **According to the EPA general guidelines and the obtained results , it is very important to use protective clothing, sun glasses and avoid being in the sun, particularly at noon time in summer months.**

References

- **Arola, A., Kazadzis, S., Krotkov, N., Bais, A., Herman, J.R., Lakkala, K., 2004. Assessment of TOMS UV bias due to the absorbing aerosols. In: Slusser, James R., Herman, Jay R., Gao, Wei, Bernhard, Germar (Eds.), Proceedings of SPIE. Ultraviolet Ground and Space Based Measurements, Models, and Effects IV, vol. 5545, pp. 28–35.**
- **Arola, A., Kazadzis, S., Krotkov, N., Bais, A., Grobner, J., Herman, J.R., 2005. Assessment of TOMS UV bias due to absorbing aerosols. Journal of Geophysical Research 110, D23211. doi:10.1029/2005JD005913.**
- **Binod Kumar Bhattarai, Berit Kjeldstad, Trond Morten Thorseth, Asadollah Bagheri ,2007. Erythemal dose in Kathmandu, Nepal based on solar UV measurements from multichannel filter radiometer, its deviation from satellite and radiative transfer simulations. Atmospheric Research 85 , 112–119**
- **Blumthaler, M., Webb, A.R., Seckmeyer, G., Bais, A.F., Huber, M.,Mayer, B., 1994. Simultaneous spectroradiometry: a study of solar UV irradiance at two altitudes. Geophysical Research Letters 21(25), 2805–2808.**
- **Dahlback, A., 1996. Measurements of biologically effective UV doses, total ozone abundances, and cloud effects with multichannel, moderate bandwidth filter instruments. Applied Optics 35 (33), 6514–6521.**
- **Diffey B. L., 1982: The consistency of studies of ultraviolet erythema in normal human skin, Phys.Med. Biol., 27, 715-720.**
- **Diffey B. L. and Farr P. M., 1989: The normal range in diagnostic phototesting , Br.J Dermatol., 120, 517-524.**

- **Gange R. W., Park Y. K., Auletta M., Kagetsu N., Blackrtt A.D., Parrish J. A., 1986: Action Spectra for cutaneous responses to ultraviolet radiation, The Biological Effects of UV-A Radiation ed F Urbach and R W Geang , New York, 57-65.**
- **Grant, R.H., Heisler, G.M., 2000. Estimation of ultraviolet-B irradiance under variable cloud conditions. Journal of Applied Meteorology 39 (6), 904–916.**
- **Ilyas, M., 1987. Effect of cloudiness on solar ultraviolet irradiation reaching the surface. Atmospheric Environment 21 (6), 1483–1484.**
- **Kerr, J.B., 2003. Understanding the factors that affect surface UV irradiation. In: James, R.S., Herman, J.R., Gao, W. (Eds.), Proceedings of SPIE. Ultraviolet Ground and Space Based Measurements, Models, and Effects III, vol. 5156, pp. 1–14.**
- **Krotkov, N.A., Bhartia, P.K., Herman, J.R., Fioletov, V., Kerr, J., 1998. Satellite estimation of spectral surface UV irradiance in the presence of tropospheric aerosols 1. Cloud-free case. Journal of Geophysical Research 103 (D8), 8779–8793.**
- **Kylling, A., Bais, A., Blumthaler, M., Schreder, J., Zerefos, C.S., Kosmidis, E., 1998. Effect of aerosols on solar UV irradiances during photochemical activity and Solar UV irradiation campaign. Journal of Geophysical Research 103 (D20), 26051–26060.**
- **Kylling, A., Dahlback, A., Mayer, B., 2000. The effect of clouds and surface albedo on UV irradiances at a high latitude site. Geophysical Research Letters 27 (9), 1411–1444.**
- **London, J. The observed distribution of atmospheric ozone and its variations, in: Whiten, R.C., Prasad, S.S. (Eds.), Ozone in the Free Atmosphere. Van Nostrand Reinhold, New York, pp. 11–80, 1985.**
- **Madronich, S., 1993. UV Irradiation in the natural and perturbed atmosphere. In: Tevini, M. (Ed.), UV-B Irradiation and Ozone Depletion, Effects on Humans, Animals, Plants, Microorganisms, and Materials. Lewis Publishers, USA, pp. 17–69.**
- **McKinlay A.F. and Diffey B.L. 1987: A reference action spectrum for ultraviolet induced erythema in human skin. In Human Exposure to Ultraviolet Radiation: Risks and Regulations, Passchier, W.R. and Bosnjakovic, B.F.M. (eds.), Elsevier, Amsterdam.**
- **Parrish J. A., Jaenicke K. F. and Anderson R. R., 1982: Erythema and melanogenesis action spectra of normal human skin, photochemistry and photobiology, 36, 187-191.**
- **Thiel, S., Steiner, K., Seidlitz, H.K., 1997. Modification of global erythemally effective irradiance by clouds. Photochemistry and Photobiology 65 (6), 969–973.**
- **WMO (World Meteorological Organization), 2003. Scientific assessment of ozone depletion: 2002. Global Ozone Research and Monitoring Project-Report vol. 47 Geneva, 498 pp.**

Table 1: Exposure category of UV index.

UV Index Prior to May 2004		The New Global Solar UV Index	
Exposure Category	Index Number	Exposure Category	Index Number
MINIMAL	0-2	LOW	1-2
LOW	3-4	MODERATE	3-5
MODERATE	5-6	HIGH	6-7
HIGH	7-9	VERY HIGH	8-10
VERY HIGH	10+	EXTREME	11+

Table 2: The EPA general guidelines of UV index.

Exposure Category	Index Number	Sun Protection Messages
LOW	1-2	• Wear sunglasses on bright days. In winter, reflection off snow can nearly double UV strength. • If you burn easily, cover up and use sunscreen.
MODERATE	3-5	• Take precautions, such as covering up and using sunscreen, if you will be outside. • Stay in shade near midday when the sun is strongest.
HIGH	6-7	• Protection against sunburn is needed. • Reduce time in the sun between 11 a.m. and 4 p.m. • Cover up, wear a hat and sunglasses, and use sunscreen.
VERY HIGH	8-10	• Take extra precautions. Unprotected skin will be damaged and can burn quickly. • Try to avoid the sun between 11 a.m. and 4 p.m. Otherwise, seek shade, cover up, wear a hat and sunglasses, and use sunscreen.
EXTREME	11+	• Take all precautions. Unprotected skin can burn in minutes. Beachgoers should know that white sand and other bright surfaces reflect UV and will increase UV exposure. • Avoid the sun between 11 a.m. and 4 p.m. • Seek shade, cover up, wear a hat and sunglasses, and use sunscreen.

EXPOSURE CATEGORY	INDEX Number	Sun Protection Recommendations
LOW	1-2	• Wear sunglasses on bright days. In winter, reflection off snow can nearly double UV Strength. • If you burn easily, cover up and use sunscreen.
MODERATE	3-5	• Take precautions, such as covering up and using sunscreen, if you will be outside. • Stay in shade near midday when the sun is strongest.
HIGH	6-7	• Protection against sunburn is needed. • Reduce time in the sun between 11am and 4pm. • Cover up, wear a hat and sunglasses, and use sunscreen.
VERY HIGH	8-10	• Take extra precautions. Unprotected skin will be damaged and can burn quickly. • Try to avoid the sun between 11am and 4pm. Otherwise, seek shade, cover up, wear a hat and sunglasses, and use sunscreen.
EXTREME	11+	• Seek shade, cover up, wear a hat and sunglasses, and use sunscreen. • Avoid the sun between 11am and 4pm • Take all precautions. Unprotected skin can burn in minutes. Beachgoers should know that white sand and other bright surfaces reflect UV and will increase UV exposure.

Table 3: The values of MEDs for different skin types.

Skin type	Tan	Burn	Hair colour	Eye colour	1MED
I	never	always	red	blue	200 J/m²
II	sometimes	sometimes	blond	blue/green	250 J/m²
III	always	rarely	brown	gray/brown	350 J/m²
IV	always	never	black	brown	450 J/m²

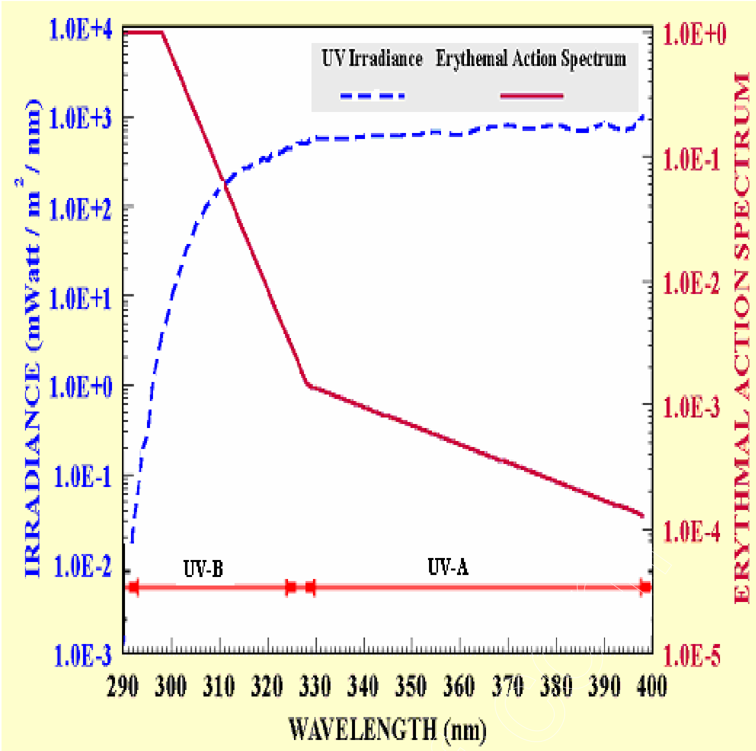

Figure (1): The CIE reference erythemal action spectrum

Figure (2): Map of Egypt, location of studied area

Figure (3): UVB-1 Ultraviolet Pyranometer

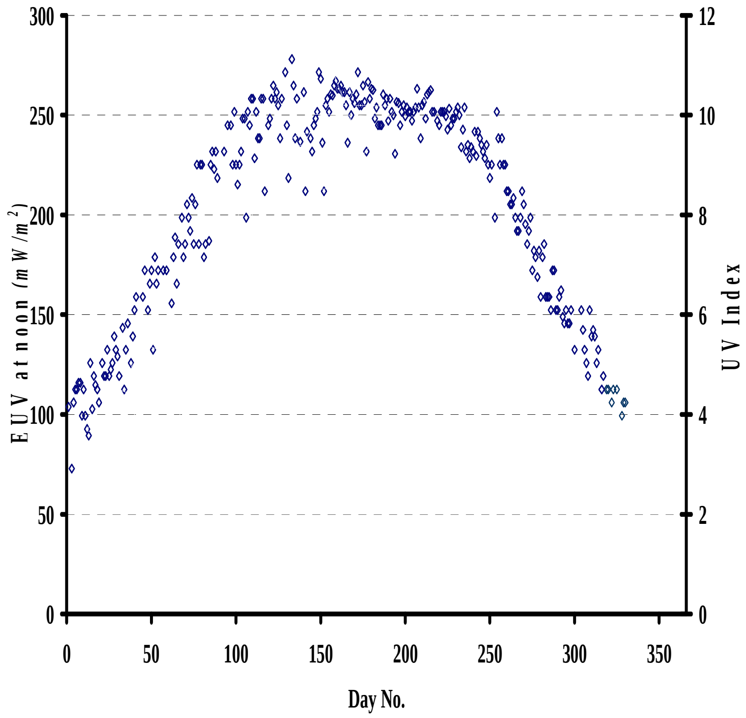

Figure (4): Clear sky ground EUV irradiation at noon (mW/m^2) and UV index in Qena Upper Egypt through the period (2001-2005)

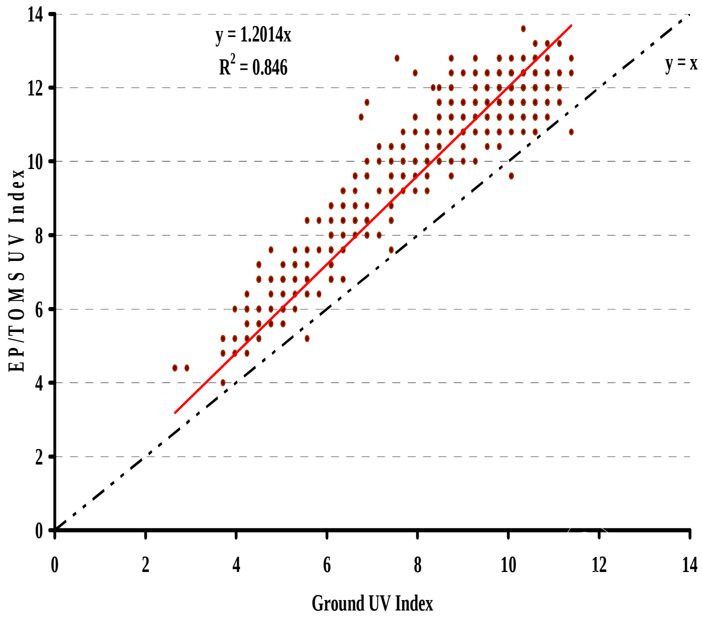

Figure (5): Scatter plot of ground UV index and EP/TOMS UV index in Qena Upper Egypt through the period (2001-2005). The solid line represents the linear fit and the dashed line is ideal regression of unit slope.

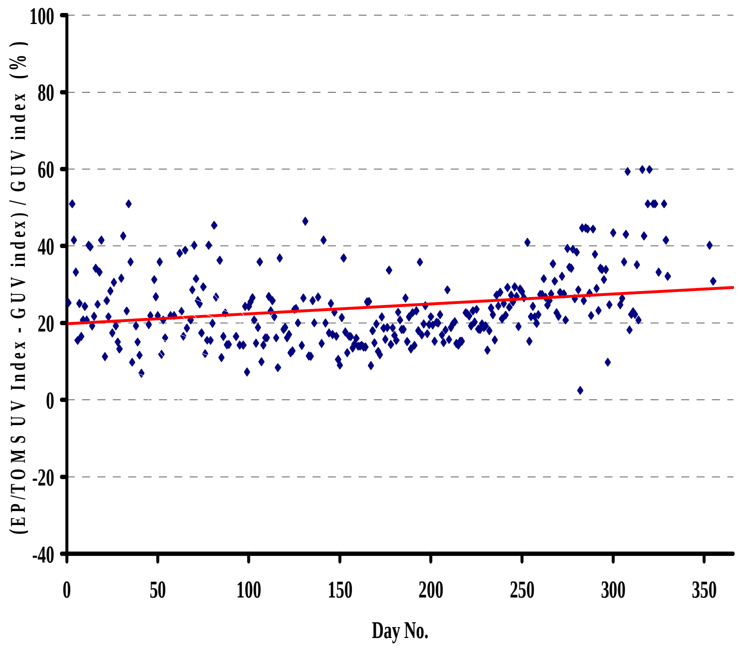

Figure (6): Daily percentage difference of ground UV index and EP/TOMS UV index in Qena Upper Egypt through the period (2001-2005). The solid line represents the linear trend line.

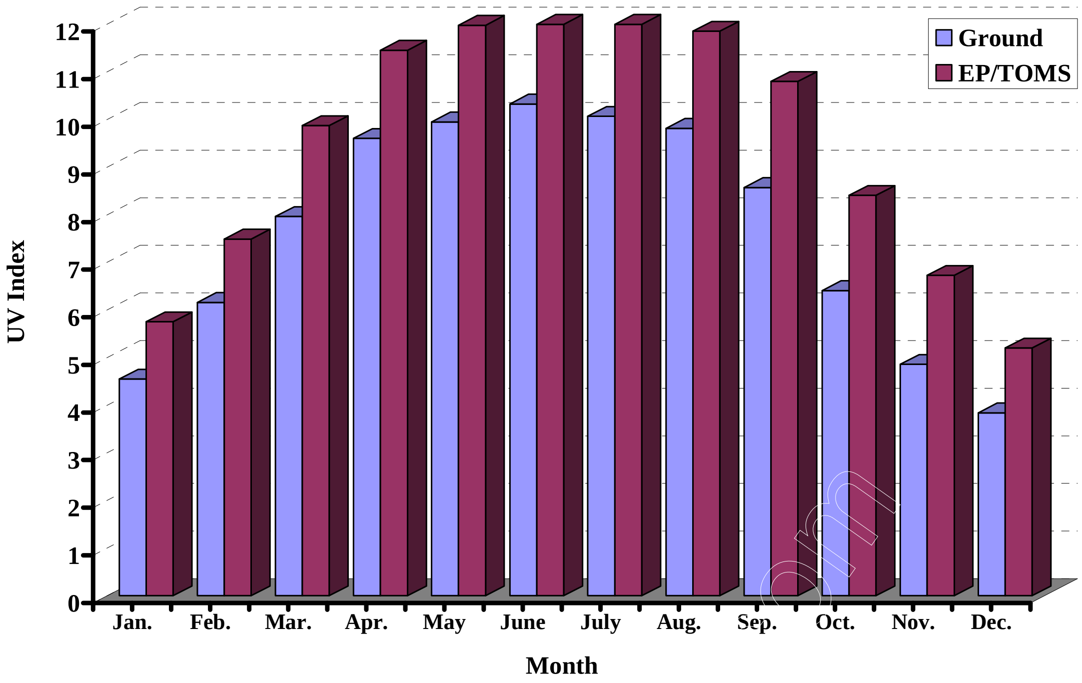

Figure (7): Monthly variation of ground UV index and EP/TOMS UV index in Qena Upper Egypt through the period (2001-2005).

EVALUATION OF POULTRY-BY PRODUCT AS FEEDSTUFF IN THE DIETS OF NILE TILAPIA

MICKDAM, E.M1, SEDDEK, A.S 1, ABDELLAH, A.M 2, SAYED A.N 2
1 Fac. of Vet. Medicine, South Valley Univ., Qena
2 Fac. Of Vet. Medicine, Assiut Univ., Assiut

ABSTRACT

The present study was performed to investigate the effect of feeding different levels of poultry by-product meal as untraditional ration constituents on fish performance, and apparent digestion coefficients.

A total number of 90 apparent healthy Nile tilapia fingerlings were randomly distributed into 5 groups, each of 18. The first group was considered as a control (T1) and was fed ad- libitum on the control diet. The other four groups (T2, T3, T4 & T5) were fed on diets containing poultry by-product meal at levels of 25, 50, 75 & 100 % respectively. The experiment was extended for 10 weeks. There were no significant ($P<0.05$) differences, in the values of body weight, body weight gain; specific growth rate, feed intake and feed conversion ratio between control, T2 and T3, while there were significant differences ($P<0.05$) between the control, T4 and T5. The apparent digestibility are matching with growth performance results and nutrient utilization that fish meal protein in Nile tilapia diets could be substituted with poultry by-product meal protein up to 50% without adverse effect on nutrient digestibility.

INTRODUCTION

The shortage in world production of fish meal, which is the main conventional protein source coupled with its increased demand in feeds for livestock and poultry is likely to reduce the dependence on it as a single protein source in aqua feeds (El-Sayed, 1999). It is evident, on the long-run, that many developing countries will be unable to depend on fish meal as a major protein source in aqua feeds. Therefore, several attempts have been made to partially or totally replace fish meal with less expensive, locally available protein sources

Total or partial replacement of fish meal with less expensive animal protein, such as poultry by-product meal may help to reduce feed costs, although these sources may be lower in digestibility, palatability and essential amino acids (Barlow, 1997; Hertrampf and Piedad- Pascual, 2000; Emre et al., 2003; Hu et al., 2008).

The present study was carried out to investigate the possibility of using poultry by-product meal as non-conventional protein source to replace fish meal protein in the diet of tilapia.

MATERIALS & METHODS

A total of 90 apparent healthy tilapia fingerlings with an average body weight (13.75±2.62 g/fish) obtained from local hatchery. The fish were randomly divided into 5 groups each of 18 fish. The first group was fed on control diet, while 2nd, 3rd, 4th and 5th group were fed on diets where fish meal protein was replaced by poultry by-product meal at level 25, 50, 75 and 100%, respectively. Five experimental diets were formulated from commercially available ingredients. The diets were isonitrogenous (32% crude protein) and isocaloric (3000 kcal/kg digestible energy).

Performance measurements:

- Average live body weight:
- Body weight gain:
- Feed intake:
- Feed conversion ratio:
- Specific growth rate

Composition (%) of the experimental diets

Ingredient	Treatments (Poultry by-product meal replacement, %)				
	T1 (0)	T2 (25)	T3 (50)	T4 (75)	T5 (100)
Fish meal	10.00	7.50	5.00	2.55	0.00
Poultry by-product meal	0.00	2.70	5.40	8.00	10.75
Soybean meal	50.56	50.50	50.60	51.20	51.10
Yellow corn	32.50	32.80	31.80	29.00	30.00
Corn oil	4.38	3.85	4.43	6.38	5.17
Limestone, ground	1.52	1.60	1.71	1.80	1.89
Methionin	0.24	0.25	0.26	0.27	0.29
Premix*	0.30	0.30	0.30	0.30	0.30
Chromic oxide	0.50	0.50	0.50	0.50	0.50

*Each2.5 kg contains: Vit. A, 12000000 IU; Vit. D_3, 2000000 IU; Vit. E, 10 g; Vit. k_3, 2g; Vit. B_1, 1g; Vit. B_2, 5g; Vit. B_6, 1.5 g; Vit. B_{12}, 10g;Nicotinic acid 30g;Pantothenic acid 10g; Folic acid 1g; Biotin 50g; Iron30g; Copper 10g; Zinc 50g;Manganese 60g;Iodine 1g; Selenium 0.10g

RESULTS

Performance of fish in the experiment

Item	Treatments (Poultry by-product meal replacement, %)				
	T1 (0)	T2 (25)	T3 (50)	T4 (75)	T5 (100)
Initial body weight (g)	13.84±2.62	13.75±2.93	13.90±3.21	14.00±3.44	14.00±1.66
Final body weight (g)	62.04±3.02^{a*}	58.67±1.83^{a}	60.77±1.07^{a}	50.95±1.77^{b}	42.94±1.82^{c}
Weight gain (g)	48.20±0.83^{a}	44.92±1.03^{a}	46.87±1.05^{a}	36.93±0.92^{b}	28.94±0.95^{c}
Weight gain (%)	348.26	326.69	337.19	263.78	206.73
Feed intake (g/fish)	85.13	80.86	74.99	73.12	65.12
Feed conversion ratio	1.77	1.80	1.60	1.98	2.25
Specific growth rate (% day-1)	2.12±1.20^{a}	2.07±1.19^{a}	2.10±1.24^{a}	1.84±0.96^{b}	1.58±0.80^{c}

*Figures in the same raw having the same superscripts are not significantly different (P<0.05).

Apparent digestibility coefficient of some nutrients

Nutrient	Diets (Poultry byproduct meal replacement, %)				
	T1 (0)	T2 (25)	T3 (50)	T4 (75)	T5 (100)
Dry matter	76.30±0.40	75.13±0.26	75.92±0.32	74.50±0.30	75.70±0.46
Crude protein	83.10±0.60[b*]	82.35±0.74[b]	85.05±.39[a]	76.30±0.45[c]	70.82±0.78[d]
Ether extract	85.30±0.45[a]	85.99±0.46[a]	87.20±0.36[a]	79.12±.97[b]	76.30±0.95[c]

CONCLUSION

It could be concluded that fish meal protein in Nile tilapia diets could be substituted with poultry by-product meal protein up to 50% without adverse effect on growth performance and nutrient digestibility.

REFERENCES

Emre Y, Sevgili, H., Diler, I. (2003): Replacing fish meal with poultry by- product meal in practical diets for Mirror carp (Cyprinus carpio) fingerlings. Turk. J. Fish Aquat. Sci. 3: 81-85.

Mohamed, S.H., (2003): partial replacement of fish meal with different animal by-product meals in diets of Nile Tilapia(Oreochromis Niloticus). Ph.D.Thesis, faculty of agriculture, Cairo Univ.

Yang, Y.; Xie, S.; Cui, Y.; Lei, W.; Zhu, X.; Yang Y. and Yu Y. (2004): Effect of replacement of dietary fish meal by meat and bone meal and poultry by-product meal on growth and feed utilization on gibel carp, (Carassius auratus gibelio). Aquacult.Nutr., 10: 289- 294.

Hu, M.; Wang Y.; Wang Q.; Zhao M.; Xiong B.; Qian X.; Zhao Y, and Luo, Z. (2008): Replacement of fish meal by rendered animal protein ingredients with lysine and methionine supplementation to practical diets for gibel carp, Carassius auratus gibelio, Aquacult. 275: 260- 265.

Macro-invertebrates as Bio-indicator for the pollution in lake Nasser, Egypt

Hoda M. Abdel-wahab, Essmat M. Nagieb
Zoology Department,Faculty of Science, Aswan, Egypt. South Valley University.

Abstract

The objective of this study was to determine which species of Macro-invertebrates "Aquatic insects" may be used as bio-indicator for the pollution in lake Nasser, Aswan, Egypt. Temperature,pH,DO,salinity, turbidity, heavy metals, water level and macro-invertebrates abundance were measured. Big difference in macro-invertebrate population were recorded along the year round which depend on pollution and physico-chemical factors.

The results indicated that the population of some insect orders are tolerance to the pollution and others are sensetive , there diversity and abundance reflex the purification of lake water. Thus, continuous monitoring of lake Nasser biota should be undertaken to follow the change in the ecosystem.

Keywords: lake Nasser; macro-invertebrates;Aquatic insect; pollution; physico-chemical factors

Introduction

Lake Nasser is the second largest man made lake in Africa, After lake Volta. It is about 480 Km long with tw parts: Lake Nasser in Egypt which extends for a bout 300 Km and Lake Nubia in Sudan which extend for 180 km. Lake Nasser is characterized by the presence of side branches named kors(85) in number. The only source of lake water is the River Nile

The outflow is the continuation of the Nile towards the north. Lake is unique in its performance because it is situated in pure desert. The Nile flood comes once a year in late August originating from the Ethiopian highlands. Aquatic insects are important of lake and stream biota. They comprise 50% to 90% of the Macroinvertebrate species. Aquatic insects may be more sensitive to certain pollutants than are fish. The wide variety of aquatic insects, some species abundance in unpolluted streams, their sensitivity to low concentration of pollutants, and some species are tolerant to pollution.

Material and Methods

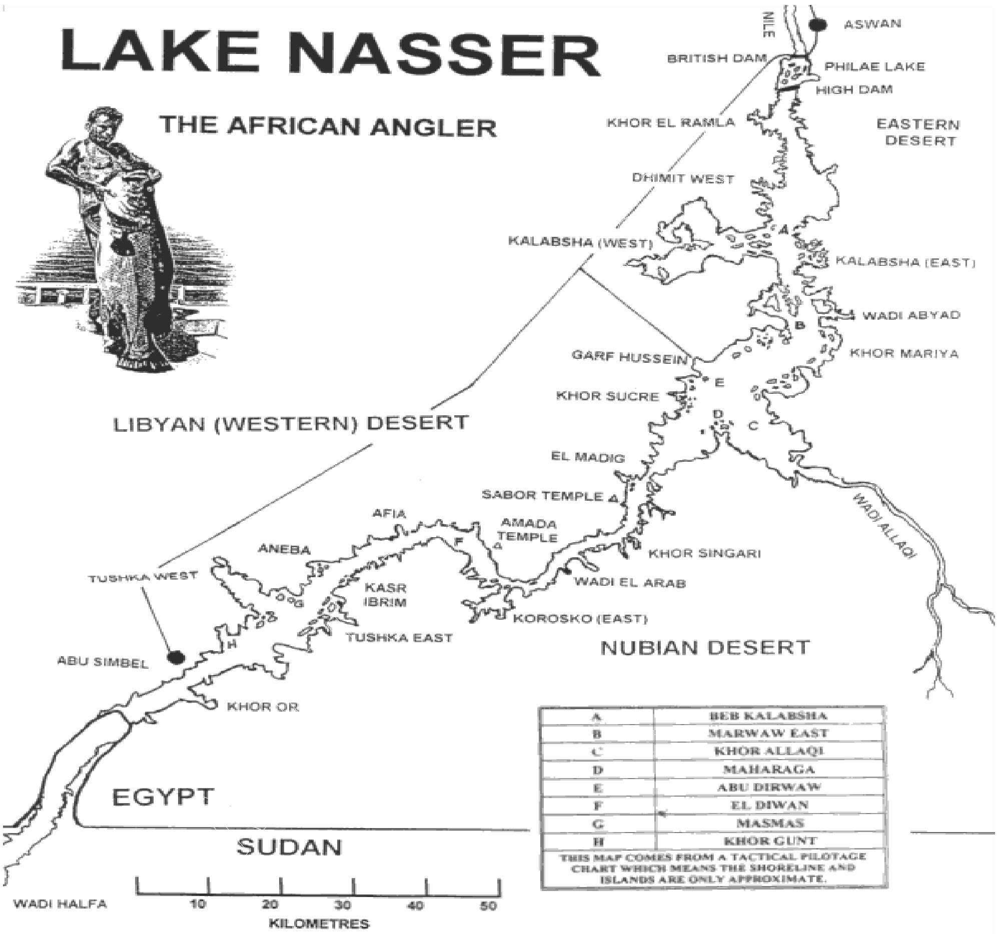

Description of site studied

Aswan High dam(AHD) reservoir lies between 22° 00′ N and 23° 58′ N in Egypt and extends southward into Sudan to 20° 27′ N as lake Nubia.

Sampling regime

The sampling were collected from two station along the pelagic water of the main channel in Lake Nasser (Egypt). Sampling was performed 12 time form May 2009 to April 2010.

Water analysis

Water samples from 0.5m below the surface were collected. Temperature, pH, and conductivity were measured in the filed immediately. Dissolved oxygen DO was determined

according to Winkler's method in the laboratory within a few hours of collection. Water temperature was measured with a standard thermometer graduate to 0.1◦ c, pH was measured by pH meter model pH 18 "Aqua litic", Water conductivity was measured with , transparency was measured by schii disc, and chlorophyll-a (chl.-a) was extracted in methanol and measured by.

Aquatic insect samples were carried out monthly during the daytime by using insect net.

Results

1- Water analysis:

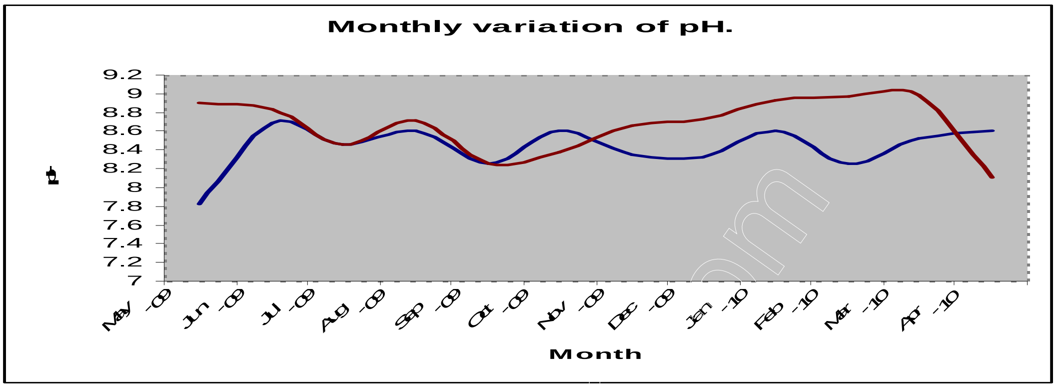

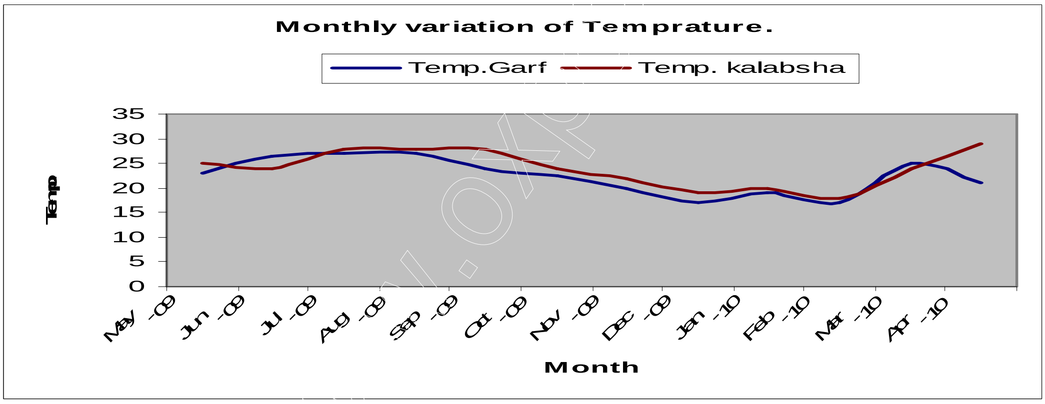

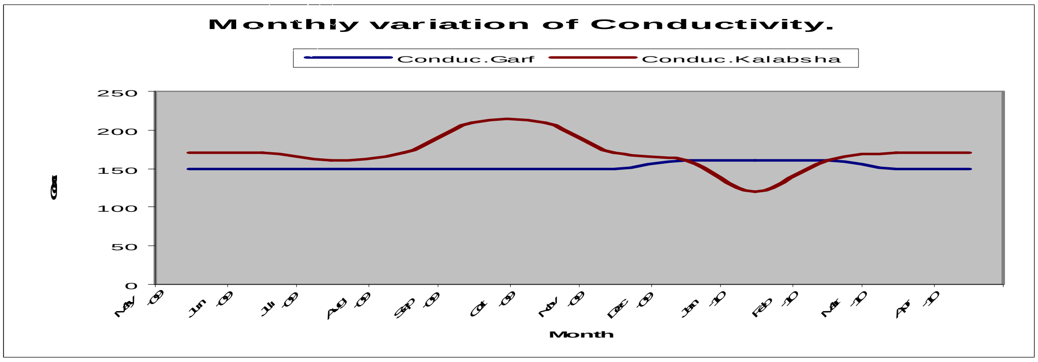

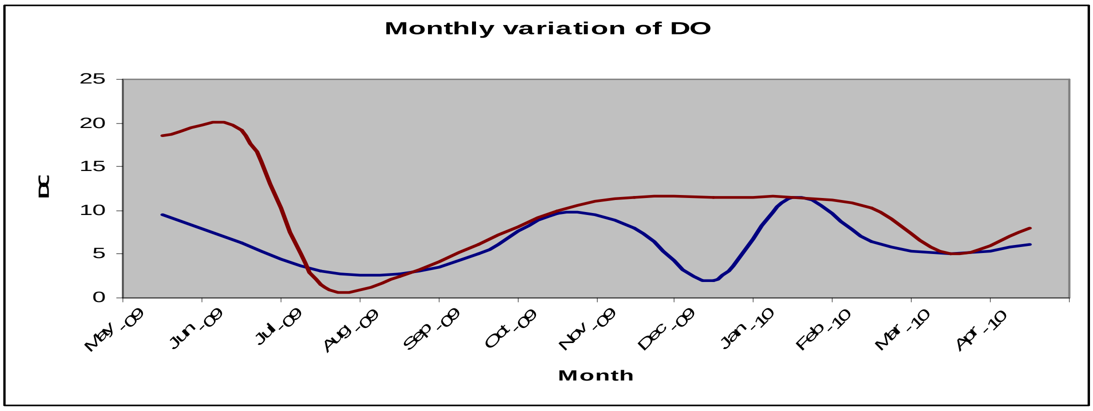
Monthly variation of DO
DO
25
20
15
10
5
0
May -09
Jun -09
Jul -09
Aug -09
Sep -09
Oct -09
Nov -09
Dec -09
Jan -10
Feb -10
Mar -10
Apr -10
Month

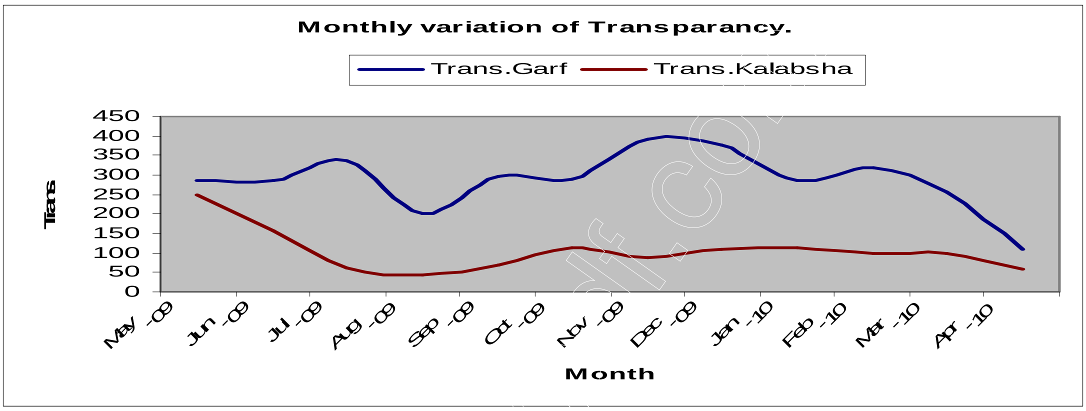
Monthly variation of Transparancy.
Trans.Garf
Trans.Kalabsha
Trans
450
400
350
300
250
200
150
100
50
0
May -09
Jun -09
Jul -09
Aug -09
Sep -09
Oct -09
Nov -09
Dec -09
Jan -10
Feb -10
Mar -10
Apr -10
Month

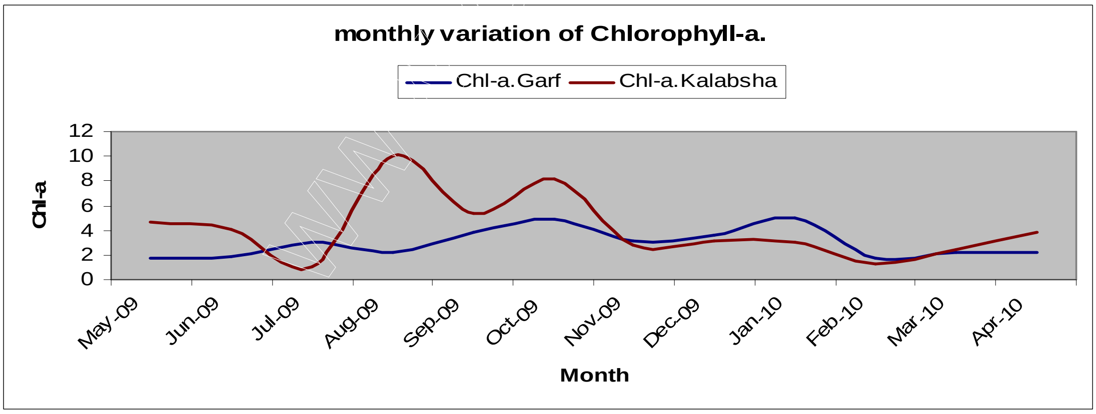
monthly variation of Chlorophyll-a.
Chl-a.Garf
Chl-a.Kalabsha
Chl-a
12
10
8
6
4
2
0
May-09
Jun-09
Jul-09
Aug-09
Sep-09
Oct-09
Nov-09
Dec-09
Jan-10
Feb-10
Mar-10
Apr-10
Month

2-Aquatic insect
Pollution sensitivity:

- Very sensitive
- Mayfly nymph

- **Tolerant**
- **Mosquito larvae and pupae**

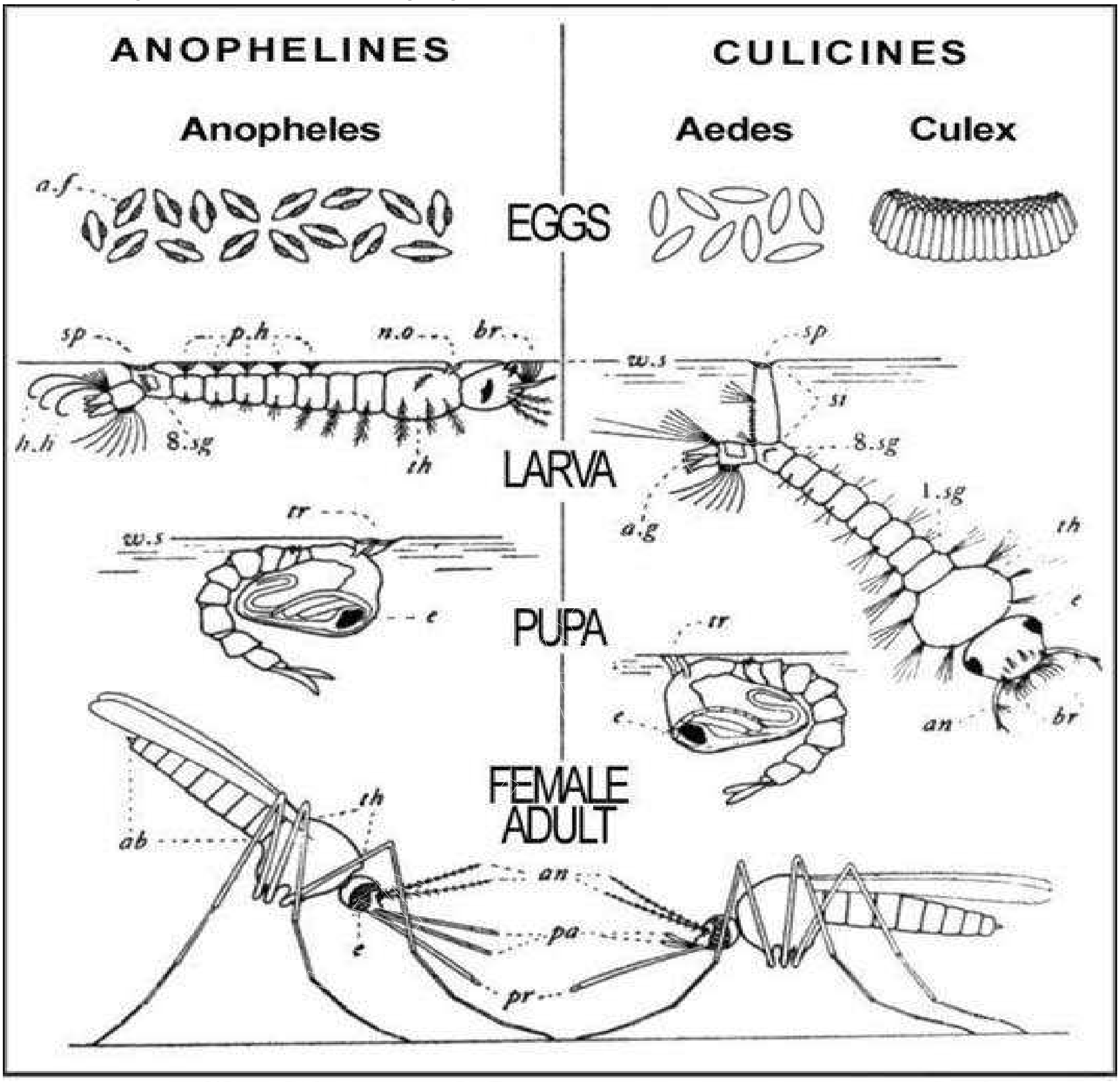

Chief distinguishing features of Anophelines and Culicines, *a.f.*, air floats; *a.g.*, anal gills; *ab.*, abdomen; *an.*, antenna; *br.*, mouth brush; *e.*, eye; *h.h.*, hooked (or grapnel) hairs; *n.o.*, notched organ; *pa.*, maxillary palp; *p.h.*, palmate (or float) hairs; *pr.*, proboscis; *1.sg.*, 1st abdominal segment; *8.sg.*, 8th abdominal segment; *si.*, siphon; *sp.*, spiracles; *th.*, thorax; *tr.*, respiratory trumpets; *w.s.*, water surface.

References:

Ali, M. M.; Mageed, A. A.; &Heikal, M. T.(2007): Important of aquatic macrophyte for invertebrate diversity in large subtropical reservoir. Limnological, 37, 155-169.

Eaton, A. D.; Clesceri, L. S.; &Rice, E. W.; Greenberg, A. E.(2005): Standerd methods for the examination of water and waste water. 21st edition: ch.8, 133.